A mi ma,
por volver (siempre) a levantarse...

"After years of stormy sailing,
have I finally found the bay?"

—Penny

Fundamental Aspects of Phase Separation MicroFabrication
PhD Thesis, Membrane Technology Group, University of Twente

This thesis has been approved by:
Prof. Dr. Ing. M. Wessling - Promotor
Dr. Ir. R.G.H. Lammertink - Assistant Promotor

Abstract

In the research featured in this PhD thesis, the fundamental aspects of Phase Separation MicroFabrication (PSµF) were studied. PSµF is a technique through which polymeric porous films with defined structures on their surfaces can be created. This is achieved by phase separation of polymer solutions that are in contact with microstructured molds. Diverse topics were covered, including the study of shrinkage during phase separation and its effect on feature replication, gas entrapment during casting of polymer solutions on molds, release of films perforated by pillars on molds (microsieves) and the development of permeable molds to yield membranes with structures on both sides. The results obtained in this research help in facilitating the successful use of PSµM in future applications.

FUNDAMENTAL ASPECTS OF

PHASE SEPARATION MICROFABRICATION

DISSERTATION

to obtain
the doctoral degree at the University of Twente,
on the authority of the rector magnificus,
Prof. Dr. H. Brinksma,
on account of the decision of the graduation committee,
to be publicly defended on
Friday 18th December 2009 at 16.45

by

Matías Bikel

Born on April 24th, 1980
in Buenos Aires, Argentina

I n the words of my promotor "there are no fundamental questions left to answer regarding transport through membranes". This might be the reason why this is one of those rare theses in the membrane field that deals with pure, exploratory science as opposed to the usual R&D concepts. In these concepts developing a membrane for specific conditions is the project; trial and error through formulation and testing is the method. Materials, synthesis conditions, operation modes… all tuned to try to meet the specific goal of a given application. However, in the rarest of occasions, something really new arises in this field. In our case, it was the possibility of patterning almost any polymeric membrane. Of course, the initial projects were launched into the R&D type: different types of applications were thought of and people got busy directly. Again, goals were to be met. Still, the basic science behind the process is not totally understood and this is what this thesis tries to explain. There are no applications in sight, no operation conditions to endure. Just undefined research… as delightful and dreadful as that sounds.

Table Of Contents

Summary

This chapter contains a short description of the project and the main question driving the research presented in this thesis.

Up to now, most of the patterning of polymers has been done through:

- Molding of a curable mixture of polymer and cross linking agent

- Molding of polymer melts

- Plastic deformation of sheets of thermoplastic polymers, heated and embossed on a mold

- Photolithography and/or etching

Several conclusions can be drawn from these facts. First, the range of processable materials is narrow. Second, the obtained films are invariably dense. Third, the defect rate of these processes is high as the solid material is directly in contact with the mold during release.

Phase Separation MicroFabrication (PSµF) is a new technique that is used for patterning the surface of polymeric films. This process relies on the phase separation of polymer solutions while they are in contact with microstructured molds. These molds are obtained through etching silicon wafers. The first disadvantage mentioned in the previous paragraph is thus trumped. Virtually all polymers for which a solvent (and a nonsolvent) can be found, can be processed with PSµF. In addition, particles (like ceramics or metals) can be suspended in the polymer solution. Upon phase separation, burning of the polymer and sintering, ceramic or metallic structures can be obtained.

As will be explained in Chapter 2, films produced via phase separation are porous, with or without a dense skin on top. Dense films can be obtained by casting a polymer solution made in a volatile solvent. Upon evaporation, the polymer is left behind as a nonporous film. The second disadvantage mentioned above is, therefore, also overcome.

The remaining disadvantage is directly overcome due to the shrinkage process that accompanies phase separation processes. During solidification, the polymer can retract from the mold walls and the film lifts off the surface of the mold by itself. As will be shown in Chapter 3, this shrinkage phenomenon is also responsible for the deformation of the replicas in certain cases. For microsieves, it makes the release from

the mold more difficult due to pulling of the polymer against the pillars.

The big question then arises. How should one design a mold so that upon phase separation (i.e. shrinkage) the features on the membrane are the desired ones? Extending this to all possible phenomena, the question becomes:

What are the *Fundamental Aspects of PSµF* that affect its performance?

This is the main challenge motivating the research presented here. In other words, what has to be taken into account to use PSµF successfully? For answering this question each of the components of the process (i.e. mold, polymer solution, coagulation bath, casting atmosphere, etc.) has been studied.

Summary

This chapter introduces the main topics in play in this thesis. Membrane morphologies are related to formation mechanisms during phase separation. The balance between thermodynamics and kinetics during this process is then presented. Applications of microstructured polymeric films are presented next, along with Phase Separation MicroFabrication. This new process allows the structuring of many different polymers to create films with interesting topologies.

1. Membranes

In the context of this thesis, a membrane is a selective polymeric barrier between two media. In other words, we deal here with plastic films which present the special ability to control the permeation of a chemical species [1]. As a result, different components of a mixture will traverse the membrane freely, whereas others will be hindered. When correctly developed, a membrane will allow separation of these components. Membranes are widely used in industry for separation processes [2]. This is largely because the development of membranes is highly advanced in certain areas.

Membranes can be made from different polymers and via different methods. The effect of the method can be largely seen on the final morphology of the membrane. This is important because the efficiency of a membrane-based separation process will depend on the interaction between the components of the feed stream and the material from which a membrane is made, as well as the morphology of the membrane. A general classification of membrane processes and required membrane morphologies can be seen in Figure 1:
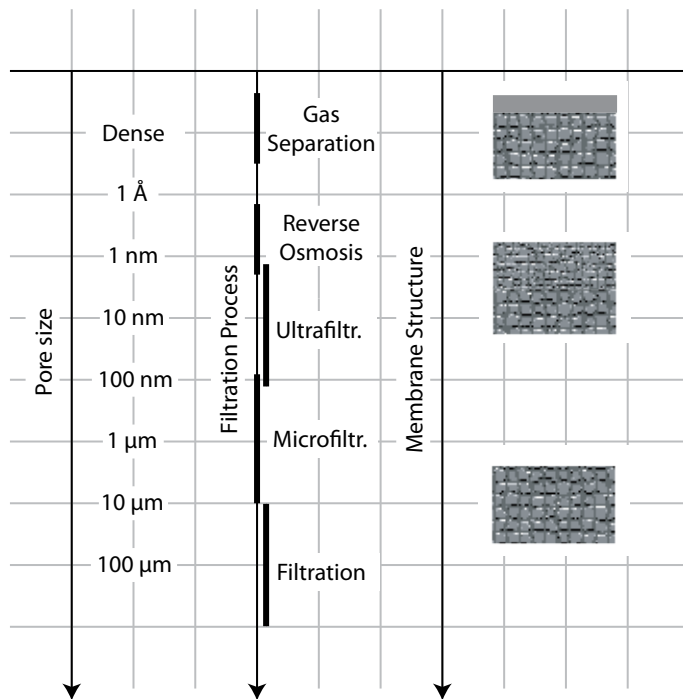

Figure 1: Classification of membrane processes.

The greatest division that can be made in the morphology of membranes is perhaps the distinction between dense and porous membranes. Dense membranes often present a high resistance to flow and rely on affinity as a separation mechanism. Their main application is gas separation. Gas molecules dissolve into the polymeric matrix of the membrane, diffuse through it and are desorbed at the permeate side. Permeation results from movement through the interstices between the chains of polymer. Given their high resistance, dense membranes are normally prepared as thin layers (coatings) deposited on thicker porous substrates. This is done for mechanical resistance.

On the other hand, porous membranes function largely as a sieve, which excludes molecules on the basis of their sizes. Affinity also plays a role through Van der Waals interactions. The permeation takes place as flow through the pores in the membrane. Their main applications are filtration, microfiltration and ultrafiltration.

This thesis deals with porous polymeric membranes made through phase separation of polymer solutions. In this process, an initially homogeneous system is caused to separate into two phases. The main difference between these two phases is the concentration of polymer. The so-called polymer rich phase undergoes precipitation processes, creating the polymeric matrix of the membrane. The polymer lean phase is often a mixture of solvent and non-solvent and as a result, does not solidify. All the pockets containing the polymer lean phase constitute the pores of the membrane.

Phase separation can be induced in many ways. Figure 2 presents diagrams of a temperature induced phase separation process (TIPS) and the process induced through addition of a third component. This can be in the liquid phase (Liquid Induced Phase Separation, LIPS) or in the vapor phase (Vapor Induced Phase Separation, VIPS). As indicated by its name, TIPS proceeds through a change in temperature of a polymer solution beyond its critical point, through the binodal curve. The region contained by the binodal is the one in which the polymer solution can no longer exist as a homogeneous phase. Therefore, it undergoes the separation mentioned above. The process can be represented in a binary phase diagram from which the composition of the different phases can be found for different temperatures. The tie lines inside the binodal link the compositions of the phases in equilibrium with each other.

In VIPS and LIPS three components are present in the system. A ternary phase diagram is used in which each vertex represents a pure component. Each side of the
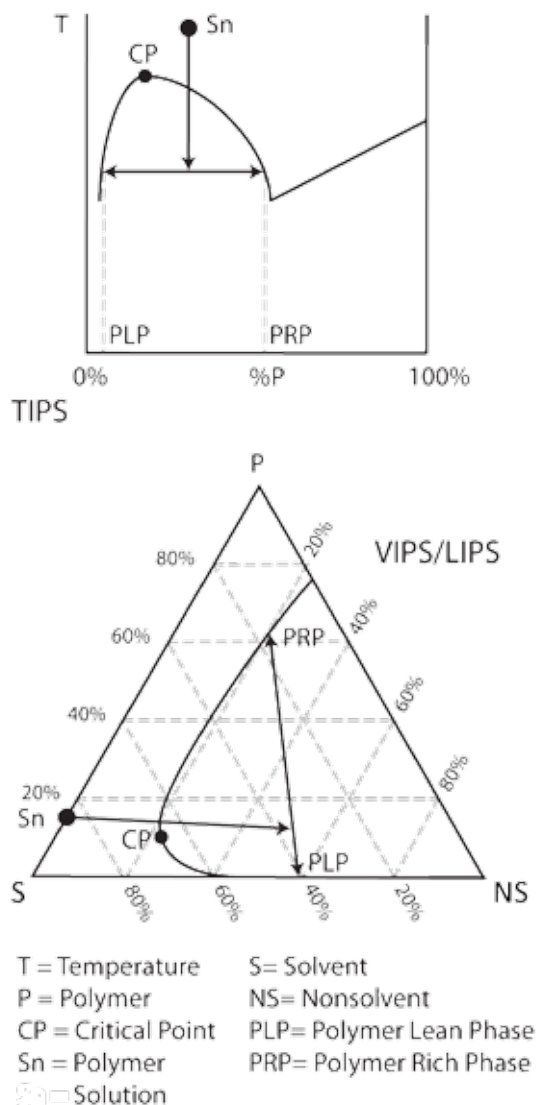
Figure 2: Phase diagrams for TIPS, VIPS and LIPS.

triangle is a mixture of the two components on the vertices. Any point inside the triangle represents the mixture of three components. The composition of the polymer solution is gradually changed until it crosses the binodal, causing the phase separation into two phases linked by a tie line. The membranes presented in this thesis are made through one or a combination of these two processes.

2. Thermodynamic Considerations

The ternary phase diagram is a representation of the thermodynamic nature of the system. It indicates which process is most favorable for each composition at a constant temperature. The one in Figure 2 is a highly simplified version. The diagrams in Figure 3 are more complete. These diagrams present separately all the information that can be obtained from one single ternary phase diagram.

Figure 3A illustrates the information regarding the amount of phases present for each composition, together with the state of aggregation. Figure 3B presents the names of certain curves, points and regions in the phase diagram. Figure 3C indicates the mechanisms governing the phase separation process in each region.

The one-phase regions comprise all the compositions for which the polymer solution is either liquid or solid. Whether the solid phase is amorphous or crystalline is a question that can only be applied to crystalline polymers which undergo a slow enough process to allow crystallization [3].

The two-phase regions consist of compositions at which the system separates into two homogeneous phases. The region enclosed by the spinodal includes unstable compositions $\left(\dfrac{\partial^2 G}{\partial x^2} < 0 \right)$ for which the separation process is spontaneous $\left(\dfrac{\partial G}{\partial x} < 0 \right)$, where G is Gibbs free energy and x the molar fraction of polymer. The mechanisms for phase separation in this region are fast and result in the generation of bicontinuous structures. These structures owe their name to the fact that both the polymer rich and lean phases are created in a way in which they reach both sides of the membranes, creating highly interconnected structures with low resistance [4]. When the phase separation is extremely fast, the polymer lean phase is formed into long and thick columns, known as macrovoids [5]. Macrovoids are an undesired type of structure, since they confer low mechanical stability to the membrane.

The regions between the spinodal and the binodal curves correspond to stable compositions $\left(\dfrac{\partial^2 G}{\partial x^2} \geq 0 \right)$ for which the separation process is spontaneous $\left(\dfrac{\partial G}{\partial x} < 0 \right)$.
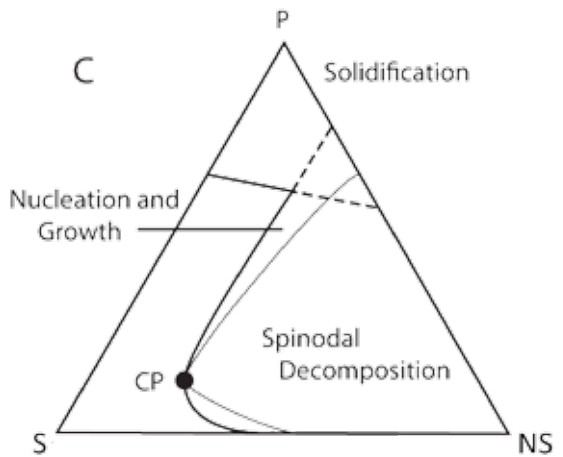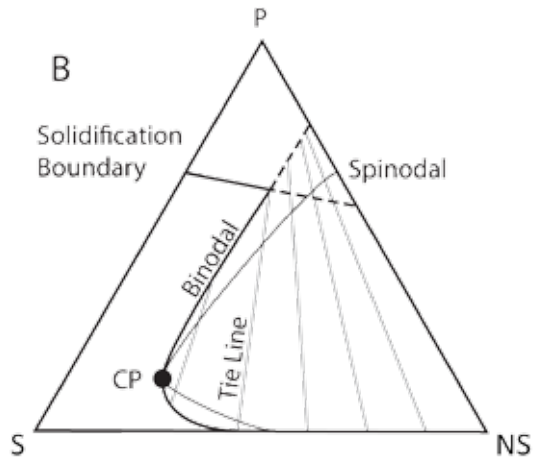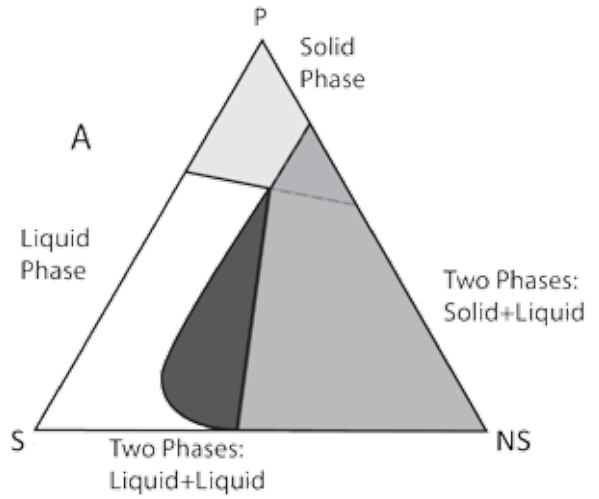
Figure 3: Phase diagramss for VIPS and LIPS.

A: Present phases and states.

B: Name of different elements in the diagram.

C: Mechanisms ruling each region.

As a result, these regions contain metastable states that proceed through phase separation slowly, via nucleation and growth mechanisms. The phase that nucleates and grows is the one present in the lower proportion. This is why, if the binodal is crossed slowly above the critical point, the nucleation and growth of the polymer lean phase takes place, leading to closed-cell structures. These structures result from the formation of droplets of polymer lean phase that grow in time, surrounded by walls of polymer rich phase. This creates a spongy structure in which the pores are separated by thin walls of polymer. If the thin walls are penetrated, an open-cell structure is formed in which the pores are interconnected [6].

When the binodal is crossed below the critical point, nucleation and growth of the polymer rich phase occurs. As a result, the membrane presents a structure made out of polymeric beads. The pores of this type of membrane are the spaces between the beads. Kesting has indicated that the generation of skins in phase separation membranes can be created through this mechanism [7]. The pores present in the skins of Reverse Osmosis and Ultrafiltration membranes might be the product of early solidification of the beads, before they can become a film.

The SEM micrographs in Figure 4 present different structures obtained from solutions based on Poly (ethersulfone) (PES, polymer), Poly (vinylpyrrolidone) (PVP, pore forming additive), N-methylpyrrolidone (NMP, solvent),and sulfonated poly (ether ether ketone) (SPEEK, polymeric additive) coagulated in different conditions. These images were obtained during the optimization of the recipe used for microsieves in Chapter 5.

Picture I shows macrovoids, product of an extremely fast phase separation. Picture II shows the structure obtained via spinodal decomposition. The bicontinuous structure can be noticed in the fact that both the polymer and the big pores are interconected. Picture III shows a membrane that consists solely of an open-cell structure created via nucleation and growth mechanisms. The pores are highly interconnected. In the case of Picture IV, the structure resembles more a closed-cell type, in which the pores are not interconnected. Furthermore, the presence of a very thick dense skin can be noticed.
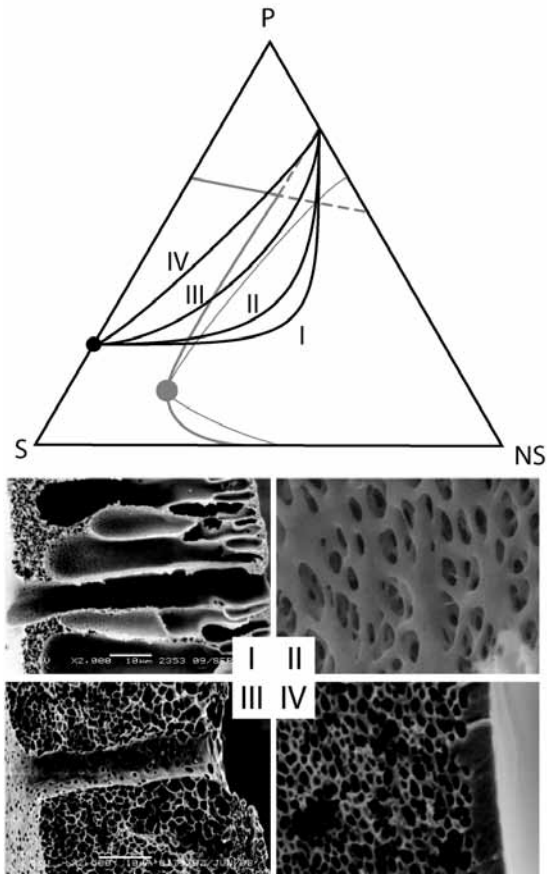
Figure 4: Different composition paths and obtainable morphologies.

3. Kinetic Considerations

Let us assume that we desire a membrane that has a structure that may be obtained via nucleation and growth of the polymer lean phase. The description in the previous section suggests that all we have to do is weigh all components in the required composition, stir well and we have what we desire. This, unfortunately, does not work for membranes. Membrane formation is often too fast. As a result, thermodynamic equilibrium may not be reached. The process of membrane formation is multifaceted and cannot be explained by thermodynamics alone. This phenomenon stems from the fact that thermodynamic descriptions are often qualitative and leave out kinetic effects of individual events [8].

Membranes must be well defined films. Their thickness affects their resistance,

both mechanical and to permeation. Their structures must be as defect free as can be managed. They are prepared as thin films of polymer solution cast onto suitable substrates (flat glass plates or nonwovens, for instance) and then exposed to nonsolvent vapor (VIPS) or immersed in a coagulation bath of liquid nonsolvent (LIPS). The amount of nonsolvent present is typically much larger than that of polymer solution. From this, one would expect the equilibrium tie line to be very close to the pure nonsolvent, where spinodal decomposition is the ruling mechanism for phase separation. However, the structure resulting from this mechanism is seldom seen in the final membrane.

In VIPS, the phase separation proceeds mainly through nonsolvent uptake. On the other hand, in LIPS an exchange of solvent and nonsolvent takes place between the polymer solution and the coagulation bath. Phenomenological equations can predict the diffusion of all three components. Models can even go as far as to include the effects on viscosity of conformational changes of the polymeric chains due to the presence of nonsolvent. However, in this system as soon as any boundary composition is reached, phase separation takes place. This creates two phases, one of which may or may not precipitate. The system becomes then too complex for the currently known equations to describe.

Considering the polymer solution in layers, each solidifying layer will impose an added resistance to the transport of solvent and nonsolvent to and from the rest of the solution. Furthermore, the polymer lean phase will mix with the diffusing nonsolvent, leading to different local compositions for each polymer solution layer. This can create, for example, pore size gradients across the membrane.

In the case of crystalline polymers, crystallization is thermodynamically the most favorable process, but it is also the slowest. Therefore, the sequence of compositions of each element of volume of polymer solution dictates its final structure. This phenomenon is commonly represented in the ternary phase diagram by means of the composition path. This path is drawn as a line that links the initial composition of the polymer solution with the final one, passing through the different compositions that the different phases have during the phase separation process. It is normally said that the composition path represents either:

- All the different compositions that a single element of volume of the membrane has during the phase separation process, or

- All the different compositions that all the elements of volume have at a single instant during the phase separation process.

From the considerations explained above, it seems unlikely that a single composition path can explain the process for an entire membrane. This is especially so when keeping into account that only dense membranes are entirely homogeneous, and these are not made via phase separation. Membranes obtained via phase separation often present differences in their structure. These differences can range from pore size variations to the presence of dense skins, crystalline regions and/or macrovoids in specific regions of the membrane.

In Figure 4, each picture is linked to a possible composition path that can explain its structure. The processes become slower as we move from I to IV. In case of picture I, the macrovoids are obtained as product of phase separations that proceed fast, skipping the metastable regions and going deep into the spinodal region. If the penetration into the spinodal region is shallower, spinodal decomposition can be obtained. This is shown in Picture II. Picture III shows a membrane obtained purely via nucleation and growth of the polymeric lean phase. In case of Picture IV, the formation of the dense skin can be better explained through solidification processes, following composition path number IV. For the inner structure of the membrane, composition path III seems more applicable.

The effects of kinetics on the system can limit the validity of certain rules of thumb. For instance, Baker indicates that an increased polymer concentration in the casting solution reduces the porosity and permeability of the membrane [1]. This conclusion can be developed from observing a phase diagram. The coagulation of a more highly concentrated polymer solution decreases the proportion of polymer lean phase, causing its nucleation and growth to create smaller and fewer pores. However, it is known that this only works within certain limits [9]. Perhaps, the increased viscosity of the polymer solution has an effect we cannot predict so easily or the composition path changes in a way we are not considering.

4. Phase Separation MicroFabrication (PSµF)

The microstructuring of polymeric films can be advantageous for several applications. The creation of highly hydrophobic surfaces, microfluidic devices, tissue scaffolds, etc., requires the patterning of substrates in the micrometer level. In the case of membranes, topologies can assist in improving the fouling behavior of some systems. For microsieves, the presence of a well defined porosity ensures a more reproducible separation process. To this day, polymers are mainly structured through the casting of curable mixtures or molten polymers onto suitable molds [10]. An alternative is hot embossing, in which a polymeric film is heated and pressed into a mold. These two processes can only be applied to thermoplastics or curable mixtures.

PSµF is a process in which polymer solutions undergo a phase separation process while in contact with a microstructured mold. The polymer solution is cast onto this mold and wets the features in it. Upon phase separation, a membrane with micropattern topology is obtained. This process was developed within our group and presented six years ago by Vogelaar et al. [11].

The process is shown in Figure 5 and different polymeric structures obtained with this method can be seen along this thesis. Vogelaar has shown that the process can be successfully used for manufacturing freestanding microstructures, microsieves, superhydrophobic surfaces and tissue scaffolds [12].

Building on the possibilities presented in Vogelaar's PhD thesis, several applications have been tried. Gironès has thoroughly explored the fabrication of microsieves for filtration purposes, as has Geerken for their use as emulsification devices [13, 14]. De Jong has used the technique for the creation of microfluidic devices with porous walls, allowing the contact of different streams and adding membrane functionality to microfluidics [15]. Papenburg has developed tissue scaffolds made out of biodegradable polymers, structured with this technique [16]. Çulfaz is actively working on the structuring of fibers, as well as on the chemical shrinkage of microsieves for obtaining pore diameters below the micron. The fundamental science related to some of these applications is presented here.

Shrinkage is inherent to phase separation processes. This means that during solidification the polymer can retract from the mold walls. This translates into a low
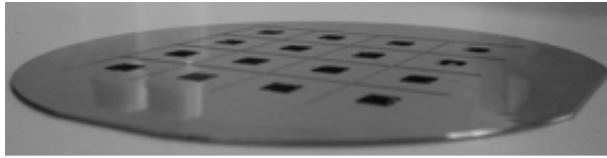
Mold
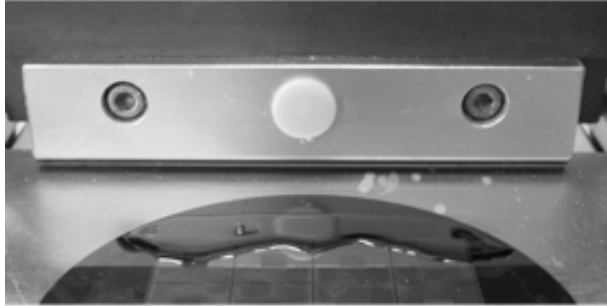
Casting of a Polymer Solution
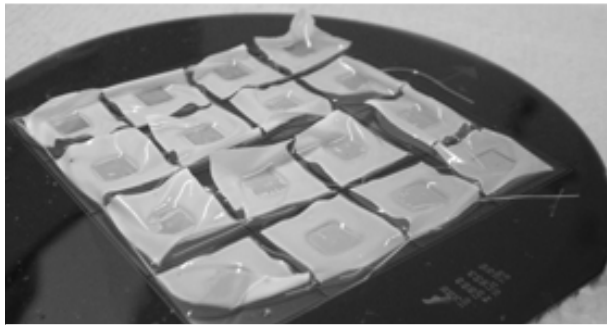
After Phase Separation
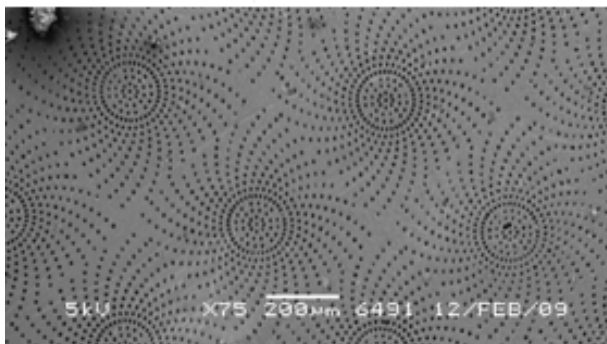
SEM Micrograph

Figure 5: Steps in the preparation of microsieves via PSμF. The solution is cast on a mold and after phase separation, a structured membrane is obtained as seen in the SEM micrograph.

defect rate. On the other hand, as will be shown in Chapter 3, shrinkage might not be desired during molding. The replication of the features in the mold can be affected.

Chapter 4 explores the intricacies of creating a membrane with pillars. This is done by using a mold with wells. However, in these wells air can be entrapped during casting of polymer solution. As a result, pillars are not always obtained, but freestanding structures are often gotten instead. A new device is introduced, used to study the dissolution of gas in the polymer solution. The result is applied to PSµF by casting membranes in a glove box purged with different gases.

Chapter 5 presents a somewhat opposite case: the use of a mold with pillars for the creation of microsieves. The shrinkage is used here to our advantage, achieving perforation of the polymeric film once it becomes thinner than the pillar height. The effects of pillar array and pitch are studied through the measurement of the force required to peel the microsieve off the mold [17].

Chapter 6 introduces the use of flexible and permeable molds made of silicone rubber. These molds bring this technology one step closer to its implementation as a continuous process. Furthermore, the use of permeable molds allows membranes to be structured on both surfaces. A new type of polymeric membrane, a *Sieving Microfence*, is presented.

Conclusions and outlook will be presented on chapter 7, followed by summaries for the general audience and acknowledgments.

5. References

[1] R. W. Baker, Membrane Technology and Applications, McGraw-Hill, (2000)

[2] M. Ulbricht, Advanced functional polymer membranes, Polymer, 7 (2006) 2217

[3] A. M. W. Bulte, M. H. V. Mulder, C. A. Smolders and H. Strathmann, Diffusion induced phase separation with crystallizable nylons. I. Mass transfer processes for nylon 4,6, J. Membr. Sci., 1 (1996) 37

[4] S. P. Nunes and T. Inoue, Evidence for spinodal decomposition and nucleation and growth mechanisms during membrane formation, J. Membr. Sci., 1 (1996) 93

[5] C. A. Smolders, A. J. Reuvers, R. M. Boom and I. M. Wienk, Microstructures in phase-inversion membranes. Part 1. Formation of macrovoids, J. Membr. Sci., 2-3 (1992) 259

[6] K. Kimmerle and H. Strathmann, Analysis of the structure-determining process of phase inversion membranes, Desalination, 2-3 (1990) 283

[7] R. E. Kesting, Four tiers of structure integrally skinned phase inversion membranes and their relevance to the various separation regimes, J. Appl. Polym. Sci., 11-12 (1990) 2739

[8] L. J. Zeman and A. L. Zydney, Microfiltration and Ultrafiltration, Principles and Applications, Marcel Dekker, Inc., (1996)

[9] A. F. Ismail and A. R. Hassan, Formation and characterization of asymmetric nanofiltration membrane: Effect of shear rate and polymer concentration, J. Membr. Sci., 1-2 (2006) 57

[10] Y. Xia and G. M. Whitesides, Soft lithography, Ann. Rev. Mater. Sci., 1 (1998) 153

[11] L. Vogelaar, J. N. Barsema, C. J. M. Van Rijn, W. Nijdam and M. Wessling, Phase Separation Micromolding - PSμM, Adv. Mater., 16 (2003) 1385

[12] L. Vogelaar, Phase Separation Micro Molding, PhD Thesis, Membrane Technology

Group. University of Twente, Enschede, The Netherlands, (2005)

[13] M. Gironès, Inorganic and polymeric microsieves: strategies to reduce fouling., PhD Thesis, Membrane Technology Group. University of Twente, Enschede, The Netherlands, (2005)

[14]   M. J. Geerken, Emulsification with Micro-Engineered Devices, PhD Thesis, Membrane Technology Group. University of Twente, Enschede, The Netherlands, (2006)

[15]   J. De Jong, Application of Membrane Technology in Microfluidic Devices, PhD Thesis, Membrane Technology Group. University of Twente, Enschede, The Netherlands, (2008)

[16]   B. J. Papenburg, Design strategies for tissue engineering scaffolds, PhD Thesis, Membrane Technology Group. University of Twente, Enschede, The Netherlands, (2009)

[17]   J. Garduño Pérez, M. Bikel, P. Z. Çulfaz, R. G. H. Lammertink and M. Wessling, Influence of Design Parameters on Microsieve Production, Master Thesis, Membrane Technology Group. University of Twente, Enschede, The Netherlands, (2009)

Summary

PSµF entails the phase separation of a polymer solution cast onto structured supports. Shrinkage of the solidifying polymer solution influences the replication precision. Through the systematic study of a PES/PVP/NMP/ water system, the relation between polymer concentration and replication performance was assessed. Normal shrinkage (thickness) is found to be dependent on polymer concentration, with pore sizes varying between two limits. Outside these limits, the pore structure does not vary with polymer concentration and shrinkage scales inversely with it. Lateral shrinkage proceeds according to the same mechanism. Yet, its extent is lower. Influence of the mold features on the shrinkage of the replicas and the deformation of the overlying film is explained in terms of feature size and distribution, along with the porosity of the film.

1. Introduction

Several industrial separation processes make use of polymeric membranes. When porous polymeric membranes are needed, phase separation of polymer solutions is the fabrication method of choice. First, a polymer solution is cast on a support. Then, phase separation is induced. A polymer rich-phase and a polymer-lean phase are created. The polymer-rich phase forms the body of the membrane, whereas the polymer-lean phase will form the porosity inside the membrane. The morphology of the membrane depends strongly on the conditions under which the phase separation is carried out [1-3].

Efforts have been made to understand the effect of many variables (including affinity between solvent and non-solvent, addition of polymeric additives to the polymer solution, variations in the composition of both polymer solution and coagulation bath, etc.) on the morphology of the final membrane [4-8]. In 1990, Kesting published an article entitled "The Four Tiers of Structure in Integrally Skinned Phase Inversion Membranes and Their Relevance to the Various Separation Regimes" [9]. In this article, four main structures or tiers were identified as contributing to the morphology of a membrane obtained via phase separation. The final dimensions of a membrane should change according to the governing mechanism for polymer precipitation. In other words, the extent of the shrinkage that usually accompanies the phase separation process will be regulated by the conditions that favor a certain "tier".

Phase separation microfabrication is a process in which the polymer solution is cast onto a structured template [10, 11]. The polymer solutions wet the feature in the mold. Upon solidification, the features on the support are replicated. This method enables defect-free processing of polymers, without some of the limitations of traditional microfabrication methods, e.g. hot embossing. Not only melt-processable polymers can be patterned, but all polymers for which a suitable pair of solvent and non-solvent can be found. Porous microstructures can prove convenient for tissue engineering [12], food applications [13], microfluidic devices [14], etc. Figure 1 depicts the process and shows the cross section of a typical poly (ethersulfone) membrane with a line pattern obtained with this method.

Shrinkage is inherent to the process of phase separation of polymer solutions. When a membrane is formed by means of precipitation from a polymer solution, the

1. Polymer solution casting

2. Liquid induced phase separation

3. Release
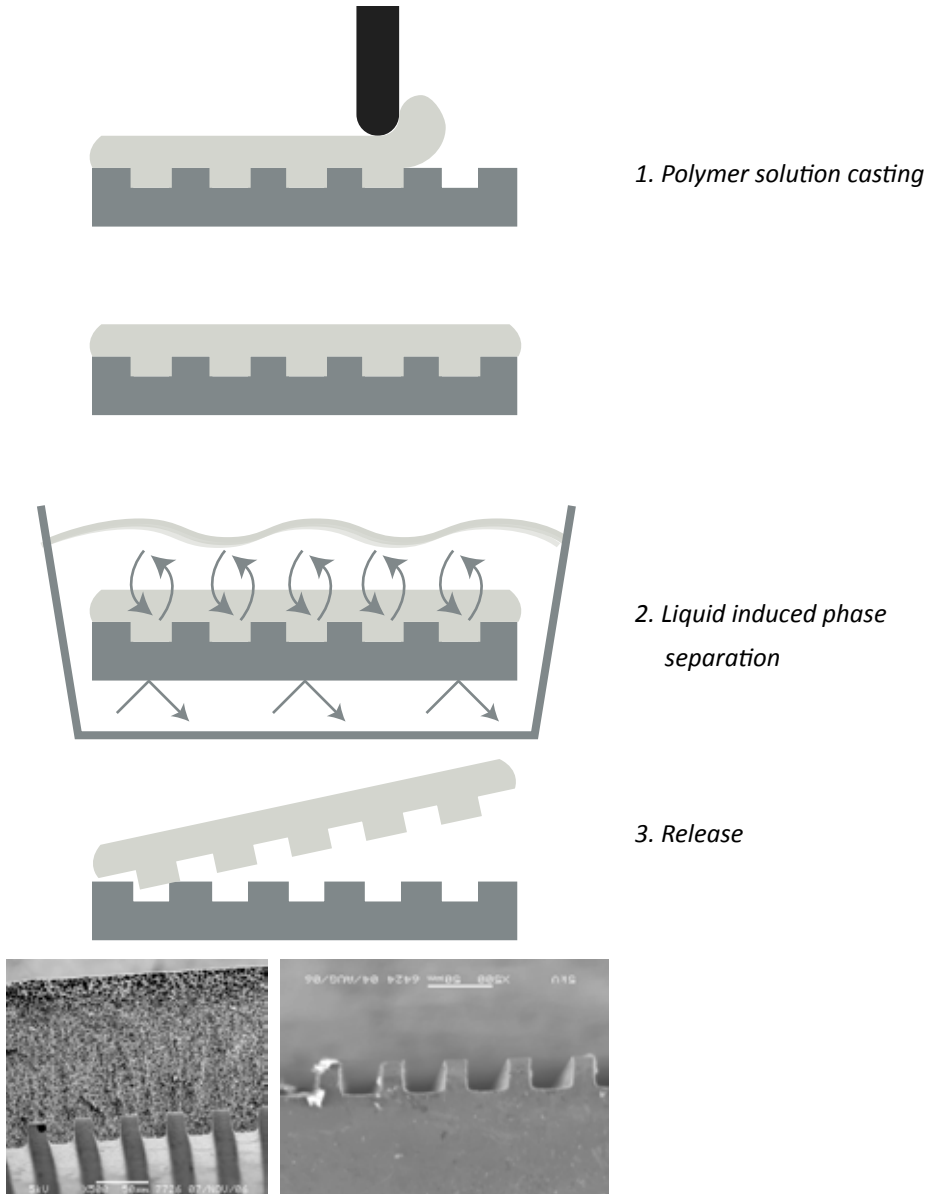
Figure 1: Schematics of the PSµF process and SEM micrographs of a structured membrane and the corresponding mold.

dimensions of this membrane are smaller than those of the cast solution. We have recently demonstrated that this mechanism allows the perforation of polymer films, creating polymeric microsieves [13]. Vankelecom and co-workers have showed that the shrinkage is related to the chemical nature of the substrate [15]. Stropnik et al. have measured shrinkage in a few membrane forming systems [16]. Their focus was on using shrinkage as evidence for their proposed mechanisms for membrane formation. Extent,

nature, and kinetics of the shrinkage have not been the object of a thorough scientific investigation yet. This is the reason why there is a need to understand the shrinkage phenomenon and its dependence on the different parameters governing a given phase separation process. These can include the composition of the polymer solution and/or the coagulation bath, temperature, used additives, structures on molds, etc.

During the preparation of polymeric membranes for emulsification, Geerken et al. noticed interesting effects of shrinkage [17]. The mold in use consisted of fields with pillars, separated by a deeper grid. For a casting solution containing poly (ethersulfone)/ poly (vinylpyrrolidone)/sulfonated poly (ether ether ketone)/N-methylpyrrolidone and a two-step coagulation bath (see Experimental section), they observed that the lateral shrinkage was directed towards the center of each field (Figure 2).

The aim of this chapter is to present a systematic study with respect to lateral and normal shrinkage with a system comprising a polymer, a solvent, a non-solvent and an additive utilizing a structured substrate. Effects of polymer solution and coagulation bath compositions, mold features and casting thickness have been investigated.
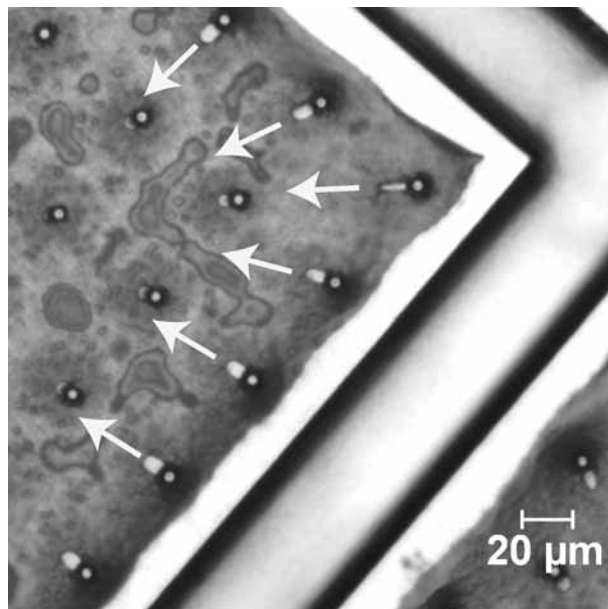

Figure 2: Shrinkage directed towards the center of each field of an emulsification membrane [17].

2. Experimental

2.1 Materials and Solution Preparation

The polymer used in these experiments was poly (ethersulfone) (PES, Ultrason, E6020P). The additive for the polymer solutions was poly (vinylpyrrolidone) (PVP K30, Fluka), commonly used to create a percolating porosity and a hydrophilic surface [18]. It also acts as a macrovoid formation inhibitor [1]. N-methylpyrrolidone (NMP, 99%, Acros Organics) was used as solvent. Tap water was used as non-solvent. All reagents were used as received, without further purification. Unless otherwise specified, solutions were prepared by weighing all the components into a plastic bottle and left on a rolling bank until complete dissolution.

Solutions were made with a constant PVP concentration of 5.0 wt.% and polymer concentrations of 12.00, 12.75, 13.50, 15.00, 16.50, 17.25 and 18.00 wt.%. In addition, another set of solutions was made with constant polymer concentration (15.00 wt.%) and additive concentrations of 4.0, 4.5, 5.0, 5.5 and 6.0 wt.%.

2.2 Casting

Solutions were cast on silicon wafers using a custom-made doctor blade with micrometric screws to regulate the casting thickness.   The silicon wafers were microstructured through standard photolithographic methods combined with deep reactive ion etching (DRIE) in clean-room facilities. Three molds are used in these experiments:

- Mold I: containing a line pattern with a width of 20 µm and a depth of 20 µm and a spacing of 30 µm.

- Mold II: with lines of 50 µm width, 100 µm depth and spacing of 500 µm.

- Mold III: with scarce, small features of different sizes and a depth of 25 µm.

The 15.0 wt.% solution was cast at 15 different thicknesses (every 10 µm between 50 and 150 µm; from then on, every 25 µm until 250 µm) and in all cases spongy, macrovoid free structures with uniform pore size along the cross-section were observed.

Therefore, the other solutions were cast at fewer thicknesses (50, 100, 200 and 250 μm) and considered representative when pore size uniformity was observed.

2.3 Phase Separation

After casting, the solution together with the microstructured wafer was immersed in a first coagulation bath consisting of 75 vol% NMP and 25 vol% water. The solutions became turbid and the polymer precipitated. In some cases the membrane lifted off after some time in this bath, indicating completion of the phase separation. When this was not the case, after 1 or 2 minutes, when the white color was uniform over the whole surface, the support holding the membrane was moved into a water bath. After several minutes, the membrane lifted from the wafer. In all cases, membranes were rinsed further with water.

In some cases, the coagulation was carried out by letting the polymer solution stand in an atmosphere with a very high relative humidity. This was achieved by purging a vessel with nitrogen at 40°C, saturated with water vapor. This vapor stream was created through bubbling of nitrogen in a water bottle at 60°C. Afterwards, the stream was cooled to 40°C. In this way, the phase separation has been initiated by vapor uptake for times varying between 10 and 60 minutes. To finalize the phase separation, the membrane was then immersed in water.

2.4 Porosity Measurements

The porosity of the membranes has been calculated as the ratio of pore volume to sample volume. The sample volume was obtained by measuring the sample with a ruler and a thickness meter (Mitutoyo). The volume of the pores was obtained by subtracting the volume of polymer from the volume of the sample. The volume of the polymer was measured with a pycnometer (Micrometrics, Accupyc 1330). The method compares the volume of a cup to the volume of the same cup containing the sample to be tested. Helium displacement is used to measure the volumes. Given the structures of the membranes, it is assumed that helium infiltrates the entire sample. The measurements were performed in duplo.

2.5 Membrane Treatment and Inspection

Membranes were rinsed with water overnight and treated afterwards with sodium hypochlorite (aqueous solution from Fluka) for 48 hours, to remove the remaining PVP. Membranes were broken in liquid nitrogen when needed for cross-section pictures. Prior to SEM inspection (Jeol JSM 5600LV), the membranes were dried overnight under vacuum at 30°C and then sputtered with gold (Balzers Union SCD040).

3. Results and Discussion

During the phase separation process, exchange of solvent and non-solvent takes place between the polymer solution film and the coagulation bath. Both normal and lateral shrinkage occur.

Replication from three molds has been investigated to assess the influence of the microstructure on the final product. Membranes were fabricated from solutions with different polymer concentrations, different additive concentrations, and using different coagulation baths. Variations in shrinkage were observed that could indicate the dependence of the porosity and replication fidelity on these variables.

3.1 Normal Shrinkage of the Overlying Film

When casting a polymer solution, we normally measure the casting thickness from the unstructured parts of the molds. Using this plane as reference, we classify features as *positive* if they are higher than this plane and as *negative* if they are deeper than this plane.

Microstructured supports consist of local height differences that create the pattern to be replicated. In some systems macrovoids appear when the polymer solution is cast thicker than a certain critical casting thickness [19]. For a microstructured support this can result in locations populated by macrovoids while others are free of macrovoids. Figure 3 shows that when pure water was the coagulation bath, the presence of macrovoids was higher inside the features (thicker parts) than it was between the features.
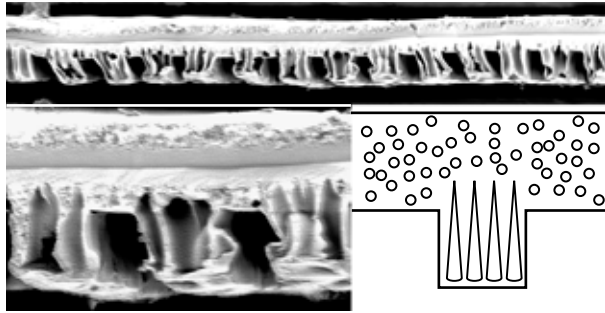
Figure 3: Macrovoid concentration inside the features.

To investigate the effect of preparation variables on the shrinkage process, it is desired to have a morphology which is independent of thickness. Adding solvent to the coagulation bath is one of the many ways to suppress macrovoid formation and it is known to work for this system [20]. No macrovoids were obtained when the NMP concentration in the coagulation bath was 75% or higher. A well defined porous structure was obtained with no noticeable pore size gradient across the thickness of the membrane.

The membranes obtained with the above mentioned coagulation bath were not fully solidified. To extract the remains of NMP in the film, a second coagulation bath with only water was used. In this way, macrovoids were avoided and fully solidified NMP-free membranes were obtained, a typical example of which can be seen in Figure 1. Variations in PVP concentration (between 4.0 wt.% and 6.0 wt.%, with 0.5 wt.% increments) had no detectable effect on the extent of shrinkage.

It is widely accepted that membranes shrink during coagulation. This can be expected if we consider the volume of polymer compared to the volume of the solution. PES has a density of about 1.4 g/mL, whereas the density of NMP is 1.03 g/mL. If we prepare 100 g of a 20 wt.% PES solution in NMP, we are mixing 14.3 mL (20 g) of PES with 77.7 mL (80 g) of NMP. Even if we consider that PES does not add volume to the solution (which is not true), the phase separation of 77.7 mL of polymer solution will only give 14.3 mL of PES. This volume is twice as big if we consider a porosity of 50%. Therefore, only roughly 30 mL of the original 77.7 mL will be occupied after phase separation. This means about 60% of shrinkage. The polymer precipitation begins in the first coagulation bath, but it is finished in the pure water. This is known because upon completion of the phase separation process, the membrane lifts off the mold on its own. Therefore, it is understood that shrinkage takes place in both baths. Unfortunately, the increased

flexibility of the membranes coagulated in the first bath only makes it complicated to measure the partial extent of the shrinkage.

The extent of shrinkage is also strongly influenced by the ratio between non-solvent in-flux and solvent out-flux from the polymer solution during coagulation [16]. Hypothetically, if we make a membrane with complete solvent removal (as can be done with evaporation of solvents) the final membrane will have a non-porous dense structure with minimum thickness. On the other extreme, if a membrane is formed just by non-solvent in-flux and without solvent extraction, it will be the thickest membrane possible for this system. We verified this by using a two-step coagulation method using VIPS followed by LIPS, for a solution containing 15 wt.% of PES. It has been noticed that if the solution is subjected to VIPS for 10 minutes and then to LIPS, shrinkage amounts to 60%. On the other hand, when VIPS is performed for 60 minutes prior to the LIPS step, the shrinkage amounts to 40%. Given the low evaporation rate of NMP, it is clear that the latter case is close to the hypothetical membrane obtained only through nonsolvent influx, the thickest possible membrane for this system.

The concentration of polymer also influences the final thickness of a membrane, as it affects the transport properties (diffusion rates of all components) within the polymer solution. To investigate this, solutions were prepared by using PES concentrations of 12.00, 12.75, 13.50, 15.00, 16.50, 17.25, and 18.00 wt.%. For each concentration, we have cast the polymer solution at different thicknesses. In an attempt to find the mean relative shrinkage for each concentration, the thickness of all films above the features has been measured via cross-sectional SEM. By means of linear regression fittings (r^2 was higher than 0.95 in all cases), the mean final thickness above features to casting thickness ratio (R) was obtained. A typical result is shown in Figure 4 for a concentration of 15 wt.% of polyethersulfone. The porosity of all the membranes was also measured. The results are summarized in Figure 5. R relates to the shrinkage as follows:

$$R(c) = \frac{d_{end}}{d_{cast}} = \frac{d_{cast} - d_{shrinkage}}{d_{cast}} = 1 - S(c)$$

where d_{end} is the final thickness of the overlying film, d_{cast} is the casting thickness, $d_{shrinkage}$ is the shrunk distance and S(c) is the relative shrinkage.

For the range of casting thicknesses studied here, the pore size was uniform across the cross-section and independent of the casting thickness. It has been
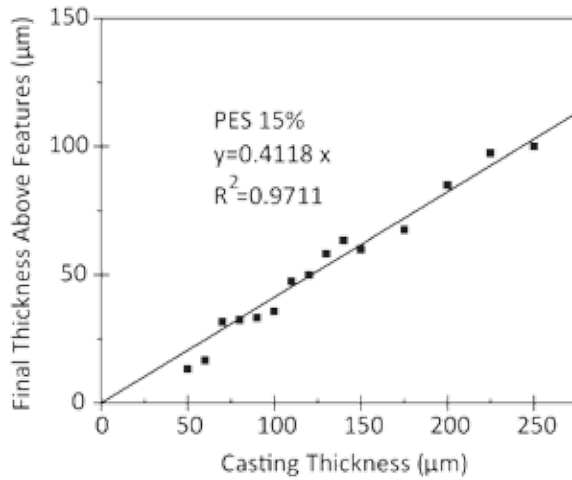
Figure 4: Linear regression for the calculation of R for a solution containing 15 wt% of PES.
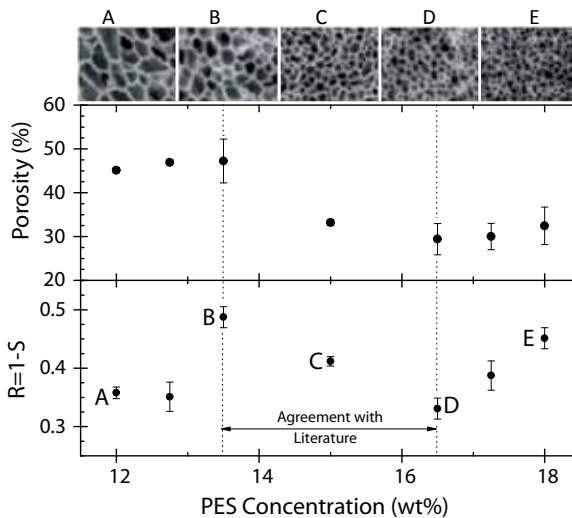
Figure 5: Variation of R and porosity with polymer concentration.

indicated in literature that a higher concentration of polymer in the casting solution leads to a membrane with smaller pore sizes. Figure 5 shows that for the polymer concentrations of 13.50, 15.00 and 16.50 wt.% this commonly assumed trend is indeed valid. An increase in polymer concentration in the solution led to lower pore sizes and thinner membranes. A thinner membrane is the effect of higher shrinkage. For these three points, a significant decrease in porosity was measured. A lower fraction of air in the sample correlates with a higher compaction, leading to increased shrinkage. The

shrinkage was between 50% and 70% in all cases which is in the order of the values previously reported by Stropnik et al. for other polymeric systems [16].

The relative decreases in porosity and shrinkage are 38% and 33% respectively, from B to D. These two values are in good agreement. Comparing B and C, the decrease in porosity (30%) and the decrease in shrinkage (16%) do not match. These values are not expected to match as different polymer concentrations can give different skin thicknesses, affecting the average porosity of the membrane. Moreover, the loss of polymeric material (both PES and PVP) during phase separation can be affected by increased viscosities. From this point of view, the similarity in values between points B and D is regarded as coincidental. However, the trend is similar for both variables. The decrease in porosity can be used to partially explain the increase in shrinkage.

Above a certain concentration the pores do not get smaller with increasing polymer concentration. This has been previously reported for the phase separation of polysulfone solutions [21]. Beyond this limit, the thickness will increase with increasing concentration at constant porosity, as can be seen in Figure 5 D and E, comparing the 16.5 and 18.0 wt.% solutions. For concentrations below 13.5 wt.%, the pores cannot get larger and the thickness decreases keeping the porosity constant. With extremely low concentrations, no continuous film is obtained after phase separation, but only loose polymer particles are formed.

The experiments mentioned so far have been realized by casting the polymer solutions on a mold which consisted of lines with a width of 20 µm and a depth of 20 µm and a spacing of 30 µm (Mold I, Figure 6). Figure 6 shows different types of shrinkage phenomena observed for various geometries and casting thicknesses, e.g. the shrinkage of the film above the replicas, of the replicas themselves and of the film around the replicas.

A mold with lines of 50 µm width, 100 µm depth and spaced 500 µm was then tried (Mold II; consider sketch in Figure 6C as opposed to Figure 6A for Mold I). At small casting thicknesses the mass of polymer solution inside the feature is larger than the mass of the solution lying directly on top of it. At a constant relative shrinkage, the absolute shrinkage inside the feature is more extensive than that of the overlying film. The increased depth of the features and the larger distance between them causes the upper film to deform, which is especially noticeable on the air side. The local thinning
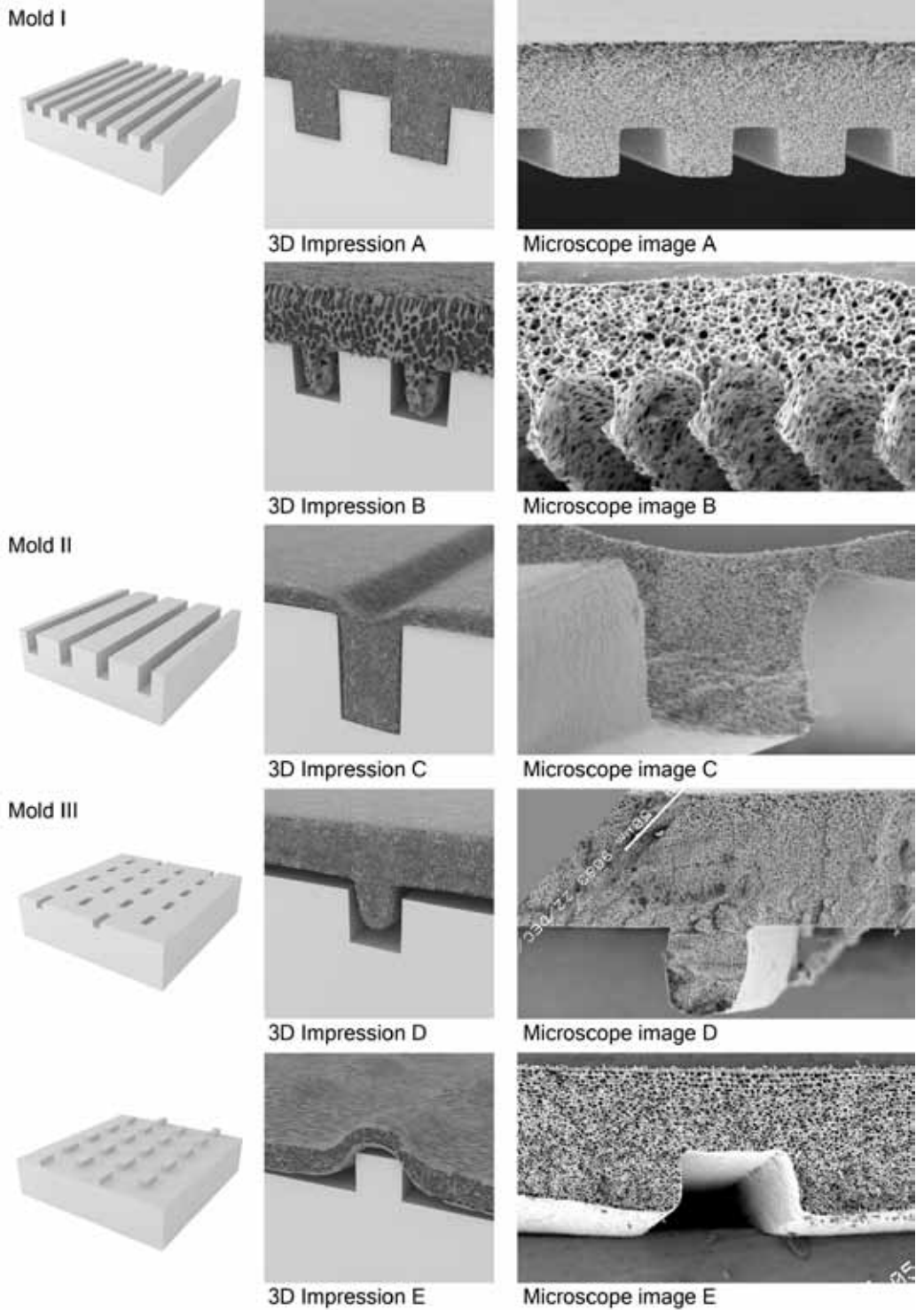
Figure 6: Mold schematics, along with 3D impressions and SEM images observed shrinkage phenomena. (Illustrations by Jonathan Bennink)

of the film is shown in Figure 6C and will be discussed in section 3.3. When the polymer solution was cast at higher thicknesses, this deformation was not observed anymore. Thicker films are stronger and can resist the shrinkage forces.

Because of the local thinning and the different resistance of the films, the final thickness cannot be fitted to a constant ratio. This shows that the shrinkage is also dependent on the amount, geometry and depth of features.

3.2 Lateral Shrinkage of the Overlying Film

The polymer solution film also shrinks in the direction parallel to the support [15]. The mechanisms for normal and lateral shrinkages have the same origin. However, their effects on the final dimensions of the micro-structured membrane are different. This can be theoretically explained considering the accumulation of the effects when considering that the solution consists of liquid layers parallel to the substrate. These layers solidify one by one, as the solidification front propagates, and each of them meets different conditions for phase separation.

The solidified polymer is pulled along during the shrinkage of the layer that is in contact with it. This lessens the shrinkage on the subsequent layers. This can lead to membranes curving upwards [22] and to distorted replication. As the coagulation front propagates down the liquid film, local compositions change continuously. As has been shown before, shrinkage depends on the compositions of both the polymer solution and the coagulation bath. The differences in solvent and nonsolvent fluxes affect directly the composition path of each volume element of the membrane. Therefore, the extent of shrinkage is different for each layer of solution.

When the phase separation occurs solely due to in-flux of non-solvent through the top of the film, the result is that the layer on the mold side shrinks less than the layer on the coagulation bath side. This is the reason why we can create asymmetric membranes: the first few layers shrink enough to make a dense skin while the following layers shrink less and give a porous support. In the cases where the non-solvent can enter the region between the polymer solution and the mold, it can also diffuse from the bottom of the film (see section 3.3). There the bottom layer shrinks to a similar extent as the top layer and the membrane has a closed skin on both surfaces.

Mold I consists of long, densely packed lines. The position and size of the replicas on the polymeric film was always in close agreement with those of the channels on the mold. When the features are smaller or not so close to one another, the position of the replicas on the membrane (used as markers for the shrinkage of the film) does not match the position of the features on the mold. This difference is dependent on the distance between the features in the mold [10] and is in the order of 10%. Conversely, the normal shrinkage amounts to 60% for these systems with all molds. These values agree well with previously reported ones for polymeric systems [15].

The effects of lateral shrinkage must be viewed in terms of relative and absolute shrinkage. Whereas relative shrinkage can be expected to be uniform for a given layer, the absolute shrinkage will depend on the actual distance between the features on the mold. As longer distances without features correlate to longer regions of polymer in the membrane, the shrinkage of these regions will produce higher forces. This means that the deformation of features depends strongly on the distance between features. Vogelaar et al. have proved that this is the case [10]. They have used a mold consisting of columns with positive lines out of the surface of the mold. The size of all lines was the same and on each column, the distance between the lines was doubled. The size of the indentations on the membranes scales linearly with the distance between the features. Extrapolation to a spacing of 0 microns leads to the original size of the features (Figure 7).

A special design requirement to consider is the replication of isolated positive features. In this case, the film thickness will not be uniform because even when the normal relative shrinkage is constant, the absolute one is not (Figure 6E). This can produce bumps on top of the features, at the air side. Also, as the lateral shrinkage is often not uniform along the thickness, the replicas become increasingly deformed [14]. Both of these phenomena can be overcome with the use of sacrificial features whose function is not needed on the final product. These features act as anchors and help hinder shrinkage in the lateral direction near the mold surface. Another way to overcome these bumps is through increasing the thickness of the film. At some point, the differences in actual casting thickness (the one due to casting on the unstructured part of the wafer vs. the one due to casting on a feature) will become negligible. However, this can be at the expense of having a membrane too thick for proper operation.
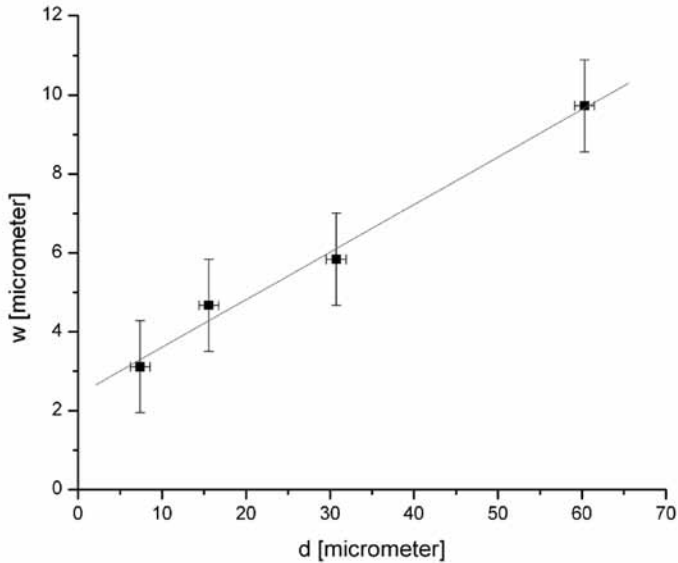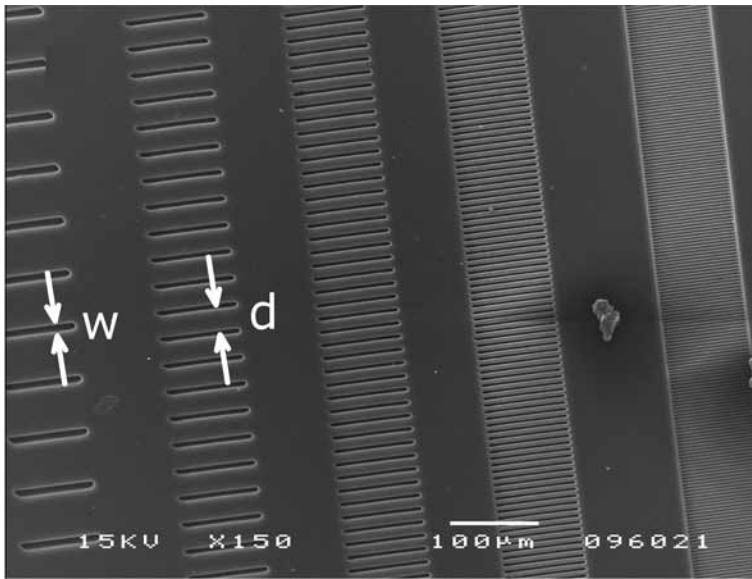
Figure 7: Distortion of features as a function of distance between them [10].
Copyright Wiley-VCH Verlag GmbH & Co.KGaA. Reproduced with permission.

3.3 Effect of Feature Geometry on Replication

Features can be classified according to their size, packing density and whether they are negative or positive. All these parameters have an effect on the quality of the replicated structures.
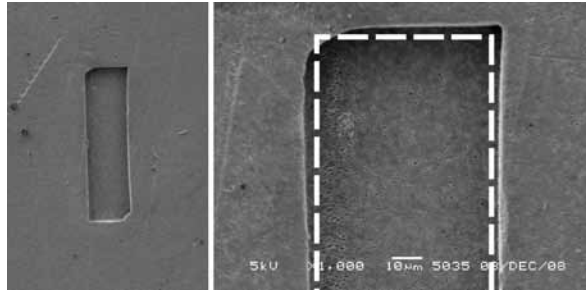
Figure 8: Distortion of an indentation on a membrane. The replica is bigger than the feature on the mold, indicated by the dashed line.

Figure 8 shows that the indentations on a membrane, which are the product of positive mold features, are slightly bigger than said features. The cause of this deformation is the lateral shrinkage of the polymer solution lying in between the features (Figure 6E). This phenomenon can be extensive when the features are far spaced, as a few percent relative shrinkage will result in a significant absolute shrinkage. On the other hand, the replicas of negative mold features can turn out to be smaller than the features in the mold. In this case, the replica itself shrinks to the same percentage (Figure 6D). The features are small and their absolute shrinkage is less noticeable but still present. No measurable shrinkage was observed for the molds with lines discussed here (Figure 6 A and C).

A shrinking polymer solution creates space between the solidified polymer and the mold. For these types of distortion to happen, these voids must be filled. In some cases the non-solvent can reach these spots only by means of transport through the membrane (Figure 6 A, B and C). In other cases, the nonsolvent can flow in between the formed membrane and the wafer (Figure 6 D and E). If it accesses this space from the sides, not only will the features shrink, but also the shrinkage of the lowest layer of the overlying film will be larger. This has been observed when comparing the lateral shrinkage of membranes cast on a mold with lines to those cast on a mold with isolated features (Mold III, Figure 6 D and E). The membrane with lines (Figure 6 A, B and C) displays no lateral shrinkage, whereas for that in Figure 6 D and E the lateral shrinkage amounts to roughly 10%. This is also evident by comparing the coagulation time. For membranes prepared with Mold III the coagulation is finalized in around half a minute in the first bath. For the molds with continuous lines, the coagulation time is well above 3 minutes and it is only finished after immersion in the water bath.

The accessibility of this space is a direct function of the amount, type and packing density of features. As the solution contained in the features begins to solidify, it tries to shrink. This phenomenon exerts a force on the overlying film, pulling it tighter against the mold with increasing feature volume. If the features do shrink away from the walls of the mold, they create cavities or voids in doing so. These voids cannot remain empty, as this would create a vacuum between the polymer and the mold. For cases A and C (Figure 6), the water that should fill the voids can only come by means of transport through the film or along the lines and cannot access the space between the film and the mold. As mentioned in section 3.1, the size of the features in the membranes with the continuous line pattern is always in perfect agreement with those of the structures on the mold, i.e. there is no retraction of the polymer from the feature walls. This indicates that the water transported through the membrane is limited which could be due to poorly interconnected pores or due to a dense skin. In fact, when the same mold was used with a recipe tuned for highly porous membranes the shrinkage of even this type of features is very noticeable [12] (Figure 6B). In this case, the voids created through shrinkage are filled with water that percolates through the membrane.

Replicas are also deformed when using vapor induced phase separation. Figure 9A shows the results from coagulating the 15.00 wt.% PES solution in NMP with Mold I following the LIPS method mentioned before. Figure 9B shows the membrane obtained by coagulating the same solution on the same mold via VIPS. In this case, the polymer solution was allowed to stand in nitrogen saturated with water vapor. In this case shrinkage is expected to be lower, as there is hardly any solvent out-flow. Furthermore, the phase separation process is expected to be faster, because the top layer of the polymer solution is mainly water, whereas in the first step of the coagulation bath it is 75% NMP. Because of this, features are not expected to shrink too much in width. However, coagulation in vapor yields more open structures and not so dense skins, allowing for fast non-solvent transport through the membrane into the voids. This
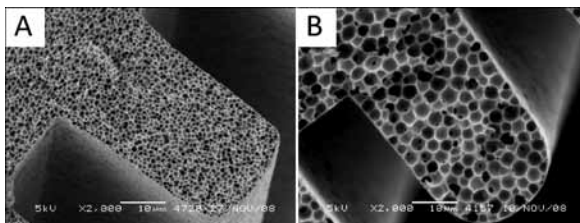

Figure 9: Distortion of replicas is not observed for LIPS (A). The replica
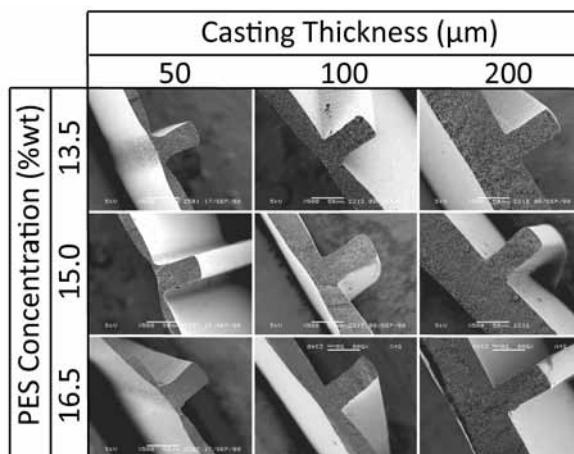*presents rounded corners when VIPS is used (B).*

Figure 10: Distortion due to pulling from deep features. Effect of polymer concentration and casting thickness.

causes the feature to have rounded corners (Figure 9B).

The shortage of non-solvent close to the features prevents the retraction of the polymer from the mold walls during the process. This produces a membrane on which the replicas agree in dimensions with the features in the mold. However, shrinkage always takes place during phase separation. If the features are deep enough the forces exerted due to shrinkage result in the deformation of the film on top of the features. This is the explanation for the phenomenon observed on Mold II (Figure 6C). Local film thinning is countered by film thickness: a thicker film is stronger and can better resist these forces. On the other hand, a variation in polymer concentration does not introduce major changes in the extent of thinning of the film (Figure 10). This thinning is the result of pulling the solid film into a solidifying replica on top of the shrinkage of the film itself.

A thick enough film will not be deformed because of these forces. However, these forces are still present and they stretch the pores where the membrane and the features meet (in the corners). Figure 11 in page 40 illustrates this phenomenon. These deformation can be drastic enough to create a tear between thicker and thinner parts of the membrane (see the tear between the beam and the pillar field in Figure 2). If said forces are not strong enough to keep the film tightly attached to the mold, the water transport in the space between the film and the mold becomes significant, increasing the shrinkage of both the features and the lowest layer of the polymer solution.
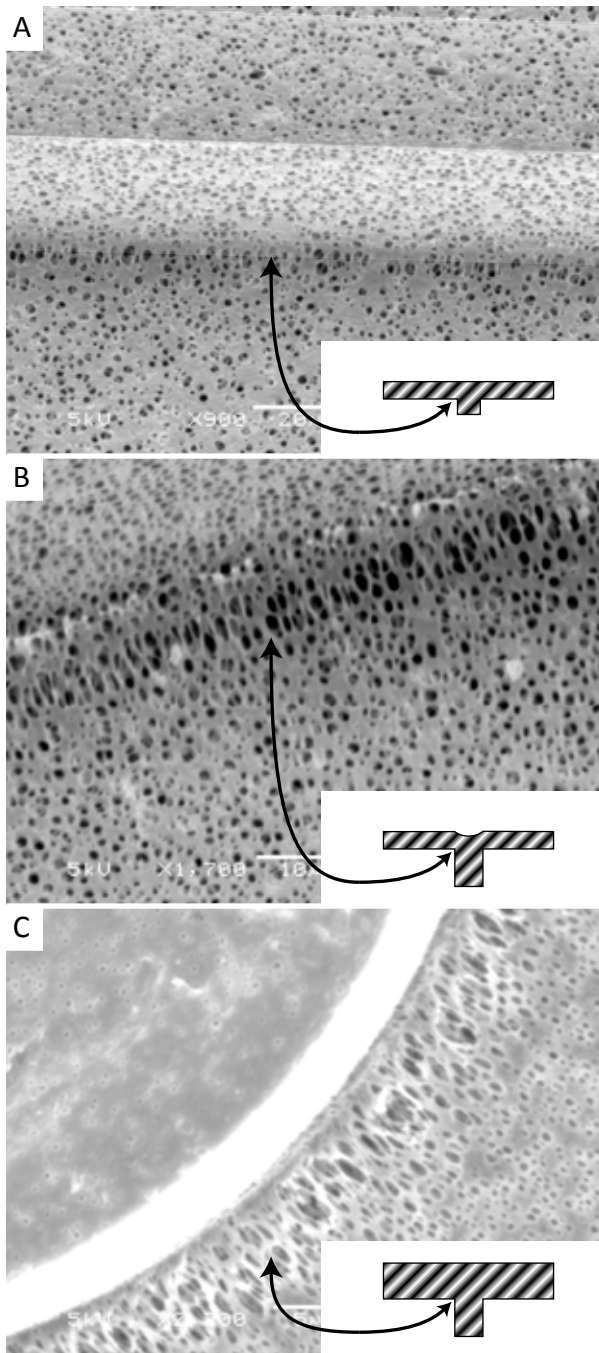
Figure 11: Balance between film thinning and pore stretching in the corners where features and films meet.

4. Conclusions

Membranes from several solutions with different concentrations of PES and PVP K30 in NMP have been prepared using three molds. The concentration of PVP seemed to be of little effect on the coagulation time and the final structure. The concentration of polymer strongly affected the porosity of the final product. With increasing PES concentrations, higher compaction levels were observed, indicated by denser and thinner membranes, for constant casting thicknesses. This variation occurred within two limits given mainly by the minimum and maximum achievable pore sizes. Outside of this range the final thickness varied in the same direction as the polymer concentration, for a constant casting thickness. The porosity of the membranes was found to follow the same trend but not to a similar extent in all cases. Therefore, changes in porosity can only partially explain the differences in shrinkage.

In the case of thickness shrinkage, each layer contributes to the total shrinkage. However, in lateral shrinkage each layer shrinks over the remaining polymer solution and in contact with the solidified layers on top. Hence, lateral shrinkage is somewhat hindered by the layers that already solidified, causing tensions on these layers. As a result, lateral shrinkage was as small as one-sixth of the normal one.

When the area occupied by the features (directly related to the amount of features, their size, and type) is low, there is little force pulling the film on top during coagulation. As a result, the non-solvent in the coagulation bath can easily access the space between the film and the mold. This is also the case when the formed membrane is skinless and extremely porous. In either case, the access of non-solvent between membrane and mold allowed for polymer retraction from the mold and inaccurate replication.

When there was not enough liquid to fill the emerging void, the features on the membrane corresponded in position with those on the mold and no evident feature shrinkage was noticed. This fact was accompanied by pulling forces on the film. When the film was not thick enough or the features on the mold were too deep, local thinning of the film above the features was observed. When the film was too thick, this pulling force was countered and local stretching on the pores near the feature corners was observed.

5. Acknowledgements

6. References

[1] R. M. Boom, I. M. Wienk, T. Van Den Boomgaard and C. A. Smolders, Microstructures in phase inversion membranes. Part 2. The role of a polymeric additive, J. Membr. Sci., 2-3 (1992) 277

[2] K. Kimmerle and H. Strathmann, Analysis of the structure-determining process of phase inversion membranes, Desalination, 2-3 (1990) 283

[3] P. Van De Witte, P. J. Dijkstra, J. W. A. Van Den Berg and J. Feijen, Phase separation processes in polymer solutions in relation to membrane formation, J. Membr. Sci., 1-2 (1996) 1

[4] A. M. W. Bulte, M. H. V. Mulder, C. A. Smolders and H. Strathmann, Diffusion induced phase separation with crystallizable nylons. I. Mass transfer processes for nylon 4,6, J. Membr. Sci., 1 (1996) 37

[5] A. M. W. Bulte, M. H. V. Mulder, C. A. Smolders and H. Strathmann, Diffusion induced phase separation with crystallizable nylons. II. Relation to final membrane morphology, J. Membr. Sci., 1 (1996) 51

[6] J. H. Kim, B. R. Min, J. Won, H. C. Park and Y. S. Kang, Phase behavior and mechanism of membrane formation for polyimide/DMSO/water system, J. Membr. Sci., 1-2 (2001) 47

[7] P. S. T. Machado, A. C. Habert and C. P. Borges, Membrane formation mechanism based on precipitation kinetics and membrane morphology: flat and hollow fiber polysulfone membranes, J. Membr. Sci., 2 (1999) 171

[8] T. H. Young, L. P. Cheng, D. J. Lin, L. Fane and W. Y. Chuang, Mechanisms of PVDF membrane formation by immersion-precipitation in soft (1-octanol) and harsh (water)

nonsolvents, Polymer, 19 (1999) 5315

[9] R. E. Kesting, Four tiers of structure integrally skinned phase inversion membranes and their relevance to the various separation regimes, J. Appl. Polym. Sci., 11-12 (1990) 2739

[10] L. Vogelaar, R. G. H. Lammertink, J. N. Barsema, W. Nijdam, L. A. M. Bolhuis-Versteeg, C. J. M. Van Rijn and M. Wessling, Phase separation micromolding: A new generic approach for microstructuring various materials, Small, 6 (2005) 645

[11] L. Vogelaar, J. N. Barsema, C. J. M. Van Rijn, W. Nijdam and M. Wessling, Phase Separation Micromolding - PSµM, Adv. Mater., 16 (2003) 1385

[12] B. J. Papenburg, L. Vogelaar, L. A. M. Bolhuis-Versteeg, R. G. H. Lammertink, D. Stamatialis and M. Wessling, One-step fabrication of porous micropatterned scaffolds to control cell behavior, Biomaterials, 11 (2007) 1998

[13] M. Gironès i Nogué, I. J. Akbarsyah, W. Nijdam, C. J. M. van Rijn, H. V. Jansen, R. G. H. Lammertink and M. Wessling, Polymeric microsieves produced by phase separation micromolding, J. Membr. Sci., 1-2 (2006) 411

[14] J. De Jong, B. Ankone, R. G. H. Lammertink and M. Wessling, New replication technique for the fabrication of thin polymeric microfluidic devices with tunable porosity, Lab on a Chip - Miniaturisation for Chemistry and Biology, 11 (2005) 1240

[15] P. Aerts, I. Genne, R. Leysen, P. A. Jacobs and I. F. J. Vankelecom, The role of the nature of the casting substrate on the properties of membranes prepared via immersion precipitation, J. Membr. Sci., 1-2 (2006) 320

[16] C. Stropnik, V. Musil and M. Brumen, Polymeric membrane formation by wet-phase separation; turbidity and shrinkage phenomena as evidence for the elementary processes, Polymer, 26 (2000) 9227

[17] M. J. Geerken, Emulsification with Micro-Engineered Devices, PhD Thesis, University of Twente, Enschede, Netherlands, 2006

[18]   I. Cabasso, E. Klein, J.K. Smith, Polysulphone hollow fibres. II. Morphology. J. Appl. Polym. Sci., 21 (1977) 165

[19] N. Vogrin, C. Stropnik, V. Musil and M. Brumen, The wet phase separation: the effect of cast solution thickness on the appearance of macrovoids in the membrane forming, J. Membr. Sci., 1 (2002) 139

[20]   R. M. Boom, T. Van Den Boomgaard and C. A. Smolders, Mass transfer and thermodynamics during immersion precipitation for a two-polymer system. Evaluation with the system PES-PVP-NMP-water, J. Membr. Sci., 3 (1994) 231

[21]   A. F. Ismail and A. R. Hassan, Formation and characterization of asymmetric nanofiltration membrane: Effect of shear rate and polymer concentration, J. Membr. Sci., 1-2 (2006) 57

[22] C. Stropnik, V. Kaiser, V. Musil and M. Brumen, Wet-phase-separation membranes from the polysulfone/ N,N-dimethylacetamide/ water ternary system: The formation and elements of their structure and properties, J. Appl. Polym. Sci., 5 (2005) 1667

Summary

I f the mold in use has a relief pattern of polygonal holes, freestanding microstructures can be fabricated in a single step. The microstructures are the result of air entrapment inside the holes while the corners and bottom of the well are filled with polymer. The mechanism responsible for the eventual filling of the holes relies on the dissolution of the entrapped air in the polymer solution and is faster for higher pressures and lower viscosities of the polymer solutions. Furthermore, casting membranes in atmospheres of other gases causes the speed of dissolution of the formed bubbles to change. CO_2 was found to dissolve much faster than N_2 or O_2.

1. Introduction

A special challenge for PSµF is the creation of polymeric pillars. For achieving this, the polymer solution must be cast onto a mold with wells. Due to the high viscosities of polymer solutions, such a well is covered before it is filled in its entirety. This causes the entrapment of a gas bubble inside the well. This bubble hinders the replication of the pillar.

Bubbles confined in microchannels are the object of much research [1], especially nowadays as miniaturization is a leading trend in engineering. Shape and behavior of bubbles in static and dynamic systems is important for applications relying on segmented flows. For example, the use of bubbles is highly desired in a catalyzed gas-liquid microreactor with a catalyst deposited on the walls of the channels [2]. The effect of channel geometry has been analyzed by Kreutzer et al. [3]. In non-circular geometries, cavities filled with the liquid phase appear in the corners, limited by circular menisci.

In our system, we are entrapping a static bubble, which causes the movement of liquid around it through its dissolution in the liquid phase. The aim of this chapter is to explore the process of creation and subsequent dissolution of bubbles during casting of polymer solutions. The first step is to present the chip we have designed to emulate the actual casting conditions. The mechanism for gas entrapment and bubble formation is then explained. The shape of the confined bubble is analyzed with a model that allows us to calculate the volume and pressure of the bubble from optical measurements. The influence of different gases is presented next, showing the different dissolution rates. Polymer solutions have been cast onto structured molds in different atmospheres to show how this affects the resulting replicas. Lastly, measurements of gas dissolution at constant volume were performed.

2. Experimental

2.1 Materials and Solution Preparation

The polymers used in these experiments were poly (imide) (PI, Matrimid 5218, Ciba) and poly (methyl methacrylate) (PMMA, M_w = 100.000 and 350.000, Polysciences).

N-methylpyrrolidone (NMP, 99%, Acros Organics) was used as solvent. Tap water was used as non-solvent. All reagents were used as received, without further purification. Unless otherwise specified, solutions were prepared by weighing all the components into a plastic bottle and left on a rolling bank until complete dissolution.

Both PI and PMMA solutions were cast on silicon substrates in air. For measurements on the microfluidic chips and on wafers in the glove box, only PMMA solutions were used. The solubility of PMMA in acetone makes it easier to clean the chips between measurements. For inspection with an optical microscope, a small amount of methyl red was added to the solutions.

2.2 Measurements on Wafers

Solutions were cast on silicon wafers using a custom-made doctor blade equipped with micrometric screws to regulate the casting thickness. The silicon wafers were microstructured through standard photolithographic methods combined with deep reactive ion etching (DRIE) in cleanroom facilities.

For measuring with carbon dioxide, a glove box was used. The glove box (0,255 m^3 volume) was purged for 150 minutes using a gas flow rate of 0.0051 m^3/min, prior to performing the casting. The measurement in air was done outside the glove box.

2.3 Membrane Treatment and Inspection

Membranes were rinsed with water overnight and broken in liquid nitrogen when needed for cross section pictures or cut with a scalpel for surface pictures. Prior to SEM inspection (Jeol JSM 5600LV), the membranes were dried overnight under vacuum at 30°C and then sputtered with gold (Balzers Union SCD040).

2.4 Measurements on Chips

The silicon microfluidic chips were microstructured through standard photolithographic methods combined with deep reactive ion etching (DRIE) in cleanroom facilities. Ports for the inlet and outlet of liquids and gases have then been fabricated by powderblasting. The chips were then sealed with a Pyrex glass wafer through anodic bonding. The whole ensemble was later diced to fit standard Micronit®

(Enschede, Netherlands) chip holders for microfluidic devices.

The chips were purged with different gases to measure the effects of their solubilities in several polymer solutions. Polymer solutions were then pumped into the channels. The process of bubble formation and dissolution was then followed through optical microscopy.

2.5 Measurements at Constant Volume

To assess the effect of the polymer on the solubility and diffusivity of the gases in the different solutions, measurements of gas uptake by said solutions were performed. These were carried out in a vessel of fixed volume (~140 mL) equipped with a pressure transducer. In all cases a liquid volume of 50 mL was used. The polymer solutions were first stirred and subjected to evacuation for 5 minutes. Afterwards, the system was left to equilibrate for another five minutes, under continuous stirring but with no connection to the vacuum pump. After turning the stirrer off, the chamber was filled with the corresponding gas. The initial pressure of all gases was kept at 1040 mbar. The pressure decay was then measured, after turning the stirrer back on. All measurements were performed in duplo.

Figure 1: Polymer solution on top of a mold with triangular wells. The side of the triangles is 16 µm in length.

S   C   S   C   S   C

5
6
7
3
4
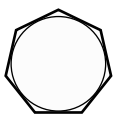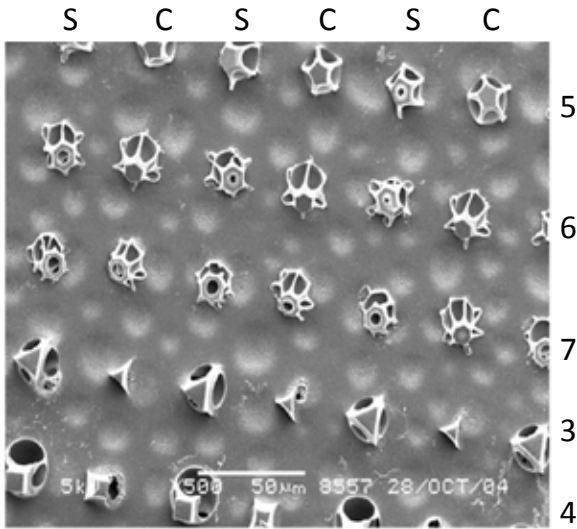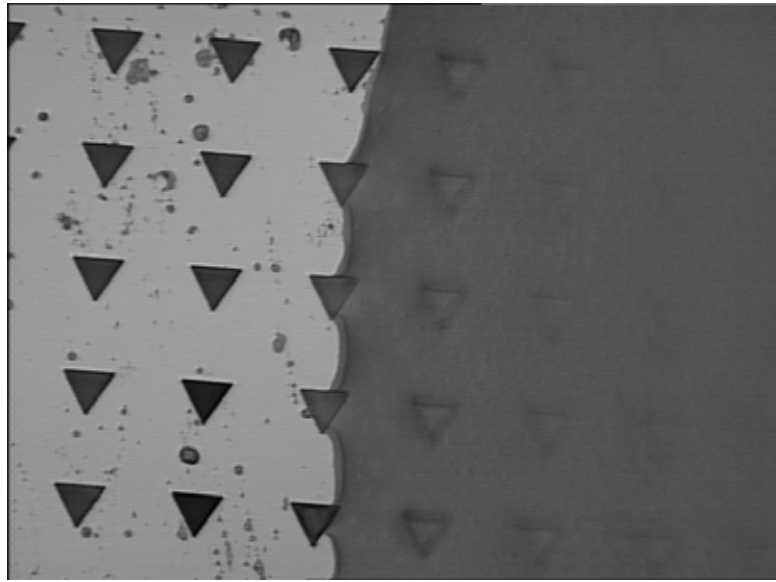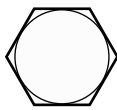
7S   6S   5S

4S   3S   3C

Figure 2: A PI membrane obtained via PSµF. The effect of the bubbles is clearly visible. The size of the bubbles increases with a decrease in the sharpness of the corners of the polygons.

3. Results and Discussion

Figure 1 shows a mold with triangular wells. For such a mold, casting of a polymer solution will result in the entrapment of gas bubbles in the wells, with the polymer solution acting like a lid for all th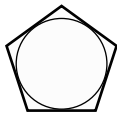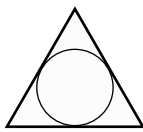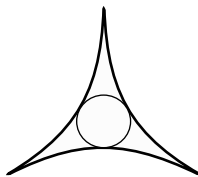e unconnected cavities. Immediately after this, entrapped bubbles rearrange achieving a certain uniform mean curvature. In other words, the replication of the wells is hindered. In its place, configurations are created that by solidifying render freestanding structures. Figure 2 shows a membrane obtained after phase separation of a polymer solution on a mold with different types of wells. The wells consist of polygonal structures with different number of sides and with straight or curved sides. The effects of the entrapped bubbles are visible in most cases. All structures consist of a freestanding top part connected to the membrane by ridges originally located in the corners of the polygons. Further progressed filling is observed for structures with sharper corners. If phase separation is not immediately induced, the volume of the bubble changes with time. Further studies have proven that this is due to dissolution of the bubble gas in the surrounding polymer solution. This process goes on until the bubble is fully dissolved.

3.1 Chip Design

Optical microscopy was used to follow the gas dissolution process in real time, while the solution is still in the liquid state. This has been realized by etching channels of varying length into a silicon wafer with a main channel for feeding the polymer solution (Figure 3). The glass wall allows inspection into the channel. Through measurements and knowing the dimensions of the channel, the shape of the bubble can be modeled (see section 3.3) and followed in time.

3.2 Gas Entrapment and Bubble Formation

The initial measurements in the chips have shown that the formation of the bubble is a very fast process. Using a high speed camera, we have captured the gas entrapment process and bubble rearrrangement.

Both during casting and in the chips, the polymer solution moves forward contained by a curved meniscus. This curved meniscus moves over the wells in the mold at speeds between 3 and 10 cm/s. When the curved meniscus moves forward
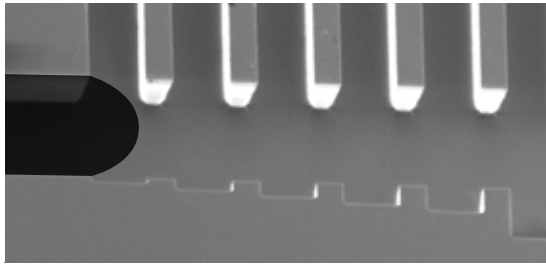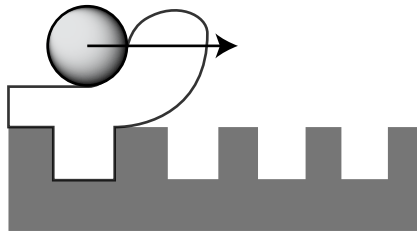
Figure 3: Emulation of casting conditions in the chips.
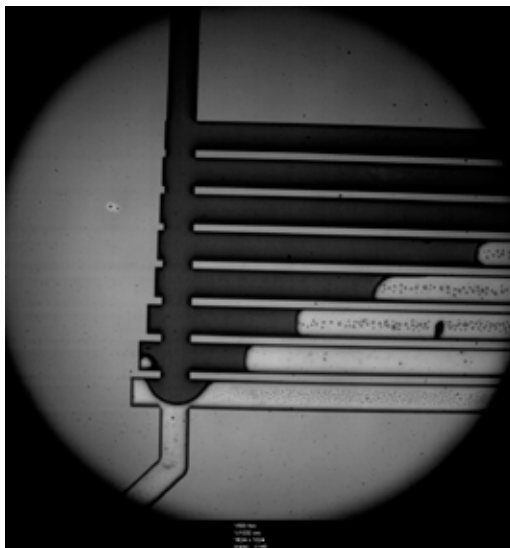
Figure 4: Gas entrapment. The channels are 100
µm in width.

from one side of the well and over it, the front of the meniscus can reach the other side of the well, before it reaches the bottom. This is illustrated in Figure 4. An entrapped bubble will almost immediately rearrange so as to have a constant mean curvature. This leads to movement away from the sharp corners of the well.

This process takes place in a number of steps. The first of them involves a radical change in the shape of the meniscus (convex to concave). Capillary forces then wick the solution in the corners of the channels. When these wicks reach the end of the well, they meet. Figure 5 illustrates the process, which takes just about 0.01 seconds. The equilibrium shape of the bubble is not shown here. However, it is known that the bubble is not round, because it is confined. The L-G interface possesses a constant mean curvature, consistent with a bubble in equilibrium with its surroundings.
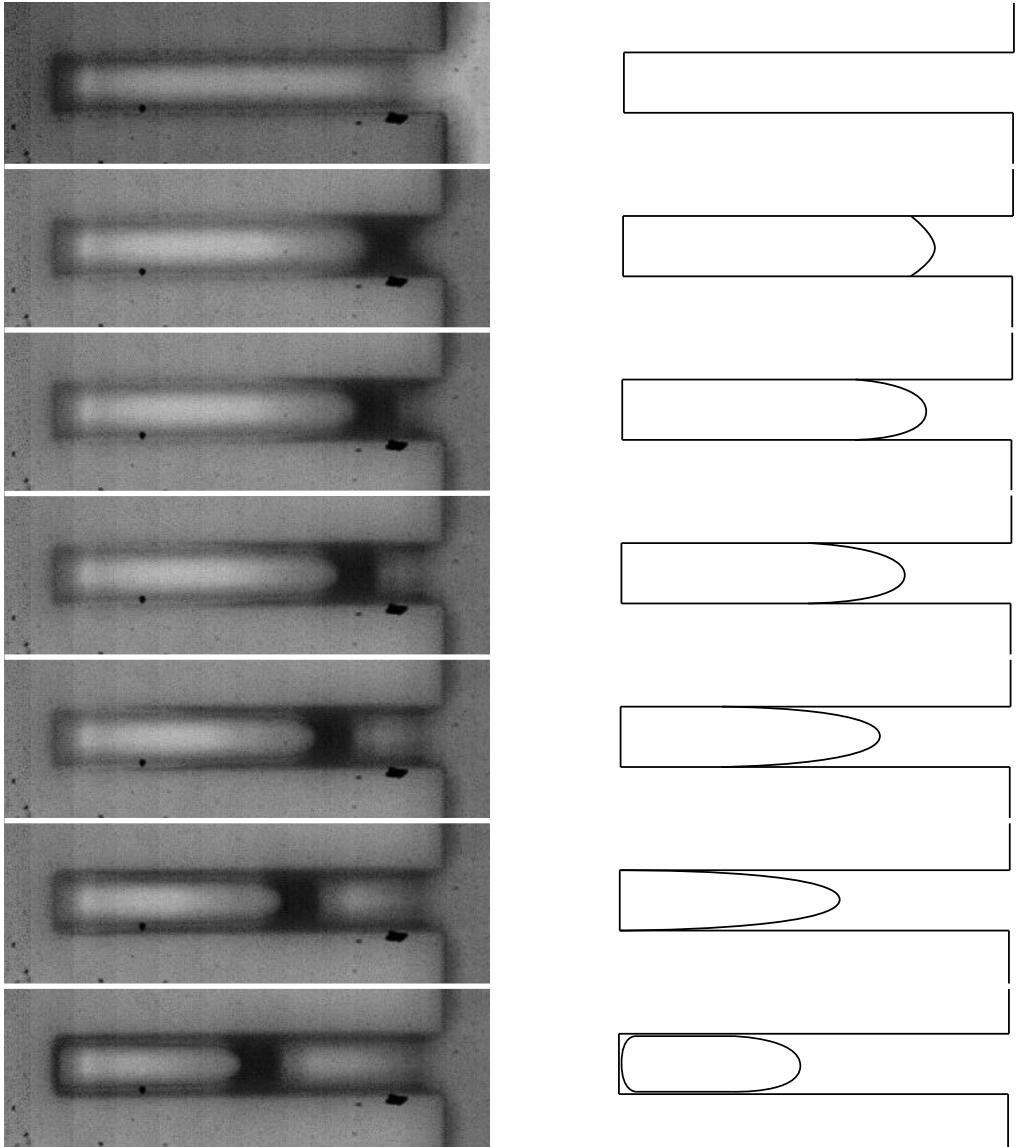
Figure 5: Rearrangement of the bubble to achieve uniform curvature. The equilibrium shape is not shown here. The channels are 15 μm in width.

This process cannot be modeled with the assumptions made for capillary rise on vertical systems. Princen et al. have proposed an approach in which the capillary force of the process pulls against the weight of the column of liquid [4]. This model has been proven to be in good agreement with experimental data by Bico and Quére [5]. There is one major difference between their system and ours. Princen's model applies to the rise of a liquid on a vertical tube with open ends. In this case the air is not confined, so the meniscus is not hindered in its movement. Besides, Princen's model requires that the properties of the liquid near the walls be known. Polymer solutions are believed to present depletion layers near walls, which might lead to local differences in properties as viscosity or interfacial tension. Furthermore, in our system gravity is not an important parameter. All the measurements in the chips were made in a horizontal position. The measurements on the wafers show no difference when the wafer is placed upside down during the waiting period. Therefore, balancing capillary forces and weight is not a good approach for calculations.

3.3 Bubble Description and Modeling

The bubble will eventually disappear through dissolution in the liquid phase. The driving force for this process is the pressure in the bubble, which is dictated by its curvature. The curvature is affected by the size and aspect ratio of the channels in which it is confined. Therefore, a correct model for volume and curvature is essential for following the process.

A sketch of a confined bubble entrapped by a perfectly wetting liquid can be seen in Figure 6. The bubble has two caps with uniform mean curvature and a long body that touches each side of the tube at two contact lines. The bubble is separated from each corner by a meniscus that has the same curvature as the caps.

It is clear that the full mathematical description of the geometry of such a bubble is not an easy task. Wong et al. have developed an intricate model with accurate results [6]. The calculation entails the use of the augmented Young-Laplace equation, eliminating the contact lines through the incorporation of disjoining thin-film forces. Its implementation is quite tedious and requires a number of parameters obtained empirically. Building on this model, Mazouchi and Homsy have given the solution for the curvature of the bubbles, by computing the contour of the cross-section of the bubbles between the caps [7]. They provide very simple solutions for regular polygons

and rectangular channels. For the latter they propose:

$$\frac{A}{2 \cdot R} = \frac{\dfrac{B}{A} + 1 + \sqrt{\left(\dfrac{B}{A} - 1\right)^2 + \dfrac{B}{A} \cdot \pi}}{2 \cdot \dfrac{B}{A}} \qquad Eq.1$$

where B is the length of the longer side of the channels, A the length of the shorter side of the channels and R the radius of curvature of the menisci in the corners of the channel (see Figure 6). The left hand side of the equation represents the curvature (reciprocal of the radius) scaled by the radius of the largest sphere that can be fitted into the channel (A/2). The right hand side of the equation shows the dependence of the radius on the aspect ratio of the channel (B/A). The only requirement imposed by this model is that the contact angle between the liquid and the solid be 0°. When the solvent in use is NMP and the substrates are silicon and glass, this is the case. The pressure inside the bubble depends on the radius of the surfaces and the surface tension of the liquid. It can be calculated from Laplace's equation, reduced for the case of a cylindrical interface to (γ represents the surface tension of the liquid):

$$\Delta P = \frac{\gamma}{R} \qquad Eq.2$$
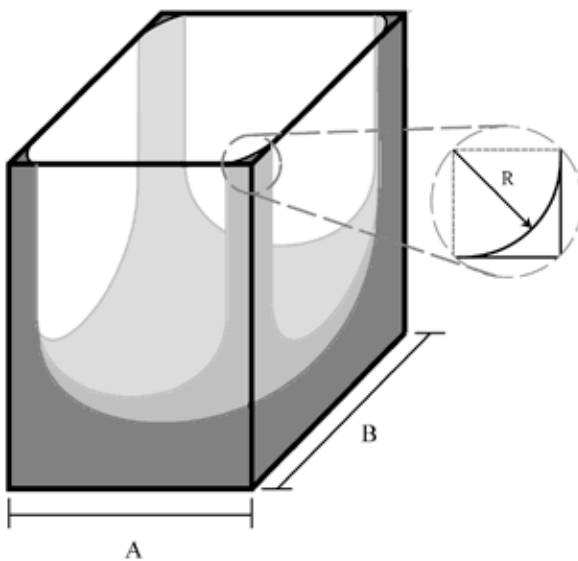
Figure 6: Scheme representing half of a bubble confined in a rectangular channel.

Now we know the aspect ratio of the channel in which the bubble is contained, the pressure inside the bubble and its curvature. The shape of the caps of the bubble can thus be obtained by using Surface Evolver (Kenneth Brakke, Susquehanna University). This program predicts the shape of surfaces evolving towards minimum area with a constant mean curvature. Different constraints can be set for the calculations. In our case, we aimed at the calculated target pressure using four constraining planes to avoid the growth of the bubble outside the channel. A typical example can be seen in Figure 7. The straight length between the caps is fixed, as it exerts no effect on pressure.

From the predicted shape, the volume of the bubble and the interfacial area are obtained. With this data, we have been able to make calibration curves of volume versus length between the caps. The straight length between the caps was then followed in time for dissolving bubbles through optical microscopy.
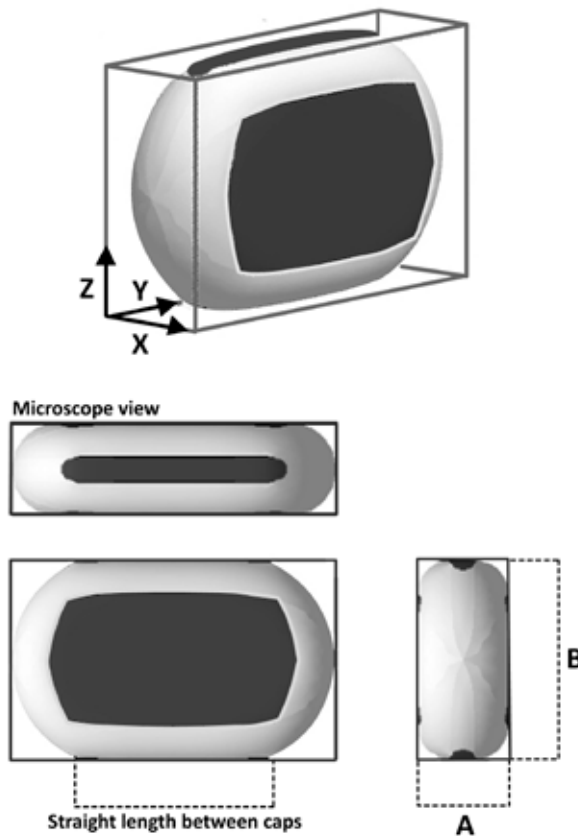
Figure 7: Shape of the bubble modeled using Surface Evolver.

3.4 Gas Dissolution

The driving force for the dissolution process is the difference between the overpressure created by the curvature of the bubble and the gas concentration in the liquid. The solutions mentioned here were not degassed prior to the measurements.

The effect of bubble size can be seen in Figure 2. This mold has been designed to include polygonal wells with 3 to 7 sides. Also, each row consists of alternating arrays of these polygons with either straight or curved sides. In all cases the area of the polygon was left constant. The figure shows that the wells fill faster when the polygon has fewer corners and even faster when the sides are curved. As the number of sides becomes lower (Figure 2), the inscribed circle that can fit into polygons with constant area becomes smaller. This means that the volume of the bubble is lower. Smaller bubbles take less time to dissolve, leading to the further progressed filling for polygons with sharper and fewer corners.
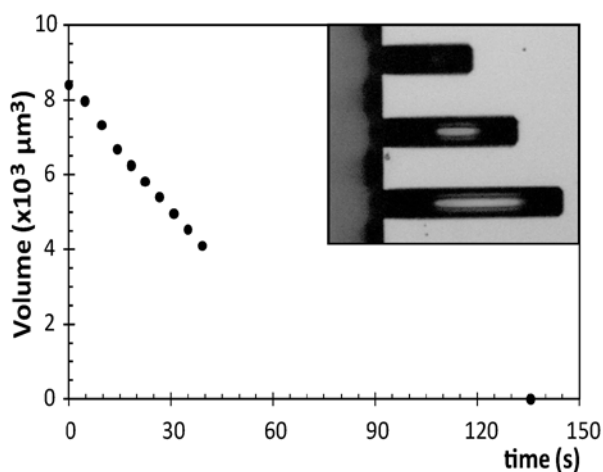
Figure 8: Dissolution profile of a bubble in a chip. The channels are 15 μm in width.

Figure 8 shows a typical image from the optical microscope next to a plot of volume versus time for nitrogen with a fresh 15% PMMA solution in NMP. The measurements show a linear decay of volume until a volume of 4000 μm^3. This volume corresponds to the moment in which the two caps meet. Up to this moment, the curvature of the bubble does not change. This translates into a constant gas pressure inside the bubble. The cap area remains constant during this process, whereas the area of the menisci in

the corners of the channel becomes lower. The dissolution must, therefore, take place mainly by means of exchange through the caps.

After the two caps meet it is unfeasible to follow the bubble volume accurately. We observed that the dissolution of the bubble proceeds more slowly beyond this point. This can be noticed when considering the average between the last two points in the graph in Figure 8: the slope of the line joining these two points is not as steep as that of the linear part of the curve. The first explanation for this is that the pressure (proportional to 1/R) does not increase enough to compensate the decrease in the area (proportional to R^2). The second one is the increased concentration of the dissolved gas in the liquid phase near the bubble, which decreases the driving force for the process. The decrease in radius of the bubble causes it to retract from the walls of the channel, difficilitating an accurate measurement of volume. However, the time until complete dissolution (disappearance) could be recorded (V=0).

For N_2 and O_2, the saturation must play an important role, as the solubility is low compared to the final achievable concentration without considering convection. Before the caps meet, the volume of the bubble changes more dramatically upon dissolution than afterwards. The constant pumping of liquid into the channel refreshes the solution near the bubble, allowing a constant dissolution rate. This does not happen so distinctly after the caps meet. CO_2 presents the same decrease in velocity towards the end of the curve, although its saturation concentration is much higher compared to that of N_2 and O_2. For CO_2, the imbalance between bubble area decrease (~R^2) and pressure increase (~1/R) must have a more prominent role than for O_2 or N_2. Nevertheless, the consequences of gas accumulation in the liquid phase must be considered.

The study of different movies has shown that the movement of the caps of the bubble is not always the same. At times, both caps move towards one another. Other times it is only one cap that moves towards the other. This makes a general description of the process including convection of the polymer solution quite hard to make. The movement of the caps causes the liquid in the space behind and in front of the bubble to mix via flow through the corner regions. This phenomenon agrees with observations from van Steijn et al. [8] during formation of bubbles by injecting gas into a liquid stream through a T-junction. In their study, they have observed that around 25% of the incoming liquid flows around the bubble through the corner regions.

This led us to the conclusion that if the cap at the end of the channel is moving towards the opening of the channel, liquid is pumped through the corners to fill all necessary space, refreshing the solution. On the other hand if the outer cap is moving in, it does so accompanied by liquid from the bulk of the solution. Most of the time, the dissolution of a bubble is a combination of both processes.

3.5 Effects of Polymer Concentration and Molecular Weight

A first set of measurements has been carried out by pumping NMP with varying PMMA concentrations through the chips with the help of syringes, after purging the chip with carbon dioxide, nitrogen or oxygen. First we have tried a solution of 7 wt% of PMMA (MW=350,000) in NMP, in chips with channels of 15 μm in width and 33 μm in depth. In a channel with these dimensions, the radius of curvature of the liquids in the corners is calculated to be 5.4 μm (Eq. 1). Considering a surface tension of 42.4 mN/m, the capillary pressure is 7.78 kPa (Eq. 2). The solutions were made according to the procedure described in the Experimental section and were not degassed prior to the experiments.

In these cases, we have noticed that the rate of change in length of a nitrogen bubble was 0.88 ± 0.17 μm/s and that of oxygen was 1.57 ± 0.20 μm/s. In the case of carbon dioxide, this value was estimated at about 800 μm/s for pure NMP. All the dissolution rates mentioned up to here were constant until both caps met.

The interaction between gas and liquid can be expressed in terms of solubility and diffusivity. The solubility of a gas in a given solvent can be lowered by the presence of polymer due to added interactions between the solvent and the polymer [9]. Also, the interactions between the gas and the polymer must be considered. The effects of polymer concentration on diffusivity must also be taken into account. An increased viscosity can correlate with lower diffusivity, although the volume fraction of polymer seems to be the controlling parameter [10].

The effect of the solubility in the process can be investigated through a decrease in the pressure of the system. From Henry's law, it can be expected that a gas at a lower pressure will present a lower solubility in a liquid phase. This was achieved by decoupling the syringe used for pumping the liquid once the bubble was formed, allowing the liquid to equilibrate with atmospheric pressure. The results for the

aforementioned solution and pure NMP are presented in Figure 9. It is clear that the initial size of the bubbles becomes much larger. Also, the volume of the bubbles decreases more slowly. The decrease of solubility seems to induce important changes in the way in which the dissolution takes place. However, from this graph it is hard to discriminate the effects of the polymer on the process. The curve for pure NMP and the polymer solution are very similar. Assuming that a small change of solubility takes place, its effects magnify along the curve. Therefore, it is hard to estimate it. A third solution was measured, with a 7 wt% concentration of PMMA but with a molecular weight of 100,000. The curve was very similar to the one shown in Figure 9 for the other solution and pure NMP, showing no significant changes. The addition of polymer and the increase in molecular weight (i.e. two steps towards higher viscosity, one step towards higher volume fraction of polymer) exert no significant effect on the curves. At a lower solubility (lower pressure), the changes in diffusivity (expected from the changes in viscosity and/or amount of polymer in the solution) do not induce a big effect on the dissolution profile of the bubbles. Because of this, it was hypothesized that the process must be solubility controlled. This hypothesis was ultimately verified through constant volume measurements, presented in the following section.
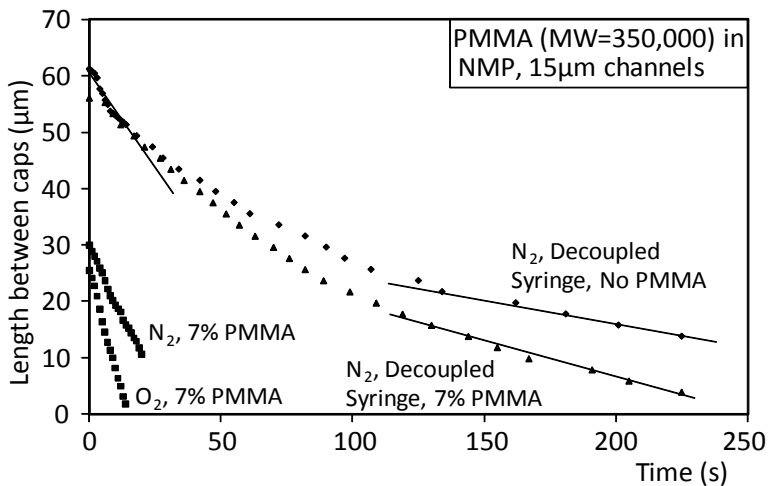
Figure 9: Examples of diverse dissolution profiles measured in the chips.

In this section we have shown that the origin of the bubbles responds to geometrical considerations. Their evolution in time depends on the interaction between the solution and the gas in the bubble. Different gases therefore lead to different dissolution rates. Figure 10 shows that a membrane cast in air presents bubble effects inside the structures even after 60 seconds. On the other hand, the membrane cast in a

carbon dioxide atmosphere presents solid pillars after only 10 seconds of waiting time between casting and phase separation.

Air, 10 second delay.
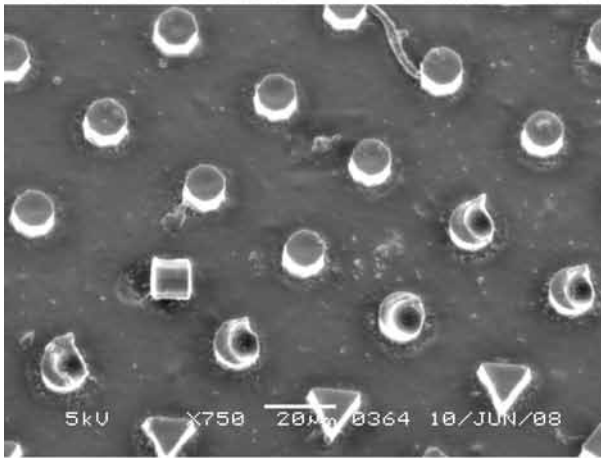
Air, 60 second delay.
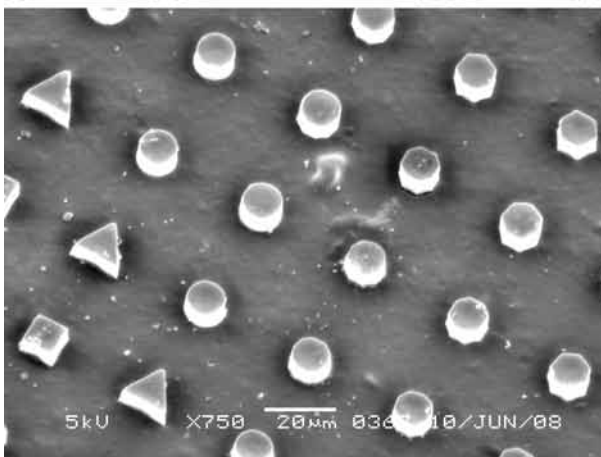
Carbon dioxide, 10 second delay.

Figure 10: effects of different gases and waiting periods on the replication of the mold.

3.6 Measurements at Constant Volume

To further assess the situation, we have performed measurements of gas dissolution in a fixed volume. For all the aforementioned solutions, we have measured the pressure decay in time of a fixed volume of gas (about 90 mL) in 50 mL of liquid. To do so, the gas volume was first evacuated and purged with the gas in question. Afterwards, an initial pressure of 1040 mbar was set.

Figure 11 represents the pressure decay due to dissolution of nitrogen and oxygen in pure NMP. Since both the volume of gas and the initial pressure were kept constant in all experiments, a lower end pressure indicates a higher mass of gas dissolved in the liquid. Since this higher mass is attained at a lower pressure, this translates into higher Henry constants or higher solubility. A steeper initial slope represents a higher permeability, which can in turn be modeled as the product between diffusivity and solubility.

The actual numbers cannot be compared with those measured in the chip. This is because the measurements in the chip were made at constant pressure, while these were made at constant volume. Furthermore, the liquid phase in this measurement presents no advancing interfaces and is stirred continuously. This is not the case in the chips. However, these measurements help us verify the observed trends. Oxygen presents a higher solubility and diffusivity than nitrogen. Their solubility is lower than that of carbon dioxide, at least by an order of magnitude.

Figure 12 shows the results obtained for nitrogen in NMP and two 7 wt% solution of PMMA in NMP, one with a polymer with Mw=100,000 and another one with a polymer with Mw=350,000. It is noteworthy that the end pressure for all three solutions remains constant. This indicates that the presence of polymer does not significantly affect the solubility of the gas. The solution of the lighter polymer and the pure solvent present very similar curves, which is a phenomenon similar to that observed in the previous section.

The process is slower for the solution of the heavier polymer. This is compatible with a lower diffusivity. As shown before, the measurements in the chips resulted in similar curves for NMP and the two solutions. It is concluded that the mechanism for N_2 is controlled by solubility, as significant changes in diffusivity cause no variations in the

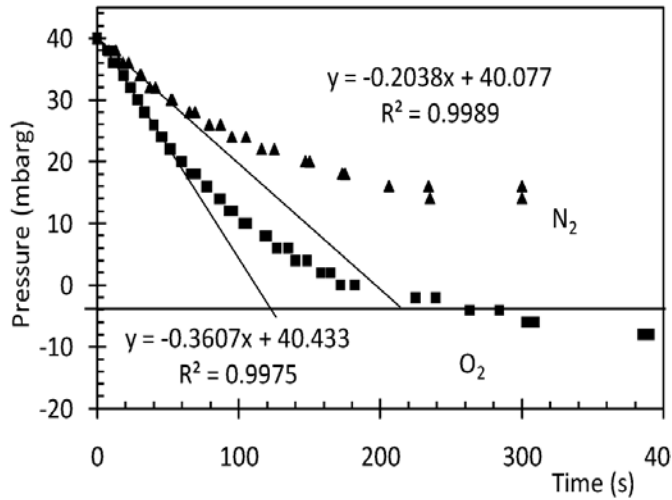measurements performed in the chips.

Figure 11: Pressure decay of nitrogen and oxygen due to absorption in pure NMP, measured at constant volume.
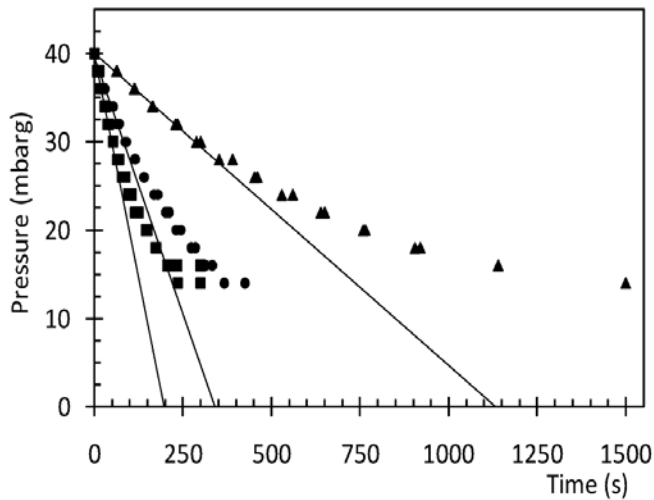
Figure 12: Pressure decay for nitrogen in different solvents:

■ *Pure NMP,*
  y=-0.2038x+40.077, R^2=0.9989

● *7 wt% PMMA (Mw=100,000) in NMP,*
  y=-0.1165x+39.704, R^2=0.9931

▲ *7 wt% PMMA (Mw=350,000) in NMP,*
  y=-0.0353x+40.037, R^2=0.9969.

4. Conclusions

Upon casting a polymer solution on a wafer with wells, the wells do not get filled directly. This is caused by entrapped air bubbles that interfere with the filling of the wells in the mold.

The variation of the volume of the bubble in time showed that the dissolution of the entrapped gas in the solution is of high importance for the filling process. This has been verified through measurements in a custom made chip. It has been seen that carbon dioxide dissolves quite quickly. Almost 800 times faster than oxygen, which in turn dissolves roughly twice as fast as nitrogen. Based on this, it can be concluded that the casting atmosphere is an important parameter in the production of polymeric structures via phase separation microfabrication. Particularly, if the mold has wells.

Experiments performed at constant volume showed that the addition of polymer to the solvent decreases the diffusivity of nitrogen. Its solubility remains unchanged. On the other hand, the presence of polymer in the solution does not induce a significant effect on the measurements performed in the chips. This indicates that the process in the chips is controlled by solubility for gases like N_2 or O_2. The amount of gas present in the bubble is higher than the amount necessary to achieve saturation. This is the main reason why the process becomes slower towards the total dissolution of the bubble.
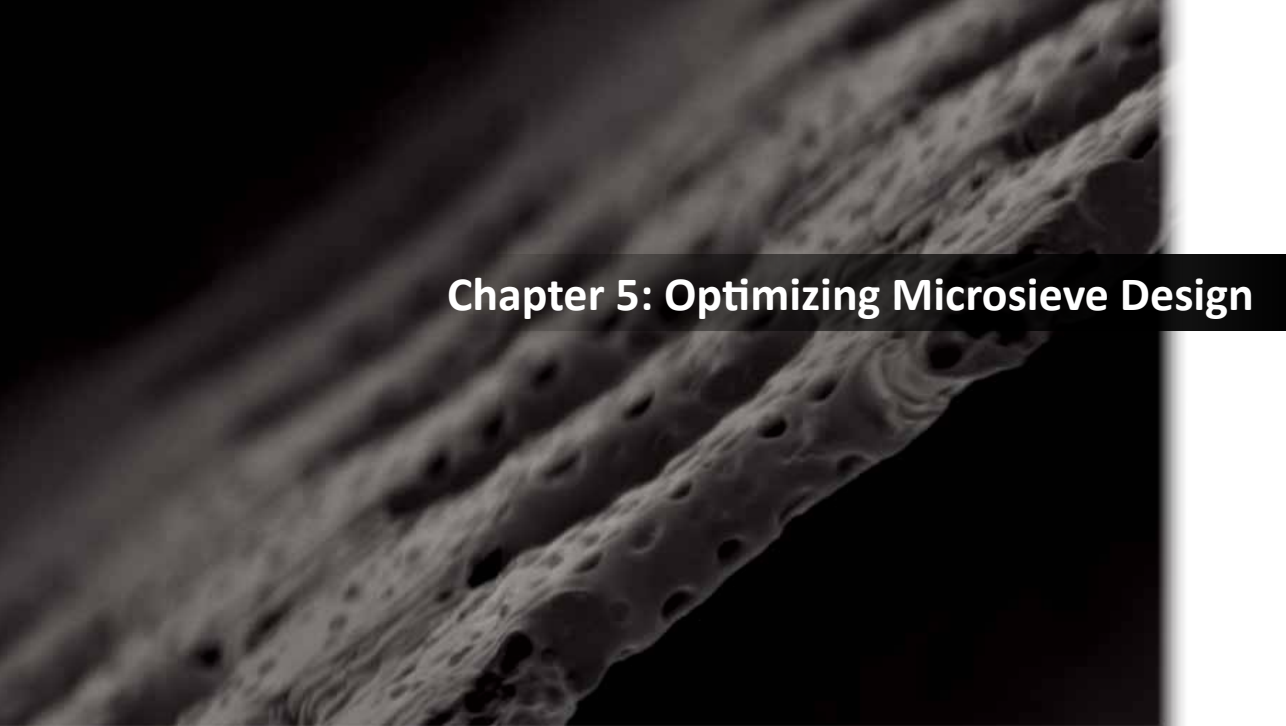
In the case of CO_2, a similar rate decrease has been observed. This gas presents a much higher solubility in the liquids in this study. The decrease in speed is then, to a greater extent, related to the decrease in interfacial area ($\sim R^2$). This is more significant than the increase in the pressure inside the bubble, proportional to $1/R$.

5. Acknowledgements

6. References

[1] V. S. Ajaev and G. M. Homsy, Modeling shapes and dynamics of confined bubbles, Annual Review Of Fluid Mechanics, (2006) 277

[2] L. Kiwi-Minsker and A. Renken, Microstructured reactors for catalytic reactions, Catalysis Today, 1-2 (2005) 2

[3] M. T. Kreutzer, A. Günther and K. F. Jensen, Sample dispersion for segmented flow in microchannels with rectangular cross section, Analytical Chemistry, 5 (2008) 1558

[4] H. M. Princen, Capillary phenomena in assemblies of parallel cylinders. II. Capillary rise in systems with more than two cylinders, J. Colloid Interface Sci., 3 (1969) 359

[5] J. Bico and D. Quére, Rise of liquids and bubbles in angular capillary tubes, J. Colloid Interface Sci., 1 (2002) 162

[6] H. Wong, S. Morris and C. J. Radke, Three-dimensional menisci in polygonal capillaries, J. Colloid Interface Sci., 2 (1992) 317

[7] A. Mazouchi and G. M. Homsy, Thermocapillary migration of long bubbles in polygonal tubes. I. Theory, Phys. Fluids, 6 (2001) 1594

[8] V. van Steijn, M. T. Kreutzer and C. R. Kleijn, μ-PIV study of the formation of segmented flow in microfluidic T-junctions, Chemical Engineering Science, 24 (2007) 7505

[9] I. Shulgin and E. Ruckenstein, Prediction of gas solubility in binary polymer + solvent mixtures, Polymer, 3 (2003) 901

[10] W. F. Pfeiffer and I. M. Krieger, Bubble solution method for diffusion coefficient measurements. An experimental evaluation, Journal of Physical Chemistry, 24 (1974) 2516

Summary

PSμF has been successfully used for manufacturing polymeric microsieves. The technique benefits from the vertical shrinkage of polymer solutions to ensure perforation by the pillars on the mold. The horizontal shrinkage causes deformation of some pores and increased peeling forces. This can lead to rupture of molds as well as inoperable microsieves. The effect of several parameters of mold design as well as peeling orientation is addressed. A peeling device equipped with a force transducer is used to measure the force required for peeling in each case. Peeling forces decrease with lower pillar densities, the use of alternative geometries for the pillars (i.e. not round pillars) and the use of alternative pillar placing (i.e. not square pitch).

1. Introduction

Porous membranes can be classified as screen filters and depth filters. Depth filters have a random array of tortuous pores. The retention of solids occurs when the particles encounter a portion of the pore that cannot be traversed anymore. This can be due to size differences or by adsorption in the bulk of the filter. On the other hand, screen filters have straight through pores. Each pore has uniform shape and diameter. As a result, rejected particles accumulate directly at the surface of the filter.

Microsieves are a special type of screen filters. Introduced a little over a decade ago [1], microsieves have been growing steadily in application span. The main feature of a microsieve is the presence of well-defined, straight pores that go through the film. This porosity is characterized by a well-defined pitch, a narrow pore size distribution and consistent pore shape.

Microfiltration processes benefit extensively from such a microsieve. Performance is increased through lower pressure drops when compared to conventional membranes. Furthermore, the flow is homogeneously distributed over the surface of the membrane, leading to a better operation of the size exclusion mechanisms [2]. As a result, this sort of membrane is highly desired [3]. Another field of application to benefit from well-defined microsieves is membrane emulsification [4]. In this process, the disperse phase of an emulsion is pumped into the continuous phase through the pores of a microsieve. Due to the narrow pore size distribution of microsieves, when the operating conditions are well controlled, monodisperse emulsions can be obtained with simplicity.

Inorganic microsieves are made through etching of silicon nitride substrates. Usually, the pattern is imprinted on the film through photolithography for pores larger than 1 µm and by means of laser interference for smaller pores [1]. These membranes have the advantage of being highly defined and resistant to extreme chemical conditions. Their surface chemistry can be readily modified through silane chemistry [5]. This parameter possesses a high influence on the performance of microsieves both as emulsification membranes as well as filtering devices [6]. On the other hand, the material is brittle and the production process requires cleanroom facilities, causing a high manufacturing cost.

Polymers are a cheaper alternative to silicon nitride. These materials can be

structured into microsieve-like geometries via techniques like interference holography [7] or track etching [8], for example. In the first case, the exposure of a negative photoresist to two UV light sources creates an interference pattern used later as a mask to etch a layer of densely linked thermosets (SU-8). Track etching membranes are produced by chemical etching of membranes bombarded with fragments produced by thermal neutron fission of U-235 nuclei. Ionization and excitation of these fragments produce tracks across the entire thickness of the polymeric film. Thus, well-defined pores with random dispositions are obtained. The complexity of these structuring methods compromises the cost effectiveness of polymers compared to silicon nitride.

Other methods have been developed for the molding of polymers from a polymer solution. A method has been optimized for microsieve production by allowing the solvent from a polymer solution to evaporate while the solution is in contact with a bed of glass microspheres [9]. This method presents three major drawbacks. The most important one is safety related, as the glass beads must be etched away using hydrofluoric acid, which is a troublesome chemical. The other two are related to the shape of the final membrane. The pattern imprinted on the membrane can only be hexagonal, as this is the way in which spheres pack, and as a result, the walls of the pores are extremely thin. Furthermore, since balls are used for molding, the pores do not have straight walls. Jahn et al. implemented inkjet technology to deposit microdroplets of a mixture of water and ethylene glycol on top of a hydrophobized aluminum foil [10]. Once this was done, a solution of poly (methyl methacrylate) in chloroform was dispersed on the film, around the droplets. Upon evaporation of the chloroform, the film can be removed. The water droplets imprint their shape on the film. Since sessile drops are used for molding, the pores do not have straight walls. On the other hand, complicated and well-defined pore dispositions can be achieved with this technique. Pores of sizes between 19 and 86 µm can be obtained with this method.

The implementation of a relatively simple patterning process makes polymers very attractive for microsieve fabrication. However, the methods presented above do not offer numerous possibilities regarding the design of the final product. An alternative technique can be found in Phase Separation MicroFabrication (PSµF) [11]. An example of a microsieve made with PSµF can be seen in Figure 1.

In this case, PSµF is implemented through casting of a polymer solution onto a structured substrate, consisting of pillar fields. The phase separation is then induced
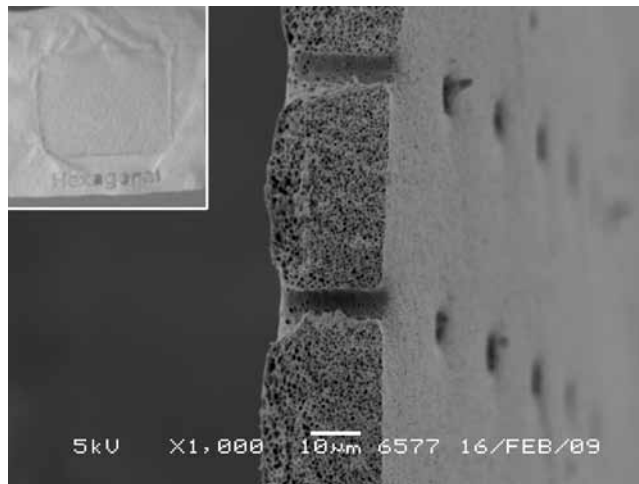
Figure 1: SEM micrograph of a microsieve obtained via PSμF. The inlay shows a picture obtained with a digital camera. The active area can be seen as a square (1 cm in side) in the center of the sample.

in a series of steps that incorporate a nonsolvent to the polymer solution. Upon solidification, a perforated membrane is obtained. This process can be used for all materials for which a miscible pair of solvent and nonsolvent can be found [12]. The disposition of the pores and their size are in good agreement with the dimensions of the mold. For smaller pore sizes, heat treatment of the solid membrane can be carried out. The collapse of the inner porosity of the polymeric matrix causes a reduction in size of the whole film, including the perforations [13].

Phase separation processes are known to be accompanied by shrinkage of the polymer solution [14]. The shrinkage in thickness enables the pillars in the mold to perforate the polymeric film. Therefore, vertical shrinkage is a desired characteristic of the process. On the other hand, shrinkage also takes place in all directions parallel to the mold. As a result, some of the pores become deformed due to pulling forces exerted by the shrinking solution. Moreover, the pulling of polymer against the pillars causes release problems. This is translated into higher peeling forces and eventual pillar rupture or membrane tearing.

The efforts on improving microsieve production with this technique are worthwhile, as their implementation is more economically feasible in terms of initial costs regarding production. Furthermore, organic microsieves present the additional advantage of their

flexibility. This is of particular interest, since backpulsing is a common method for the removal of foulants with microsieves [15, 16]. This method is used because microsieves tend to present in-pore fouling [2]. For inorganic sieves, backpulsing induces a flow reversal that sweeps the particles from the pores. Since organic sieves are flexible, backpulsing causes less flow reversal, combined with the movement of the entire sieve. This induces vibration, which helps shake the foulants off the surface of the microsieve more effectively than rigid (inorganic) microsieves [17].

The aim of this chapter is to explore alternative designs for molds, in order to ensure an easier release of the microsieves from the molds. A set of experiments was carried out using a peeling device equipped with a force transducer. This device allowed us to compare the molds in a broader scale. In this part of the research the effects of pillar density, pillar dispositions, pillar shapes and peeling direction were investigated.

2. Experimental

2.1 Materials and Solution Preparation

One polymer solution has been used for all the experiments presented here. poly (ethersulfone) (PES, Ultrason, E6020P) was the polymer in use in a concentration of 9 wt.% in N-methylpyrrolidone (NMP, 99%, Acros Organics), in a concentration of 48 wt.%. Poly (vinylpyrrolidone) (PVP K30, Fluka), commonly used to create a percolating porosity and a hydrophilic surface [18], was used as polymeric additive in a concentration of 3 wt.%. It also acts as a macrovoid formation inhibitor [19]. Acetone (Merck, analytical grade) was used as a volatile additive, in a concentration of 40 wt.%. All reagents were used as received, without further purification. Unless otherwise specified, solutions were prepared by weighing all the components into a plastic bottle and left on a rolling bank until complete dissolution. Tap water was used as non-solvent.

2.2 Casting

Solutions were cast on silicon wafers using a custom-made doctor blade with micrometric screws to regulate the casting thickness. Casting thicknesses were varied between 20 and 100 µm above pillar level. A polymer solution must be ideally cast as
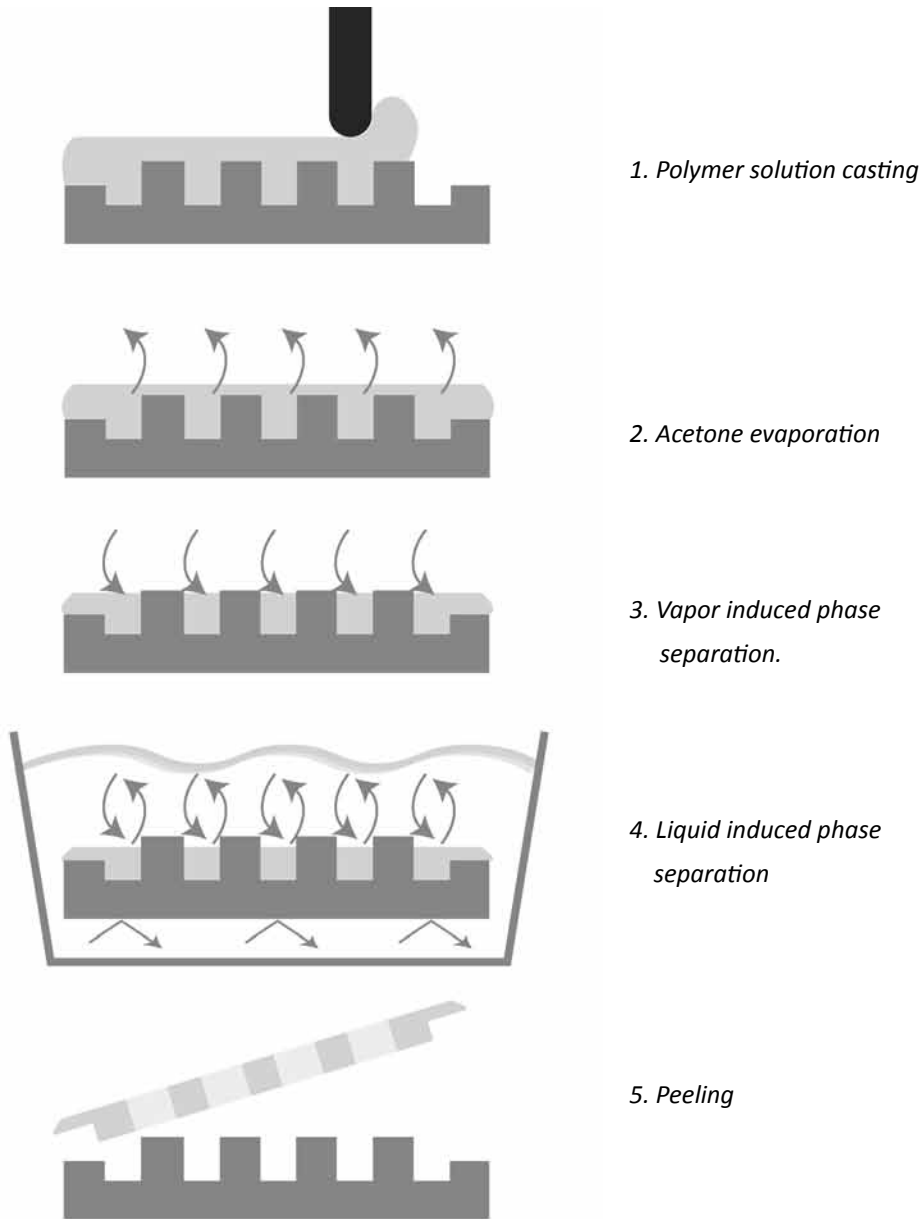
Figure 2: PSµF process adapted for microsieve production.

close as possible to the top of the pillars. This ensures perforation during the phase separation process. Afterwards, the acetone was allowed to evaporate to decrease the thickness of the solution. This was done in a chamber continuously purged with dry nitrogen. See Figure 2 for schematics of the process, this corresponds to steps 1 and 2.

The silicon wafers were microstructured through standard photolithographic

methods combined with deep reactive ion etching (DRIE) in cleanroom facilities. Four molds were used in these experiments:

- Mold A: Fields of round pillars of 10 µm in diameter. Pillars were arranged on a rectangular array. In one direction, pillars were located every 20 µm, center to center. In the other direction, the distance varied between 30 and 150 µm.

- Mold B: Fields of round pillars of 10 µm in diameter. Pillars were arranged on a rectangular array. In one direction, pillar distances were 20, 25, 30 and 40 µm for each row respectively. In the other direction, distance between pillars was 15, 20, 25 and 30 µm for each column respectively.

- Mold C: Fields of round pillars of 10 µm in diameter. Pillars were arranged in different arrays, keeping the pillar density approximately constant and equal to that of a square array with pillars every 20 µm (center to center). SEM micrographs of the mold can be seen in Figure 3.

- Mold D: 9 fields of pillars of 10 µm in characteristic length. Bottom row: round pillars, square array, 50 µm pitch. Middle row: round pillars, three different dispositions (Circles, Circular and Swirl, see Figure 3) with a comparable pillar density to that of the bottom row. Top row: square array (50 µm pitch) of pillars of different shapes (round, cross and hexagonal).

2.3 Phase Separation

Once all acetone is evaporated, the mold and the polymer solution are exposed to a stream of nitrogen at 40°C saturated with water vapor for 3 minutes. The goal of this step is to begin the phase separation in a slow way (vapor induced). Afterwards, the phase separation was completed by immersion in a coagulation bath of water (liquid induced). (Steps 3 and 4, Figure 2)

2.4 Peeling

Peeling experiments were performed with the help of a custom-made peeling device, illustrated in Figure 4A. This device is equipped with two stepper motors that move with a set velocity. One of them moves a forced transducer (range 0-2 N)
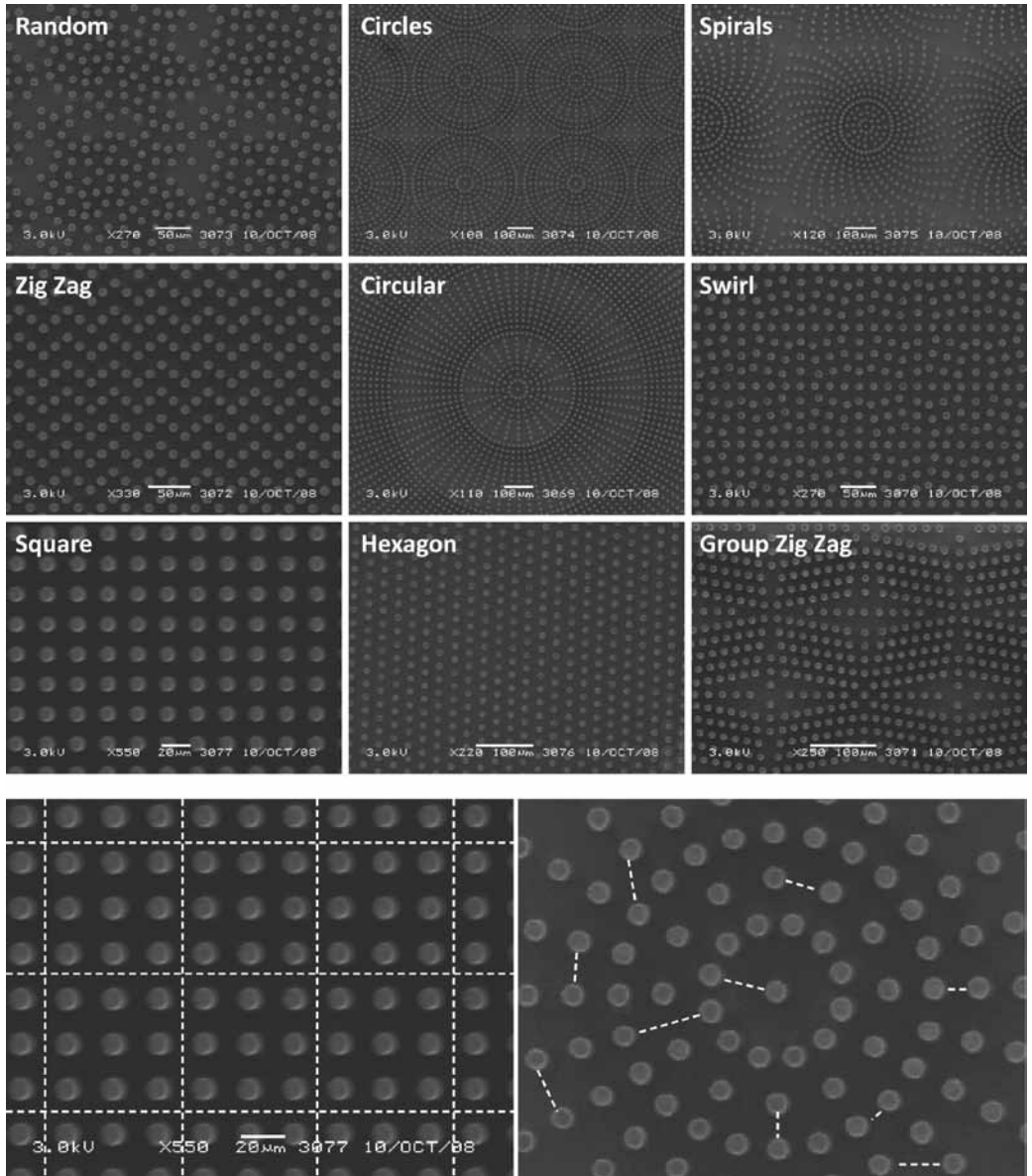
Figure 3: Different pillar dispositions in Mold C. The bottom pictures show a few of the shrinkage lines in the Square and Circular dispositions.

vertically. A clamp is attached to the force transducer and is used to grab the membrane for peeling. The second motor is equipped with a platform to which the mold (still containing the membrane) is attached. This platform moves horizontally, to ensure that the peeling angle remains constant.
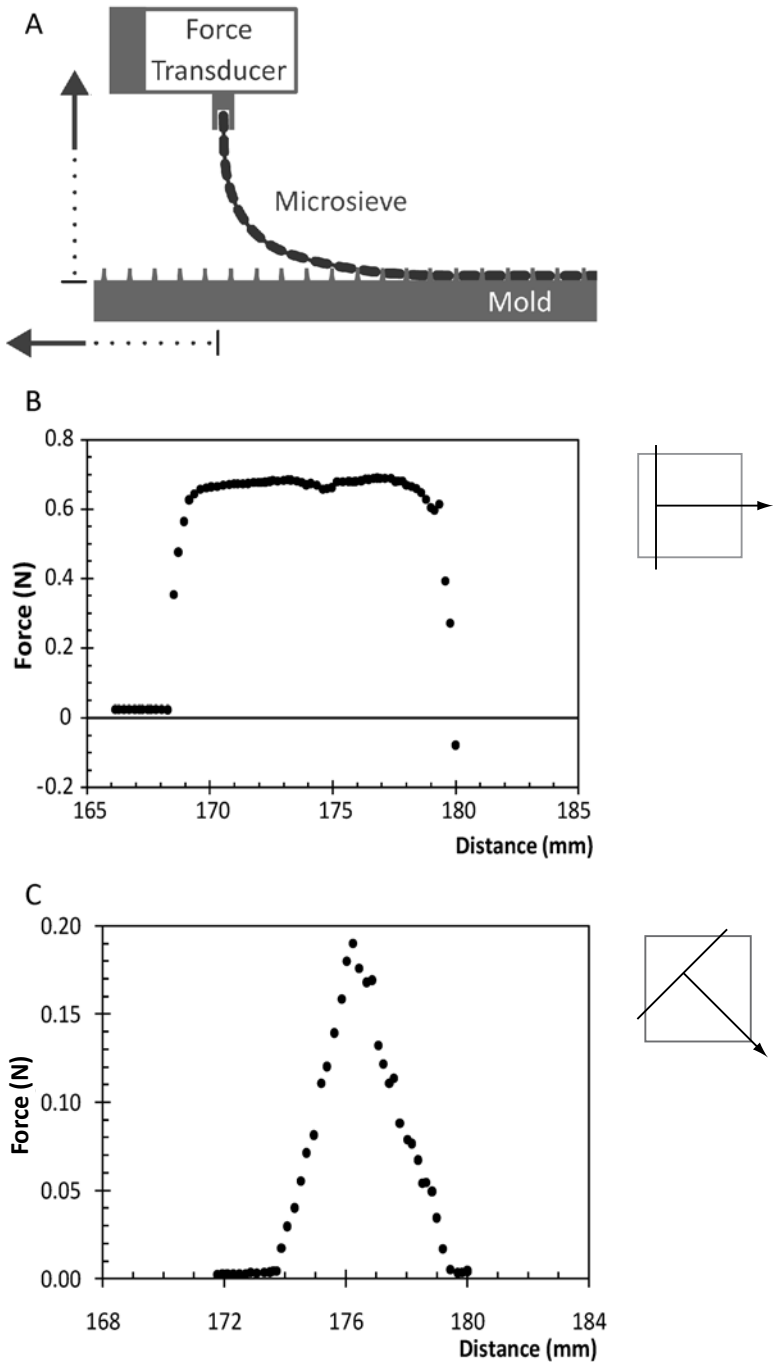
Figure 4: A. Schematics of the peeling device. (Illustration by Jonathan Bennink)

B. Typical result obtained when peeling a microsieve in a direction parallel to one of the field sides.

C. Typical result obtained when peeling a microsieve following the diagonal of a field.

2.5 Membrane Treatment and Inspection (SEM)

Peeled membranes were rinsed with water overnight and were broken in liquid nitrogen when needed for cross section pictures or cut with a scalpel when needed for surface views. Prior to SEM inspection (Jeol JSM 5600LV), the membranes were dried overnight under vacuum at 30°C and then sputtered with gold (Balzers Union SCD040).

3. Results and Discussion

Preliminary tests have shown that both casting thickness and pillar height are important parameters for the process. For membranes with the same thickness, the peeling from molds with higher pillars proceeds with more force. For different castings on the same mold, the use of higher casting thicknesses allows for peeling from fields with higher pillar densities.

Figure 4B shows a typical result obtained with the peeling device. The graph shows the approach towards the first line of pillars at a constant value of 0 N (the measurement is corrected for the weight of the clamp), the increase towards a plateau and the decrease once the whole field is peeled. The representative value for each field was taken as the average value of the plateau. That the force is constant over the whole field has to do with the fact that rows are peeled consecutively. Therefore, the values of force presented here for mold A are normalized by the amount of pillars in each row. For molds B, C and D the amounts in pillars in each row does not vary extensively. Therefore, these values are presented without normalization.

Figure 4C shows the result from peeling a field along its diagonal. When this is done, each row contains more and more pillars until the other diagonal is reached. From this point on, each row contains fewer pillars. The representative value for these tests was taken as the maximum divided by the square root of 2.

3.1 Dependence on Pillar Density and Peeling Orientation

To study the effect of these parameters, mold A was first used. In this mold, the pillars were separated 20 µm in one direction for all fields, whereas the distance in the

other direction varied between 30 and 150 μm. The height of the pillars was 50 μm. The polymer solution was cast on this mold at 40 μm. Peeling tests on perpendicular directions were performed.

In the first case, the peeling was done in the top to bottom (TB) direction, meaning that each row that was peeled contained always pillars separated by 20 μm and the distance between rows varied between 30 and 150 μm. In the second case, the peeling was done in the left to right (LR) direction. In this way, the distance between rows was kept constant at 20 μm. The distance between pillars in the rows varied between 30 and 150 μm. The orientations are indicated in Figure 5.
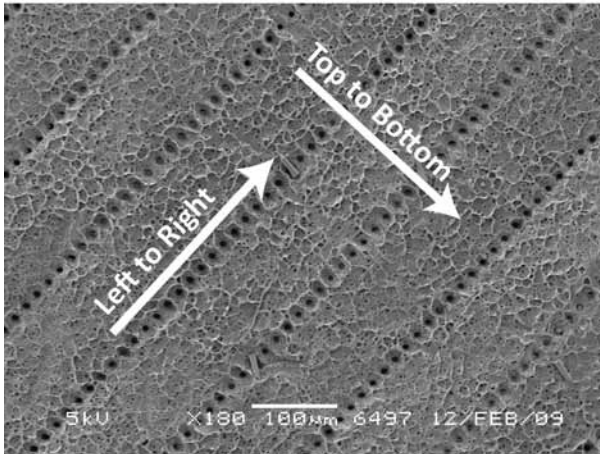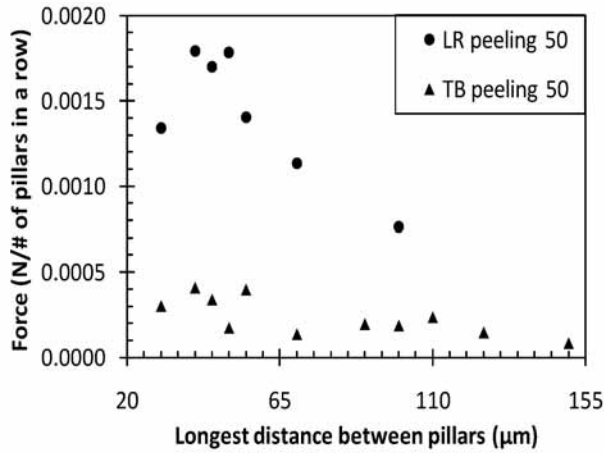
Figure 5: Peeling orientations for mold A and normalized measured forces.

Figure 5 also presents the force values for all the fields in both cases, normalized by the amount of pillars in each peeled row. We use this normalization because the

force is constant over the whole length of the field. As all rows are peeled consecutively, the number of pillars per row is more representative than the number of pillars per field. The values are the average of two determinations. It can be seen that the values for TB peeling are seemingly constant which can be explained by the fact that the peeled rows always possessed the same amount of pillars. For LR peeling, a downward trend for increasing pillar distance can be seen. In this case, the distance between rows is always the same, but the rows have fewer pillars as the distance increases. From this, it can be seen that the amount of pillars on each peeled row plays an important factor in determining the force required for release of the microsieves.

It should also be noted that the effect between rows is also important. All the points for the LR peeling are higher than those for the TB peeling. In LR peeling, each peeled row is 20 µm away from the following one and the distance between pillars is 30 µm or higher. Therefore, it can be concluded that it is harder to peel a row with fewer pillars if the following row is too close by. In other words, the distance between rows plays a more important role than the distance between pillars in a single row.

The same type of study was made then on mold B, casting the solution at 40 µm. The pillar height in this case was also 50 µm. Figure 6 shows the results obtained for one of the peeling orientations. The result in the other orientation is similar in trend. Both of the aforementioned effects (change in the quantity of pillars per row and distance between rows) are combined in this mold. A downward trend can be seen for increasing distances between pillars and rows. A lower density of pillars is therefore
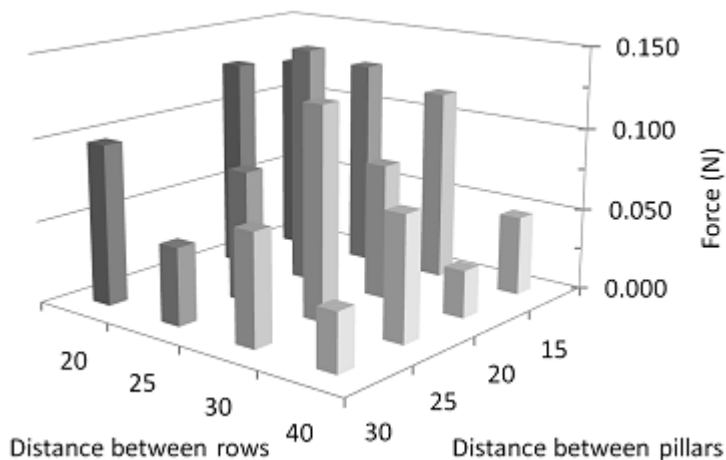
Figure 6: Effect of pillar densities on peeling force (Mold B).

more favorable for the production of microsieves with this technique.

As a last test, microsieves were also peeled from the same mold following the diagonal of the square fields. Since this increases the distance between pillars, the force values required for peeling decreased by 10—30% for the different fields at the same casting thickness of 40 µm. This shows that for a constant pillar density, the actual disposition of the pillars with respect to the peeling front must be taken into account.

3.2 Dependence on Pillar Disposition

Keeping the pillar density constant and similar to that on molds A and B, the effect of pillar placement was studied next using Mold C. In this case, the polymer solution was cast at 60 µm on a mold with a 40 µm pillar height. The pillar dispositions in this mold were already presented in Figure 3 and the results are shown in Figure 7.
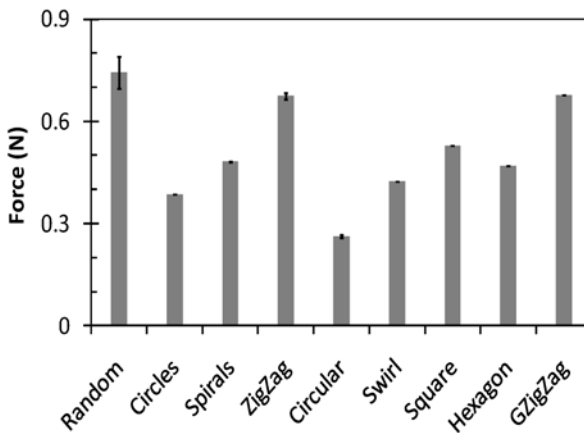
Figure 7: Effect of pillar dispositions on peeling force (Mold C).

It can be easily seen that the organization of the pillars on the mold affects the peeling force. It is also noticeable that the Square disposition is average regarding its performance. Random, Zig Zag and Group Zig Zag are worse than Square. The probable reason for this is that in some places in these dispositions, the pillars get too close to one another, making the peeling difficult.

Swirl on the other hand, represents an advantage when compared to Square. The only difference between these two dispositions is a rotation of 15 degrees for groups of 9 pillars contained between lines of pillars in their original position. This already gives

an improvement of 20%. The Circular disposition decreases the peeling force by half while the one with repeating Circles only by 25%. Circular is the only disposition that is not made from repeating units, but is one big array for the whole field.

As mentioned before, shrinkage during phase separation processes takes place both in the vertical as the lateral direction. Relative shrinkage is uniform, whereas absolute shrinkage depends on the actual length of the segment that shrinks. In the case of microstructured molds, the length of these segments is given by the distance between two features. The standard square array presents a distance equal to the pitch from center to center of the pillars. However, between pillars the shrinkage lines are as long as the field itself (see Figure 3, bottom left picture).

This means that upon shrinkage, the polymer is pulled against the pillars with the maximum available force for this field size. This is the reason why different dispositions were tried to assess the effect of the shrinkage lines on the peeling force. The idea behind the design of the mold was to try and break the maximum number of shrinkage lines possible, making them shorter (see Figure 3, bottom right picture). The absence of straight lines between the repeating units (lines that are as long as the field) creates a noticeable difference. From the results in Figure 7, it can be concluded that this approach was successful and our hypothesis is thus confirmed.

3.3 Dependence on Pillar Shape

Lastly, mold D was tested. This mold contained 9 fields in three rows. In the bottom row, a normal square array of round pillars (10 µm diameter, 50 µm pitch) was repeated in three fields. In the middle row, with a density similar to that of the bottom row, the pillar organization was changed to Circles, Circular and Swirl, the ones with the lowest peeling forces. In the top row, two alternative pillar shapes were introduced: crosses and hexagons. The height of the pillar was 40 µm and the casting thickness of the polymer solution, 50 µm.

The results are presented in Figure 8. The trend for the Square, Circle, Circular and Swirl dispositions is verified. Cross shaped and hexagonal pillars present lower values than round pillars. The reason for this can be seen in Figure 9 (right). Due to the lateral shrinkage in this particular system, the pillar shape is not replicated and actual pores tend to be circular. This decreases the contact area between polymer and pillar. This in
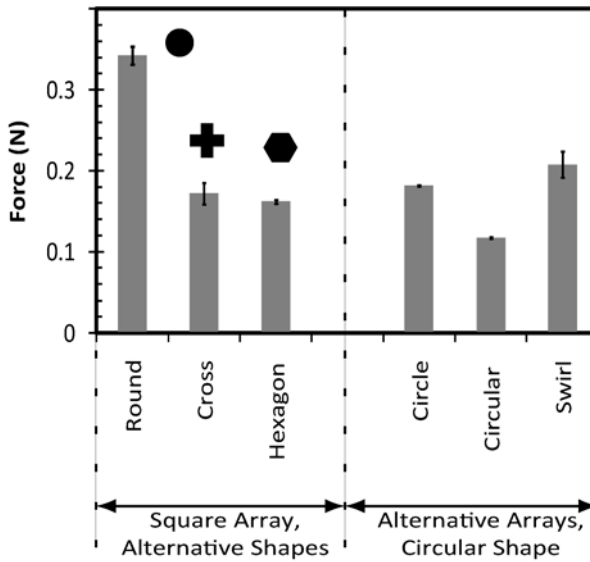
Figure 8: Effect of pillar shapes and dispositions on peeling forces (Mold D).

turn, decreases the friction and translates into a lower peeling force.

While this is good for improving the release conditions of the microsieve, it is not desirable for applications in which the shape of the pores must conform to specific requirements. The lack of replication fidelity has to do with the coagulation method, for a given polymer solution. The left hand picture in Figure 9 shows improved replication when coagulating in water vapor, followed by a butanol bath. A good replication of the hexagonal pillar can be seen. This is explained due to the mildness of butanol as a nonsolvent.

4. Conclusions

PSµF has been shown to be a simple, cost effective way to make polymeric microsieves. The technique can be applied to all polymers for which a suitable pair of solvent and nonsolvent can be found.

Pillar density has been presented as one of the main parameters affecting the quality and feasibility of release from the mold. It has been proven that square arrays of pillars with fewer pillars per row or higher distance between rows contribute to lower peeling forces. Furthermore, the effect of the distance between rows is more important than that of the distance between pillars in a single row. The increased

Coagulation in butanol. The pore replicates the
shape of the pillar due to decreased shrinkage.
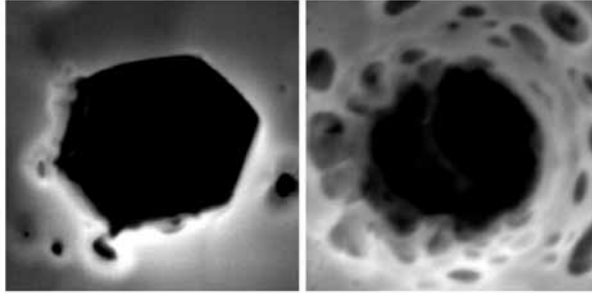
Coagulation in water. The polymer shrinks
away from the pillar, rendering a circular pore.

Figure 9: Effect of different nonsolvents used for coagulation.

distance between pillars caused a decrease in peeling force varying between 10 and 30% for different pillar densities.

Different pillar dispositions showed the importance of breaking shrinkage lines along the fields. In fields with repeating units, the lines between these units are occupied entirely by polymer solution, without features. As a result, the shrinkage of these lines pulls the polymer against the pillars, increasing friction, with the highest possible force for this system. Therefore, it is required to cut these lines shorter. In case of the square disposition, these lines are abundant, so almost any change is an improvement. However, the largest decrease in force was obtained with a circular array of pillars. This is ascribed to the fact that it consists of one single array for the whole field, therefore removing all the shrinkage lines between the repeating units.

Shrinkage is also responsible for improper replication of the pillar shape. Because of this, all pores in the membrane tend to round away from the mold walls. This is beneficial for peeling, as a lower contact area between pillar and membrane translates into lower friction and into lower peeling forces. If replication of the pillar shape is required, the use of milder nonsolvents has been shown to achieve this.

Microsieves are highly useful in microfiltration processes. The implementation of PSμF is a powerful tool for manufacturing them. The extensive choice of processable materials is now complemented with a thorough study of mold release properties

for a number of geometries. Carefully developed mold designs, polymer solution compositions and coagulation conditions ensure the attainability of products suitable for many applications.

5. Acknowledgements

6. References

[1] S. Kuiper, C. J. M. Van Rijn, W. Nijdam and M. C. Elwenspoek, Development and applications of very high flux microfiltration membranes, J. Membr. Sci., 1 (1998) 1

[2] G. Brans, A. van Dinther, B. Odum, C. G. P. H. Schroën and R. M. Boom, Transmission and fractionation of micro-sized particle suspensions, J. Membr. Sci., 1-2 (2007) 230

[3] M. Ulbricht, Advanced functional polymer membranes, Polymer, 7 (2006) 2217

[4] G. Veldhuis, M. Gironès and D. Bingham, Monodisperse microspheres for parenteral drug delivery, Drug Delivery Technology, 1 (2009) 24

[5] M. J. Geerken, R. G. H. Lammertink and M. Wessling, Tailoring surface properties for controlling droplet formation at microsieve membranes, Colloids and Surfaces A: Physicochemical and Engineering Aspects, 2-3 (2007) 224

[6] M. Gironès, Z. Borneman, R. G. H. Lammertink and M. Wessling, The role of wetting on the water flux performance of microsieve membranes, J. Membr. Sci., 1-2 (2005) 55

[7] A. M. Prenen, J. C. A. H. Van der Werf, C. W. M. Bastiaansen and D. J. Broer, Monodisperse, polymeric nano- and microsieves produced with interference holography, Adv. Mater., 17 (2009) 1751

[8] I. M. Yamazaki, R. Paterson and L. P. Geraldo, A new generation of track etched membranes for microfiltration and ultrafiltration. Part I. Preparation and characterisation,

J. Membr. Sci., 2 (1996) 239

[9] C. Greiser, S. Ebert and W. A. Goedel, Using breath figure patterns on structured substrates for the preparation of hierarchically structured microsieves, Langmuir, 3 (2008) 617

[10] S. F. Jahn, L. Engisch, R. R. Baumann, S. Ebert and W. A. Goedel, Polymer microsieves manufactured by inkjet technology, Langmuir, 1 (2009) 606

[11] L. Vogelaar, J. N. Barsema, C. J. M. Van Rijn, W. Nijdam and M. Wessling, Phase Separation Micromolding – PSµM, Adv. Mater., 16 (2003) 1385

[12] L. Vogelaar, R. G. H. Lammertink, J. N. Barsema, W. Nijdam, L. A. M. Bolhuis-Versteeg, C. J. M. Van Rijn and M. Wessling, Phase separation micromolding: A new generic approach for microstructuring various materials, Small, 6 (2005) 645

[13] M. Gironès, I. J. Akbarsyah, W. Nijdam, C. J. M. van Rijn, H. V. Jansen, R. G. H. Lammertink and M. Wessling, Polymeric microsieves produced by phase separation micromolding, J. Membr. Sci., 1-2 (2006) 411

[14] Chapter 3 of this Thesis.

[15] M. Gironès, L. A. M. Bolhuis-Versteeg, R. G. H. Lammertink and M. Wessling, Flux stabilization of silicon nitride microsieves by backpulsing and surface modification with PEG moieties, Journal of Colloid and Interface Science, 2 (2006) 831

[16] C. Ning Koh, T. Wintgens, T. Melin and F. Pronk, Microfiltration with silicon nitride microsieves and high frequency backpulsing, Desalination, 1-3 (2008) 88

[17] M. Gironès i Nogué, I. J. Akbarsyah, L. A. M. Bolhuis-Versteeg, R. G. H. Lammertink and M. Wessling, Vibrating polymeric microsieves: Antifouling strategies for microfiltration, J. Membr. Sci., 1-2 (2006) 323

[18] I. Cabasso, E. Klein, J.K. Smith, Polysulphone hollow fibres. II. Morphology. J. Appl. Polym. Sci., 21 (1977) 165

[19] R. M. Boom, I. M. Wienk, T. Van Den Boomgaard and C. A. Smolders, Microstructures in phase inversion membranes. Part 2. The role of a polymeric additive, J. Membr. Sci., 2-3 (1992) 277

Summary

M icrostructured polymeric films are fabricated by a novel replication method. A polymer solution is applied and contained between two substrates of which at least one is a patterned PDMS mold. The ensemble is then put in an atmosphere containing water vapor, which diffuses through the PDMS. The absorption of water into the polymer solution causes the phase separation of the polymer while in contact with the microstructured molds. The thickness of the PDMS slab can be exploited to tune the water vapor transport and hence the phase separation kinetics and resulting polymer morphology. Removal of excess polymer solution from between two PDMS slabs, followed by vapor induced phase separation, can also result in microperforated polymer films with great control over the dimensions.

1. Introduction

As mentioned in Chpater 3, shrinkage is inherent to the phase separation of polymer solutions. While this facilitates the release from the mold, it can also deform the replicas of the features [1]. Another common disadvantage in play with PSμF is that the phase separation is always induced from the nonstructured side (i.e., the side that is not in contact with the mold and is open to the coagulating agents). As the nonsolvent diffuses into the polymer solution, it drags along solvent with it. This creates a variation in local concentration of nonsolvent across the membrane, leading to pore size differences. As a result, the selective layer of a membrane is located on the unstructured side. This is the side where the smallest pores are formed.

In this chapter, we introduce flexible silicon rubber molds on nonwoven supports for use in Vapor Induced Phase Separation Microfabrication (VIPSμF), illustrated in Figure 1. The high permeability of PDMS for nonsolvent vapor makes it an ideal mold material. To the best of our knowledge, this is the first time PDMS is used as a permeable mold that allows the addition of a nonsolvent to a polymer solution, yielding (also as a first) bistructured porous polymeric films. This is interesting because of all the attention PDMS has gained lately as mold material, which has expanded the range of patterning processes to layer oxidation and buckling [2], laser molding [3], etc. Curing protocols have been optimized to the point of facilitating the production of 40-nm-big features [4]. The laser method is especially appealing as it can be readily used for big areas, which would make the production of belts feasible for continuous processing.

1. Polymer solution casting

2. Addition of the second mold

3. Vapor induced phase separation

4. Release

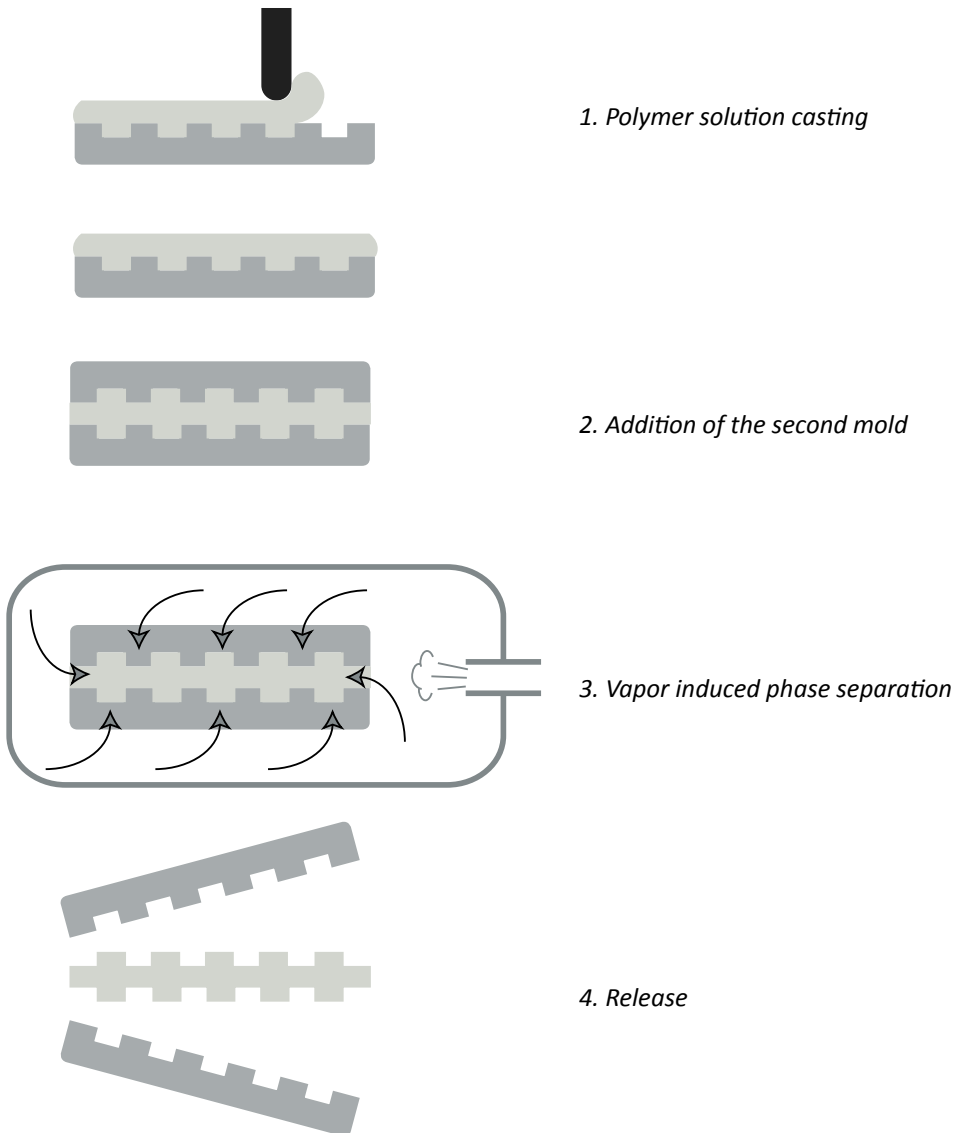*Figure 1: VIPSμF process.*

2. Experimental

2.1 PDMS Mold Preparation

SU-8 (Microchem) was used to create the master from which the PDMS molds were replicated. SU-8 is an epoxy based negative resist that is sensitive to ultraviolet radiation. Silicon wafers with SU-8 structures with the desired features were prepared in cleanroom facilities. Where needed, multiple layers of SU-8 were processed.

Subsequently, the wafers were hydrophobized through contact with trichloro-perfluorooctylsilane vapor (FOTS, Aldrich Chemicals) at 120°C for 2 hours, then cooled to room temperature and heated again to 100°C for 1 hour.

A 10:1 poly (dimethylsiloxane) (PDMS, Silicone RTV 615 A/B, General Electric) pre-polymer–cross-linking agent mixture was degassed for 0.5 h and cast onto the hydrophobized wafer at a 100 µm thickness. After 15 minutes at 60°C a polyethylene nonwoven support layer was put on top of the liquid. The PDMS was then allowed to cure for a total of 4 h at 60°C.

2.2 Materials and Solution Preparation

Two polymer solutions were used in these experiments. The first one was made of poly (ethersulfone) (PES, Ultrason, E6020P) in a concentration of 15 wt.% in N-methylpyrrolidone (NMP, 99%, Acros Organics). Poly (vinylpyrrolidone) (PVP K30, Fluka) was added to the solution. PVP is commonly used to create a percolating porosity and a hydrophilic surface [5]. It also acts as a macrovoid formation inhibitor [6]. Its concentration was 5 wt.%.

The second solution was made by dissolving poly (L-lactic acid) in a concentration of 10 wt.% (PLLA, kindly provided by D. Grijpma, Department of Polymer Chemistry and Biomaterials, University of Twente) in dioxane (Merck, analytical quality). This solution was only used for the experiment depicted in Figure 5.

Tap water vapor was used as nonsolvent. All reagents were used as received, without further purification. Unless otherwise specified, solutions were prepared by weighing all the components into a plastic bottle and left on a rolling bank until complete dissolution.

2.3 Membrane Fabrication

The polymer solution was always administered with the help of a pipet and cast with casting knives of 100 µm clearance. If a flat glass plate or a silicon wafer were used, the polymer solution was cast onto them and the PDMS mold was later laid onto the liquid layer. If both sides were structured with PDMS molds, a bit of polymer solution was cast onto both molds, which were then brought in contact and pressed lightly with

a roller. For perforated membranes, the molds were pressed against each other with the help of a lamination machine.

When the ensemble was ready, it was suspended in a pot above the surface of boiling water. The pot was covered with its lid, which possessed a small hole for purging. In this way, an environment of pure water vapor (air free, thus not 100% relative humidity, but 100% water vapor) could be created for the coagulation of the membranes, which usually took less than 10 minutes.

2.4 Membrane Treatment and Inspection

Membranes were rinsed with water overnight and broken in liquid nitrogen when needed for cross-section pictures or cut with a scalpel for surface pictures. Prior to SEM inspection (Jeol JSM 5600LV), the membranes were dried overnight under a vacuum at 30°C and then sputtered with gold (Balzers Union SCD040).

3. Results and Discussion

3.1 VIPS through PDMS

Inducing phase separation in a polymer solution with vapor requires a sustained and significant flow of this vapor into the solution. This is the reason why the mold material should present very high water permeability. Table 1 shows a list of water vapor permeability values for common polymers. It can be observed that PDMS is indeed highly open for water vapor transport.

PDMS is a readily accessible material and as it can be acquired as a curable liquid, it can be molded in a very easy way. It is mechanically and chemically stable and according to our experiments does not swell extensively when in contact with NMP (very common solvent for polymer solutions). All these characteristics make it the ideal candidate for molding in our systems. The layers in use were usually around 100 µm thick. To ease handling, a layer of a nonwoven support was introduced at the unstructured side early during the curing process. In this way, a more robust film was obtained.

Polymer	Abbreviation	H$_2$O Permeability (Barrer=7.5 10^{-18} m^2 s^{-1} Pa)	Reference
Poly (ethylene)	PE	12	[7]
Poly (vinylalcohol)	PVA	19	[7]
Poly (propylene)	PPO	68	[7]
Poly (amide 6)	PA-6	275	[8]
Poly (vinyl chloride)	PVC	275	[9]
Poly (acrylonitrile)	PAN	300	[8]
Poly (imide) (Kapton)	PI	640	[9]
Poly (styrene)	PS	970	[7]
Poly (carbonate)	PC	1400	[8]
Poly (sulfone)	PSF	2000	[8]
Natural rubber	NR	2600	[8]
Poly (ethersulfone)	PES	2620	[8]
Poly (phenyleneoxide)	PPO	4060	[9]
Cellulose acetate	CA	6000	[7]
Sulfonated poly (ethersulofone)	SPES	15000	[10]
Ethyl cellulose	EC	20000	[9]
Poly (dimethylsiloxane)	PDMS	40000	[11]
Sulfonated poly (etheretherketone)	SPEEK	61000	[12]
1000$_{PEO}$56$_{PBT}$44	PEO-PBT	85500	[13]

Table 1: Water vapor permeability for various polymers at 30°C, extrapolated to 0 water vapor activity.

PDMS controls the vapor transport during the VIPS process. We have carried out experiments to help us assess its effect on the final morphology of the film. These experiments involved the casting of a 100 μm thick layer of polymer solution on a smooth glass plate and covering it with a smooth PDMS film (100 μm or 300 μm thick). Figure 2 shows the effect of the PDMS layers on the porous morphology of the cross section of the polymeric film. As can be seen, a layer of 100 μm of PDMS does not cause significant changes on the cross section of the membrane compared to an uncovered film. The 300 μm layer of PDMS causes a noticeable growth of the pores.

Work on poly (ether imide) membranes formed from an NMP solution through VIPS with water vapor show a similar behavior when the amount of vapor in the coagulation atmosphere is lowered. The size of the cells decreases with increasing relative humidity [14]. Furthermore, cellular structures are only obtained when the relative humidity of the vapor bath is above 27%. It seems that this affects the position where the binodal

is entered and how fast this is done [15].
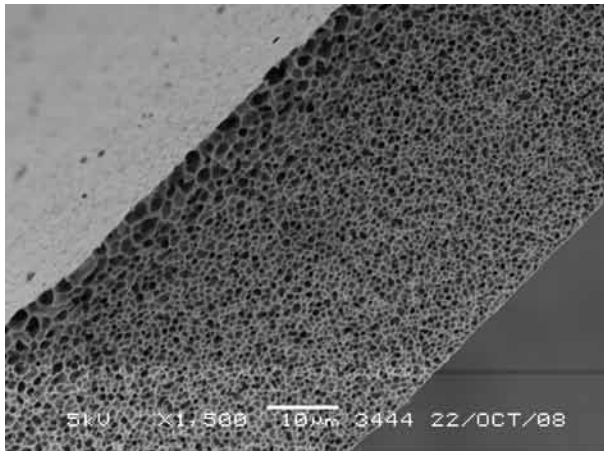
No PDMS
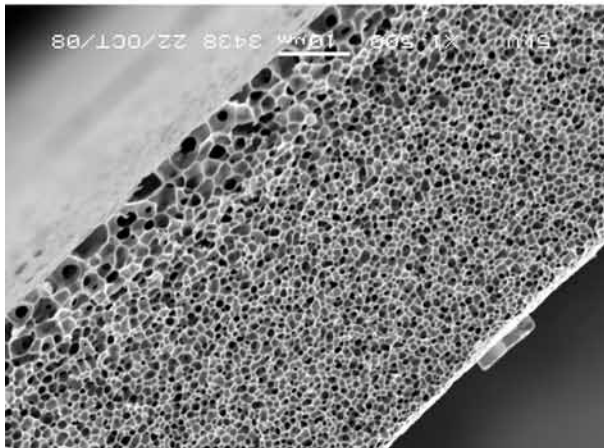
100 µm thick slab of PDMS
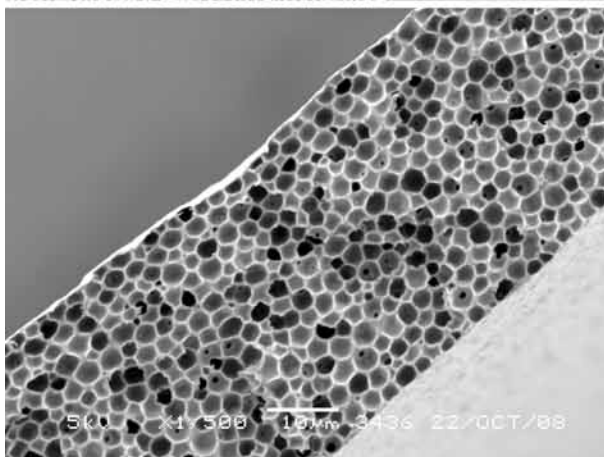
300 µm thick slab of PDMS

Figure 2: Effect of PDMS on phase separation process. The side in contact with the PDMS slab is facing up.

Having observed that PDMS is a suitable material for controlling water vapor permeation, we have made different molds. Following the methods described in the experimental section, multiple structures can be created with PDMS. See Figure 3 for different examples of molds with lines or pillars. The introduction of gutters to facilitate the distribution of the excess of polymer solution is also shown.

Lines

Pillars

No Gutters   *With Gutters*
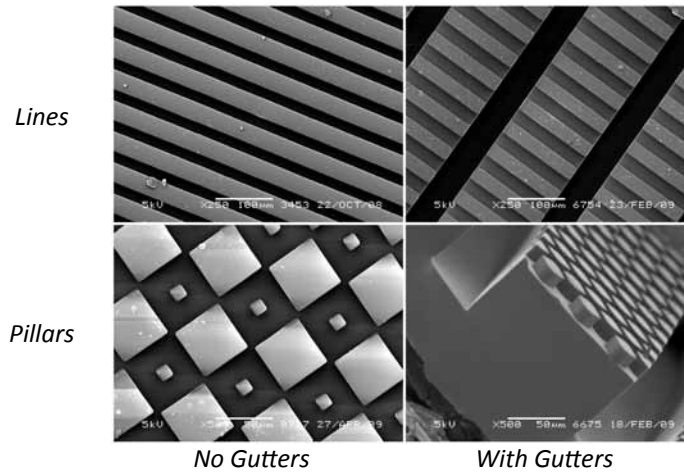
Figure 3: Molds made of PDMS.

PES
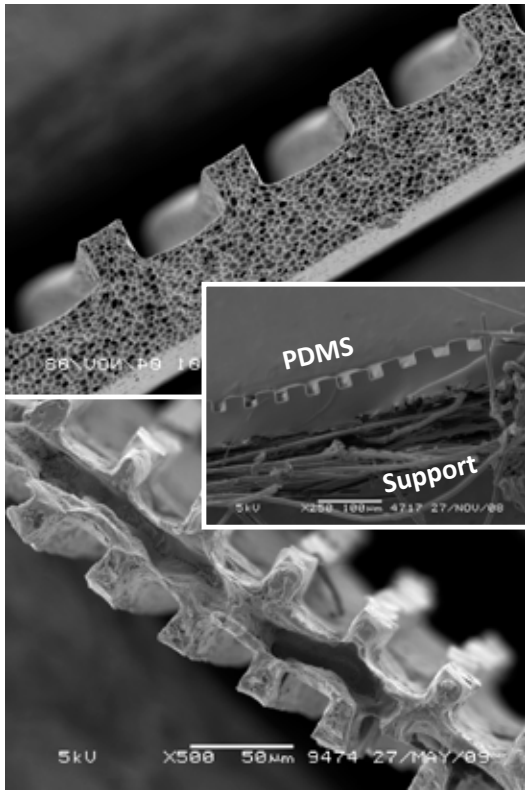
Mold

PLLA

Figure 4. TOP: membrane made from PES, between a glass plate and the shown mold. BOTTOM: membrane made from PLLA between two of these molds.

VIPSµF

PSµF
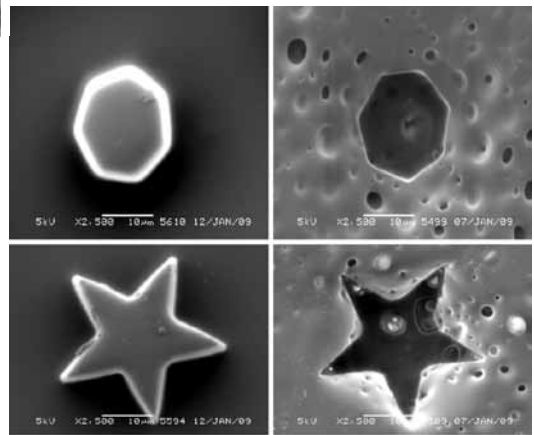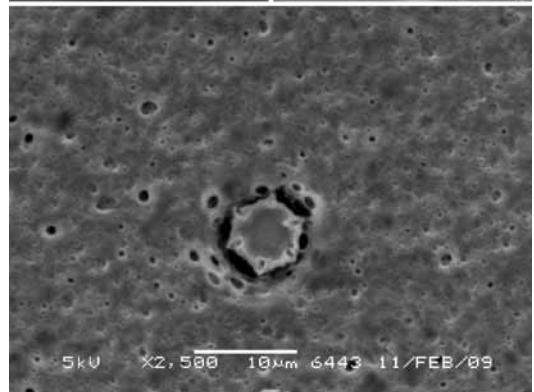
Figure 5: VIPSµF exceeds PSµF in replication fidelity.

3.2 Replication from Permeable Molds

Figure 4 depicts two membranes with line patterns and the flexible mold used to obtain them. In the top case, the polymer solution was applied on a glass plate. After casting with a knife, a PDMS mold with a line pattern (inlay in the middle the figure) was laid on it. The replication of the features is successful, with no disagreement in dimensions between mold and membrane. In the bottom case, the PLLA solution was contained between two PDMS molds. Shrinkage related phenomena as observed with solid silicon molds is not observed here [16].

The same experiment was carried out using a PDMS mold with pillars of different shapes. Figure 5 shows the replication of pillars in the shape of a star and a heptagon. In the picture presented here, the structures are replicated perfectly. These features would suffer from shrinkage in regular Phase Separation MicroFabrication [16]. The bottom picture in Figure 5 shows the lack fidelity in the replication of a hexagon via regular PSμF, resulting in rounded corners. This phenomenon is not observed here, where the star in the membrane matches the star on the mold with excellent agreement. A reason for this could be that the polymer solution begins to solidify at the layer containing the features. The walls of the features themselves are the first ones to solidify. In other words, in VIPSμF through PDMS the nonsolvent comes from the structured side. This is not the case in regular PSμF.

This effect can be notoriously seen in Figure 6. This membrane was obtained through phase separation of a membrane contained between a silicon wafer (left side in the figure) and a PDMS mold (right side), both containing line patterns. The agreement between the membrane and the mold on the PDMS side is again remarkable. This is the first layer to solidify upon contact with vapor. The nonsolvent cannot penetrate through the silicon wafer. The features on the left side are rounded even though the mold is sharp edged. This layer is the last one to solidify. The nonsolvent required comes through the PDMS mold and diffusing through the solidified polymer solution in between. Shrinkage plays, therefore, a major role. An interesting phenomenon is the deformation of the pores on the PDMS side, required to comply with the confinement of the mold. This is not observed on the silicon side.

The advantages of using PDMS molds regarding shrinkage can be exploited on both sides of a membrane by replacing the silicon wafer mentioned before with

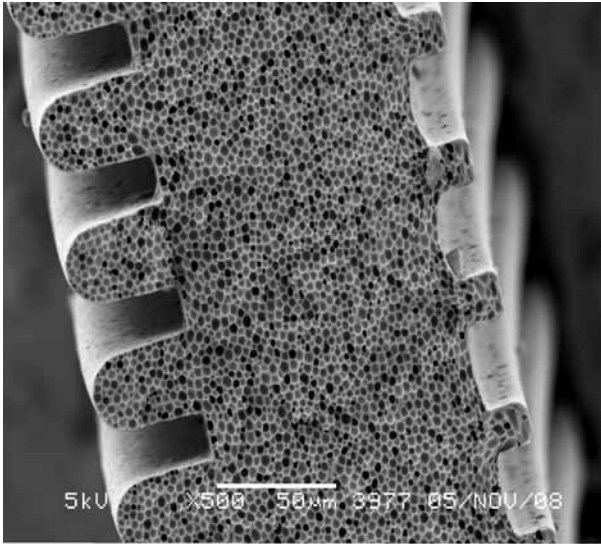*Figure 6: PES membrane made between a silicon wafer (left side of the membrane) and a PDMS mold (right side). Shrinkage is observed on the side in contact with the impermeable mold.*

Cross Section
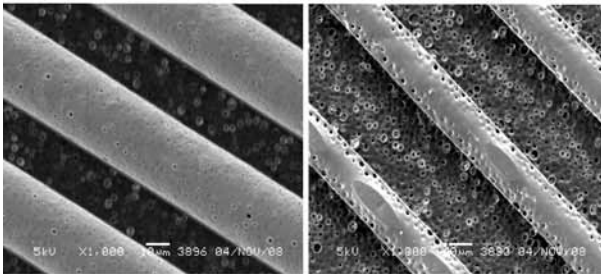
Surface Views:
Silicon Mold side - PDMS Mold side

Cross Section
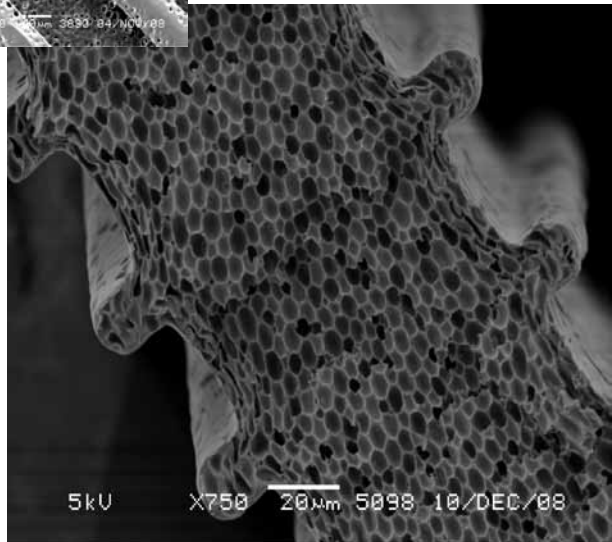
Surface Views
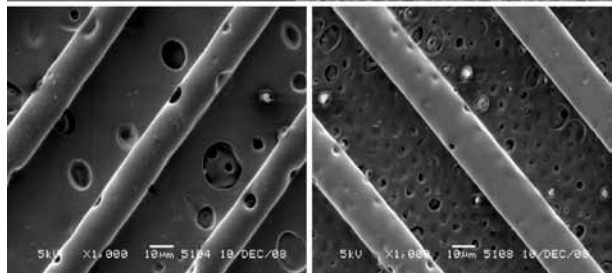
Figure 7: PES membrane made between two PDMS molds. No significant shrinkage is observed.

another PDMS mold. The vapor can, in this case, enter from both sides. Figure 7 shows a membrane obtained using said configuration. This membrane shows well replicated structures on both sides, with comparable size. An added advantage to this type of arrangement is the shortening of coagulation times, because of water diffusion from both surfaces of the membrane.

3.3 Perforated Membranes

The arrangement of pores with well-defined size and ordering is desirable for different applications [17]. The so-called microsieves present this functionality. While there are inorganic microsieves made of silicon nitride, polymeric microsieves present many advantages. Polymeric microsieves are more flexible, less brittle [18] and cheaper to produce.

Gironès et al. have demonstrated the use of PSμF to make polymeric microsieves [19]. The solution is cast onto a silicon wafer containing pillars with size corresponding to the desired pore diameter. Upon solidification and release, a perforated membrane is obtained. This method is straightforward and relatively simple. The shrinkage phenomena taking place on the horizontal direction can cause some deformation on the pores, through stretching of the polymer against the pillars. This complicates the release from the mold. Furthermore, the silicon molds are quite sensitive toward damaging during the process. (See Chapter 5)

We have fabricated microsieves by using VIPSμF with PDMS molds. For this, the polymer solution was cast onto a smooth PDMS slab with no structures. Afterwards, the solution was covered with another PDMS mold consisting of pillar fields. The ensemble was pressed together to ensure that the top of the pillars would touch the smooth PDMS layer. In this way, the excess polymer was pushed away. The ensemble was then put in water vapor environment to induce the phase separation. Figure 8 presents a microsieve obtained using this method, with a pore diameter of about 25 μm and a membrane thickness of 8 μm. The pores are separated 50 μm from each other. The mold in question presented pillars of 20 μm in diameter, about 15 μm in height and located 50 μm from each other. The size of the pores is about 25% bigger than the diameter of the pillars. This can be the effect of squeezing the pillars. Also, the membrane is much thinner than the height of the pillars.
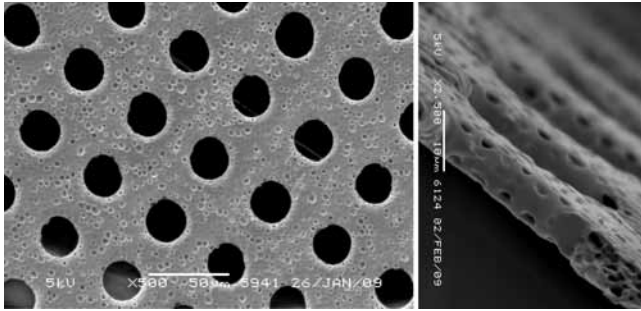
Figure 8: A microsieve made via VIPSµF.
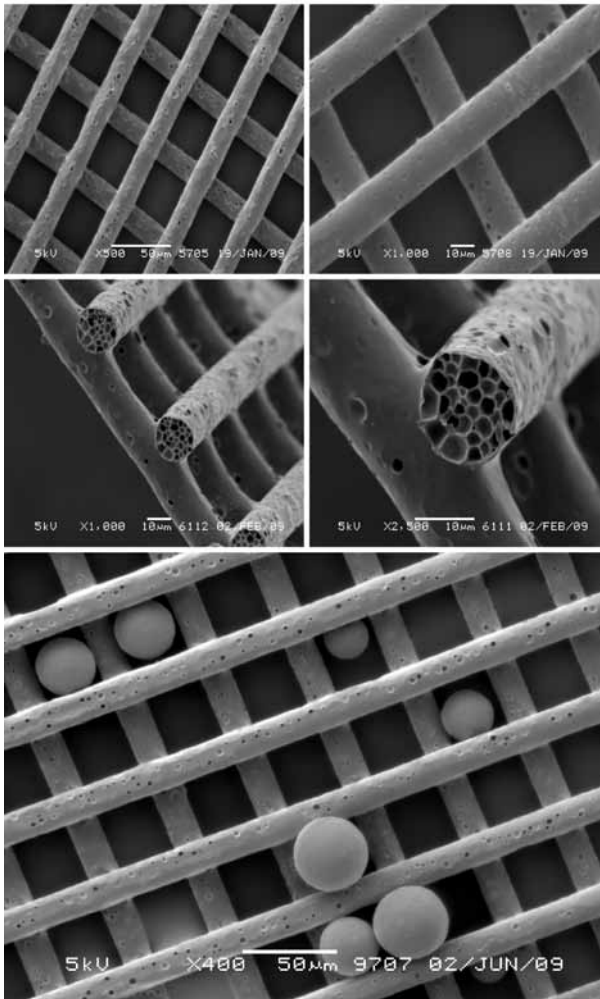
Figure 9: A Sieving Microfence made via VIPSµF.
Bottom: Use of a Microfence for the filtration of polymeric beads.

In another approach, we have tried using two PDMS molds containing a line pattern, but rotating one of the molds 90 degrees with respect to the other. By doing this, the polymer solution was allowed to fill the lines on both molds, leaving gaps where the two molds touch each other. The molds were pressed together to squeeze out the excess of polymer solution. Figure 9 shows a good example of a Sieving Microfence with square pores of 20 μm. As can be seen, the structure is well-defined. The fabrication method does not rely on perforation and the mold does not contain pillars. This allows for durable molds, easy processing and trouble-free release. Figure 9 also shows that the filtration of polymeric beads is possible with these filters.

A disadvantage of the process is the lack of homogeneity in distributing the polymer solution by pressing the two molds against one another. Isolated thicker regions can be easily spotted on the newly formed membrane once it is peeled off the mold. In an effort to overcome this challenge, we have designed molds with gutters of increased depth, located every 100 μm. The result was a great improvement in the homogeneity of the membrane.

4. Conclusions

In this case, we have shown that the use of PDMS makes for flexible, permeable molds. This is of high importance for a better replication of the structures. The opportunity to start the solidification process from the structured size guarantees that the features are extremely well replicated. Their structure is fixed and the layers of solution underneath them will not have an effect on them. This is not the case for PSμF on silicon wafers, as these are impermeable.

The use of permeable molds on both sides of the polymer solution allows for membranes with structures on both sides. Furthermore, pressing these molds against one another creates mold contact regions where no polymer solution is present. Upon solidification, these voids become pores through the film. Using this phenomenon and two molds containing line patterns, microfences were made. These fences present an arrange of square pores produced without need for perforation by the mold, simplifying the process of micromesh making. These filters present the advantage of generating turbulence on both of their sides, due to the presence of ridges.

PDMS is a widely known material, structured through multiple methods. Its inclusion in PSµF extends the accessibility of this technique. In this way, the molding of polymers through phase separation can be implemented by researchers with considerable simplicity. Furthermore, no cleanroom facilities are required.

5. Acknowledgements

Ineke Pünt, for the extensive practical work made for this chapter.

6. References

[1] L. Vogelaar, R. G. H. Lammertink, J. N. Barsema, W. Nijdam, L. A. M. Bolhuis-Versteeg, C. J. M. Van Rijn and M. Wessling, Phase separation micromolding: A new generic approach for microstructuring various materials, Small, 6 (2005) 645

[2] A. Chiche, C. M. Stafford and J. T. Cabral, Complex micropatterning of periodic structures on elastomeric surfaces, Soft Matter, 12 (2008) 2360

[3] D. B. Wolfe, J. B. Ashcom, J. C. Hwang, C. B. Schaffer, E. Mazur and G. M. Whitesides, Customization of poly(dimethylsiloxane) stamps by micromachining using a femtosecond-pulsed laser, Adv. Mater., 1 (2003) 62

[4] X. Ye, H. Liu, Y. Ding, H. Li and B. Lu, Research on the cast molding process for high quality PDMS molds, Microelectronic Engineering, 3 (2009) 310

[5] I. Cabasso, E. Klein, J.K. Smith, Polysulphone hollow fibres. II. Morphology. J. Appl. Polym. Sci., 21 (1977) 165

[6] R. M. Boom, I. M. Wienk, T. Van Den Boomgaard and C. A. Smolders, Microstructures in phase inversion membranes. Part 2. The role of a polymeric additive, J. Membr. Sci., 2-3 (1992) 277

[7] J. A. Barrie, Diffusion in Polymers, (1968)

[8] S. M. Allen, M. Fujii and V. Stannett, The barrier properties of polyacrylonitrile, J. Membr. Sci., 2 (1977) 153

[9] J. A. Barrie, Proceedings of the Fourth BOC Priestly Conference, (1986) p. 89

[10] L. Jia, X. Xu, H. Zhang and J. Xu, Permeation of nitrogen and water vapor through sulfonated polyetherethersulfone membrane, Journal of Polymer Science, Part B: Polymer Physics, 13 (1997) 2133

[11] M. Mulder, Basic principles of membrane technology, Kluwer Academic Publishing (1991)

[12] S. Liu, F. Wang and T. Chen, Synthesis of poly(ether ether ketone)s with high content of sodium sulfonate groups as gas dehumidification membrane materials, Macromolecular Rapid Communications, 8 (2001) 579

[13] S. J. Metz, W. J. C. Van De Ven, J. Potreck, M. H. V. Mulder and M. Wessling, Transport of water vapor and inert gas mixtures through highly selective and highly permeable polymer membranes, J. Membr. Sci., 1-2 (2005) 29

[14] H. Caquineau, P. Menut, A. Deratani and C. Dupuy, Influence of the Relative Humidity on Film Formation by Vapor Induced Phase Separation, Polymer Engineering and Science, 4 (2003) 798

[15] S. P. Nunes and T. Inoue, Evidence for spinodal decomposition and nucleation and growth mechanisms during membrane formation, J. Membr. Sci., 1 (1996) 93

[16] Chapter 3 of this Thesis.

[17] M. Ulbricht, Advanced functional polymer membranes, Polymer, 7 (2006) 2217

[18] M. Gironès i Nogué, I. J. Akbarsyah, L. A. M. Bolhuis-Versteeg, R. G. H. Lammertink and M. Wessling, Vibrating polymeric microsieves: Antifouling strategies for microfiltration, J. Membr. Sci., 1-2 (2006) 323

[19] M. Gironès i Nogué, I. J. Akbarsyah, W. Nijdam, C. J. M. van Rijn, H. V. Jansen, R. G. H. Lammertink and M. Wessling, Polymeric microsieves produced by phase separation micromolding, J. Membr. Sci., 1-2 (2006) 411

Summary

I t has been shown throughout this thesis that PSµF is a powerful technique for the structuring of polymeric films. In this chapter, the main findings of this research are summarized. An outlook on the future of the field and suggestions for further research are also given.

1. Conclusions

Chapter 2 describes the formation of polymeric membranes through phase separation processes in terms of a balance between thermodynamic and kinetic aspects. It is explained that the most favorable processes (like crystallization) from a thermodynamic point of view are not always undergone. This is because of the nature of phase separation of polymer solutions. The creation of solid boundaries results in a regulation of the transport of all the components involved. The diffusion of these components creates local variations in composition, yielding asymmetric membranes. The resulting morphology can be tuned through the variation of different parameters and this knowledge has been used through the rest of this thesis.

The phase separation of polymer solutions is accompanied by shrinkage phenomena. This has been studied in Chapter 3. The shrinkage has been proven to vary with the polymer concentration of the casting solution. For concentrations below and above certain values, the shrinkage decreases with increasing concentration. This is related to the presence of more polymeric material per unit volume of solution. Between these two values, the trend is reversed due to a higher compaction of the polymeric material, which leads to denser and thinner membranes. The extent of the vertical shrinkage is much larger than that of the horizontal one. The effect of shrinkage on the replication of features has been found to increase for as the amount and/or size of the features decreases. Deeper features can cause thinning of the overlying film and can lead to rupture at the points where they meet the film.

Chapter 4 deals with the effect caused by bubbles on structure replication when molds with wells are used. The mechanism for bubble formation has been identified as the rearrangement of the gas enclosed in the features of the mold during the application of polymer solution on the mold. These bubbles disappear through dissolution in the polymer solution. The speed with which this happens is directly related to the affinity of the gas for the components in this solution. Carbon dioxide has been found to dissolve much more quickly than nitrogen or oxygen. The polymer in use has been found to have no significant effect on the solubility of nitrogen in the solution, but the diffusivity of nitrogen decreases upon an increase in its concentration.

The design and production of microsieves has been explored in Chapter 5. The process has been optimized through the creation of different molds and the

introduction of a peeling device. General trends indicate that a lower density of pillars in the mold facilitates the release of the microsieves from it. This can be related to the friction between the solidified polymer and the mold material, as well as to the spacing of the pillars on the peeling direction. Further improvements can also be achieved by introducing alternative pillar geometries and placements on the molds. Different pillar geometries work by decreasing the contact area between polymer and pillar. The shrinkage of the polymer solution around the pillar decreases the contact between the almost circular pores and the non-circular pillars. The use of alternative pillar placements helps in breaking shrinkage lines that are responsible for pulling the polymer against said pillars.

Chapter 6 presents the use of permeable molds made of PDMS for the structuring of polymeric films. These molds have the advantage of allowing the structuring on both sides of a film. This is done through the addition of nonsolvent through the molds. The possibility of inducing the phase separation from the structured side enhances replication fidelity. By pushing away the excess of polymer solution between the molds and bringing them into contact, perforated membranes can be made with ease. Microfences have been fabricated following this method, greatly simplifying the production of polymeric meshes.

2. Outlook

Membrane separation processes are gaining increasing attention. In most cases, this is mainly due to the fact that most of the challenges awaiting the world in the years to come require appropriate separation performance at the molecular level. The production of drinking water (from salt water or through recycling of waste water) must still be optimized. The capture of carbon dioxide from different mixtures and its subsequent storage are challenges for which no satisfying solution has been found yet. When biomass is used as a source of energy, the product and byproduct streams tend to contain high amounts of water and are produced in high amounts. The dehydration of these streams is, therefore, a challenge.

In other cases, this has to do with the higher energy efficiency of these techniques, compared to traditional purification methods. The role of membranes in energy related

applications is growing. The development of fuel cells and flow batteries increases the options for clean, portable energy. The research into pressure retarded osmosis brings about a new method for securing energy in larger quantities.

Literature indicates that up to now, the development for membranes and polymeric films was limited to the choice of material. Considering the requirements posed by the application, the right polymer is chosen. It can be according to its performance in the desired separation, due to its chemical, mechanical or thermal stability, or even due to how quickly it can be degraded after it has served its function. It is only very recently that attention is being devoted to structuring these films. Still, the right methods for creating it are not well known.

From this thesis, it can be seen that PSµF is a very powerful and versatile method for creating a wide range of topologies on polymeric films. These products can be used in different fields, offering different advantages to each of them. In filtration processes, the inclusion of surface topologies can be of great influence on fouling behavior of systems. This applies also for fibers. In the case of microsieves used for clarification of streams, the use of a highly ordered and well defined porosity can help in the fractionation of particles by size. For emulsification devices, the creation of a monodisperse emulsion is easily attainable through the control of the variables in play. In the case of tissue scaffolds, the ease with which biodegradable materials can be structured helps in ensuring good cell growth, combined with the needed alignment and signaling for the creation of different types of tissue. For the fabrication of stamps for Micro Contact Printing, the high control on the dimensions of the replicas makes for a very well defined system. In microfluidics, the use of porous polymeric films adds a membrane functionality to the walls of microreactors. For superhydrophobic surfaces, PSµF offers the possibility of varying the roughness of surfaces to the micron and submicron scales. These are the applications we have been working on, but many more can be thought of. Considering the virtually limitless possibilities of PSµF and the growing interest in polymers, it is expected that the interest in this field will increase in the following years.

We started by exploring the available literature for the phase separation of polymer solutions. The first thing that we observed is the lack of uniform terminology for referring to the different components, variables and mechanisms involved in this process. It takes a lot of deciphering to read an article and the general impression is

that only a very basic knowledge of this phenomenon has been gained so far.

This can be ascribed to different factors but it is my personal belief that coupling this process to accurate models and in situ measurements is quite complicated. Current models do not capture all the events taking place in such a complicated system. Measurements are often affected by all the solid boundaries that are formed during the process. However, most of the effort must be devoted to these two areas. It is only through these experiments that a thorough comprehension of the process can be achieved and general conclusions can be derived.

We have tried acoustic reflectometry for measuring the phase separation and the shrinkage process online. Not much success was attained due to the relative short amount of time available for it. The technique, however, seems to be able to follow this process well. However time consuming it may be, it is strongly advised to use it for measuring the shrinkage process. The discovery of the dynamics of this process can be enlightening for the understanding of phase separation in general. Especially, if different phase separation mechanisms can be followed. The lack of contrast between solid and liquid phases will limit this technique to VIPS, as the interface between the precipitated polymer and the coagulation bath cannot be detected. Because of this same reason, the interface between the precipitated polymer and the remaining polymer solution is also tricky to identify. This problem can be overcome through the use of transducers with high frequencies.

As mentioned several times throughout this text, the main advantage of PSµF is its universality. Virtually all polymers can be structured in a simple way. Besides, considering the different structures shown in all chapters of this book, the process is versatile and allows for the formation of a large range of patterns. The main disadvantage of the technique is linked to the same universality. Namely, a change in polymer solution or mold often leads to a re-optimization of the process. However, a strong message that can be derived from this thesis is that it is only a matter of trying until the right nail is hit on the head. Chapter 3 constitutes a good guide in foreseeing the problems that can arise for using a specific mold. For the use of different polymer solutions, it might be possible to explore if there is a correlation between shrinkage and physical parameters such as viscosity, diffusivity, solubility parameters, etc. In this way, general criteria for more systems can be developed.

The recommendation regarding this aspect of the research is the allocation of time and resources for preliminary research before embarking upon an ambitious project. PSµF is a technique that can be used for different systems and to create multiple structures. This does not mean that it can be used directly. However, the simplicity and relative low manufacturing cost that can be achieved through it justify the time invested in ensuring that the product is indeed what we desire to obtain.

This groundwork includes the compositions of the polymer solution and coagulation bath and especially, finding a clever way to design the mold that will enable us to obtain the features we want. The optimization of mold design is not only limited to the disposition, size and depth of the features. Different etching techniques can be used that generate features of varying geometry (Figure 1). In our case, we have used Deep Reactive Ion Etching, which leads to features with straight walls at straight angles from the surface of the substrate and the bottom of the feature. Wet etching, on the other hand, is isotropic, rendering features of circular walls. The etching can also be done along oblique crystalline planes, giving features with walls at 45 degrees from the surface of the mold. Replicas of this type of features could greatly improve the performance of features as spacers, greatly diminishing the regions of stagnant flow.

Deep Reactive
Ion Etching

Etching along an Oblique
Crystalline Plane
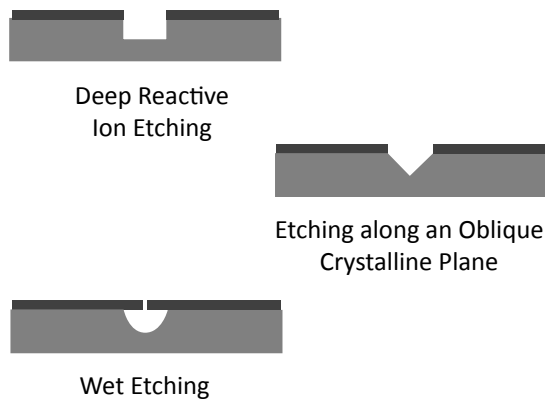
Wet Etching

Figure 1: Different etching techniques and results obtained.

The work on microsieves presented in Chapter 5 is a good example of mold optimization. Keeping the pillar density constant and changing the disposition in the molds, it has been proven that the interruption of shrinkage lines greatly diminishes the force required for peeling microsieves. This agrees well with previous findings of Vogelaar (see also Chapter 3) that proved that the distortion between features is proportional to the distance between said features. As we said, relative shrinkage can be expected to be uniform for each layer. Therefore, the larger the distance between
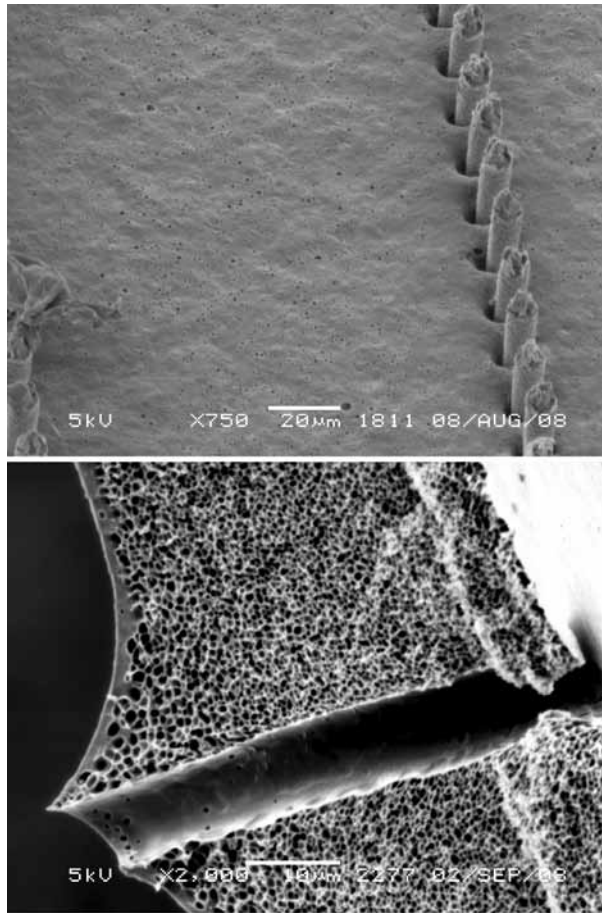
Figure 2. TOP: Due to increased friction, the pillars of this mold have been peeled along with the microsieve. BOTTOM: Chimney-like structures.

two features, the larger the absolute shrinkage will be. This translates into higher forces pulling the polymer against the pillars, inducing higher deformations due to stretching and larger friction for the release. This effect is minor towards the center of the pillar fields. If friction is too high, the pillars will be peeled off the mold along with the microsieve (Figure 2, top).

If a very mild nonsolvent is used during phase separation, a dense, thick skin is formed before further shrinkage starts. As the phase separation progresses, the shrinkage of the rest of the polymer solution pulls this skin against the pillars. Perforation takes place along with the stretching of this skin, creating chimney like structures. This kind of pores can help in emulsification applications due to pinning of the contact line,

limiting drop growth and coalescence (Figure 2, bottom). Another advantageous use of shrinkage in manufacturing microsieves can be introduced through changing the shape of the pillars. Due to shrinkage, upon solidification, the polymer retracts from the walls of the pillars. This retraction yields pores that are closer to a circular shape. As a result, a decrease in contact area between the pillar and the polymer is achieved. It has been shown here that this greatly contributes to decreasing the force required for peeling a microsieve off a mold.

The combination of alternative pillar shapes and dispositions is yet to be tried. However, the effects are not expected to superimpose linearly. The reason for this is that since the alternative dispositions of pillars are used to interrupt the shrinkage lines, less shrinkage takes place. Therefore, the retraction of the polymer from the walls of the pillars could be less pronounced. The extent of shrinkage can be varied through changes in the coagulation method of polymer solutions of varying compositions. This should also affect the force required for peeling. Unfortunately (and strangely enough), only little information is available in literature regarding shrinkage phenomena.

Chapter 4 has shown the effects of air entrapment during casting of a polymer solution onto a mold with wells. These wells are ultimately filled through the dissolution of the bubbles formed inside the features of the mold during casting. As a result, the dissolution speed is dependent on the gas that is entrapped and its solubility and diffusivity in the polymer solution in use. The casting of membranes in a glove box purged with different gases showed that this is relevant for PSμF. The time required to obtain solid polygonal pillars decreases greatly when changing the atmosphere from air to carbon dioxide.

This knowledge can be used to ensure the fabrication of polymeric pillars on a membrane through the selection of a highly soluble gas and the proper solvent for the polymer solution. On the other hand, the creation of freestanding structures can be induced using a gas with a low solubility, like nitrogen in our case. In this way, the bubble stays inside the feature and takes longer to dissolve away. The polymer solution occupies the corners and the top of the wells, allowing the bubble to achieve a uniform curvature. The phase separation of such a structure renders membranes on which flat sheets with the shape of the wells are connected to the membrane through bars originally present on the corners of said wells. To fully optimize this process, the interaction between gases, solvents and polymers must be measured. The use of a

sorption balance might be useful for this purpose.

Permeable PDMS molds have been tried as a means for initiating the phase separation from the structured side. The phase separation of a polymer solution contained between a PDMS mold and a silicon mold shows improved replication on the PDMS side. The structures on the PDMS mold are replicated with no distortion. PDMS molds with pillars of intricate shapes rendered membranes with indentations with outstanding geometrical agreement. By using two PDMS molds, membranes with structures on both sides were obtained. The benefits of diminished shrinkage were extended to the features on both surfaces on the membrane. Furthermore, by pressing the two molds together, contact regions are created.
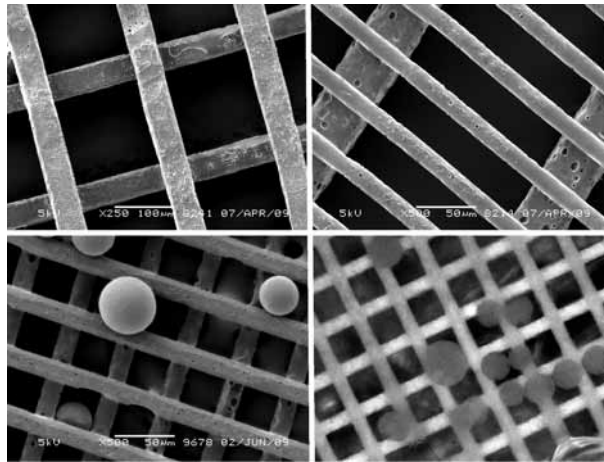
Figure 3: Different examples of Microfences. The bottom right picture has been obtained with the optical microscope, whereas the rest are SEM micrographs.

These regions are free of polymer solution and upon phase separation, membranes with perforations are obtained. By doing this, a new type of filter has been created: the Microfences (Figure 3). The properties of these filters in actual process conditions must still be tested. However, a high permeability is expected. The presence of structures on both sides is anticipated to affect local shear rates in both the feed and the permeate streams. Cleaning procedures are expected to be simple, since these filters can present virtually no in-pore fouling.

For the pore sizes presented in this thesis, these filters can find potential in the field of biology. The separation of cells is often size related and the geometry of the fence

ensures that pore blockage is minimum due to particle retention. This is expected since particles that are blocked sit on the ridges of the filter, never fully blocking the pore. This phenomenon is similar to that of filtration on microsieves with slit pores, where retained particles cannot block the entire pore. For cell culturing and tissue scaffolding, the openness of the filter is very appealing. The amount of polymeric material present in these filters is relatively low and the filter presents a mechanically stable structure. The versatility introduced by the use of PDMS molds allows to create fences with pores of different shapes and sizes. This makes for a platform technology with high potential.

In terms of the expected growth of PSμF as a process for the patterning of polymer films, PDMS molds offer a major contribution. This stems from the fact that the phase separation is induced from the structured side. This creates a structured skin or, in other words, increases the active selective area. This is fundamental in enhancing the performance of processes like ultrafiltration and reverse osmosis. The techniques in place nowadays for the structuring of PDMS slabs make the creation of long belts relatively simple. The implementation of PSμF as a continuous process becomes, therefore, possible in a cheap and reliable manner (Figure 4). The greater control on replication dimensions is an additional bonus. Furthermore, by varying the thickness of the PDMS molds, the flow of vapour towards the polymer solution can be controlled. The inner porosity of the products, as well as the porosity of the skin, can be tuned through the manipulation of this parameter.
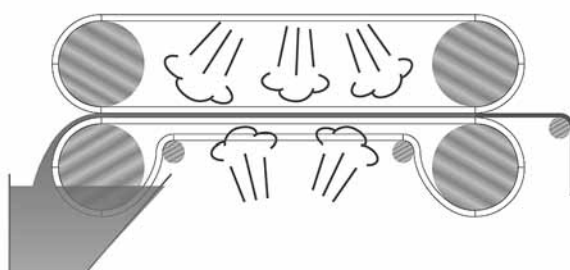
Figure 4: Scheme of a possible implementation of VIPSμF as a continuous process.

By integrating the knowledge presented in this thesis, PSμF can be used for many applications. As can be seen, the major objective set for this thesis has been achieved. The fundamental aspects of PSμF have been studied. In doing so, knowledge has been gained that helps in using the process for new applications. More importantly, the

innovations produced while doing so create new opportunities for the development of new techniques and methods. Some of them are relevant to the structuring of polymeric films. Others, help as introductions into new and exciting fields of research.

Membranes can be defined as a barrier between two media. This is a barrier of a very special kind, though: it allows certain components to go through, while rejecting others. It is sort of like a passport check at the border between two countries: you have some people at one side, different people at the other side and you can only go through if you have the right visa.

Unlike a passport control at Customs, membrane filtrations follow much stricter rules regarding what can go through or not. If a membrane is not porous, it can be used for separating gases. Gases are usually very small and would go through pores without any hindrance and no two gases could be separated from one another. Therefore, dense membranes must be used. The gases have to become part of an intimate mixture with the membrane material. They first dissolve into the membrane, then they swim through it and they get out at the other side. This means that the reason for separating different gases has to do with the different affinity between gases and the material the membrane is made of.

Porous membranes are commonly used for liquids. Liquids consist of bigger molecules that make up for viscous fluids (compared to gases). Liquid mixtures (or solid containing liquids) go through the pores in the membrane, which separates the components mainly due to size differences. Something is either small enough to fit inside a pore and go through or it is not.

The material from which the membrane is made is dictated normally by the substance we wish to separate. Ideally, these substances will not attack the membrane, allowing it to perform for a longer period. In this way, when the application involves solvents, the choice of material is more limited than when everything is water based.

The production of a porous membrane can be done in many ways. In this thesis I used a process called phase separation. A 'phase' is a portion of a system that has uniform properties, just as a polymer solution. It may sound strange but it is exactly the same as coffee: we have water and we add something that is present homogeneously in all the filled volume of the cup. The idea is, therefore, that we will cause this homogeneous phase two separate into two other phases. It is not exactly important

how this happens, but the whole concept is that the original polymer solution becomes two other solutions: one with a high amount of polymer (H) and one with a low amount of polymer (L). Phase L is dispersed through phase H, in the form of droplets, much like oil in water if we mix well enough. In time, the high amount of polymer in H will cause H to become a solid. All the droplets of L have so little polymer that they stay liquid, forming the pores in H. This process is explained in Chapter 2 of this thesis.

This is the most used process for making porous membranes. Normally, the polymer solution is smeared on a smooth glass plate and then the phase separation is induced. Thus, we get a membrane with two smooth surfaces. The novelty presented here is the use of a mold with very small structures instead of a glass plate. The structures in the mold become filled with polymer solution that becomes a solid when the phase separation ends. As a result, we get a membrane with a structured side (the one in contact with the mold) and a smooth side (see page 24).

This technique has been in use in our group for several years. Optimization is nowadays being performed for different materials and different applications. Yet, some of the fundamental questions are still unanswered. These different aspects affect the performance of our process in many different ways, which are studied throughout this thesis, namely in chapters 3 to 6. The motivation behind this research is to identify factors that affect the performance in creating different structures on a membrane. By knowing this, the whole process (from the mold to the polymer solution, including the atmosphere in which the process is made, etc.) can be tuned to meet desired goals. Chapter 3 explores shrinkage and its dependence on the composition of the polymer solution, as well as the features on the mold. Chapter 4 shows the problems to be expected when producing membranes with polygonal pillars. Chapter 5 presents a study on microsieves, perforated membranes with defined channels of small diameter. These are the ultimate membranes for the separation of solids, as they present high openness on an extremely regular structure.

Chapter 6 presents what is, perhaps, my biggest contribution to this technology: the introduction of flexible molds. With these molds, the implementation of our technology as a continuous process becomes much easier. These flexible molds have the added advantage of allowing the phase separation to occur through them. This allows us to obtain membranes with structures on both sides (see page 90).

This describes the contents of this thesis, except the conclusion chapter and the acknowledgements that follow.

Een membraan kan beschreven worden als een barrière tussen twee media. Maar dan wel een zeer bijzondere barrière: het laat specifieke componenten door, terwijl het anderen tegenhoudt. Het is vergelijkbaar met een paspoortcontrole bij de grens tussen twee landen: aan beide zijden heb je mensen en je mag alleen passeren als je het juiste visum hebt.

In tegenstelling tot de paspoort controle door de douane, volgen membraan filtratie processen veel strengere regels met betrekking tot wat doorgelaten wordt en wat niet. Als een membraan niet poreus is, kan het gebruikt worden om gassen te scheiden. Gassen bestaan doorgaans uit kleine moleculen waardoor ze ongehinderd door de poriën kunnen bewegen zonder dat er scheiding plaats vindt. Zodoende dient een dicht membraan gebruikt te worden. De gassen moeten zo een intiem mengsel met het membraan materiaal aangaan. Eerst lossen ze op in het membraan, dan zwemmen ze er doorheen en komen er aan de andere kant weer uit. Het scheiden van gassen met behulp van membranen hangt dus af van de affiniteit die een gas heeft met het materiaal waarvan het membraan gemaakt is.

Poreuze membrane worden veelal gebruikt voor het scheiden van vloeistoffen. Vloeistoffen bestaan uit grotere moleculen die door onderlinge interactie leiden tot visceuze fluidi (vergeleken met gassen). De poriën in het membraan scheiden vloeistof mengsels (of deeltjes bevattende vloeistoffen) voornamelijk op basis van grootte. Als de component klein genoeg is dan past het in de porie en kan het er doorheen. Is het te groot, dan lukt dit niet.

De keuze voor het materiaal van het membraan wordt doorgaans bepaald aan de hand van de substantie die we willen scheiden. Idealiter zal deze substantie het membraan niet degraderen, zodat het voor een langere periode mee kan gaan. Zodoende is voor toepassingen waar oplosmiddelen gescheiden moeten worden de materiaalkeuze beperkter dan voor toepassingen op waterbasis.

Een poreus membraan kan op verscheidene manieren gemaakt worden. In dit proefschrift heb ik een process gebruikt dat fasescheiding wordt genoemd. Een "fase" is een deel van een systeem dat uniforme eigenschappen heeft, zoals een polymeer

oplossing. Het mag dan vreemd klinken, maar het is hetzelfde als koffie: we hebben water en we voegen iets toe dat homogeen verdeeld is in het hele kopje. Het idee is om de homogene fase te scheiden in twee andere fasen. Het gaat er niet om hoe dit precies gebeurt, maar het concept is dat de originele oplossing twee andere oplossingen wordt: een met een hoge concentratie polymeer (H) en eentje met een lage concentratie polymeer (L). Fase L is gedispergeerd in fase H als kleine druppeltjes, vergelijkbaar met olie in water als we maar goed genoeg mengen. Na verloop van tijd zal de hoge concentratie polymeer in H ervoor zorgen dat H uithardt. De druppeltjes L bevatten zo weinig polymeer dat ze vloeibaar blijven, op deze manier de poriën vormend. Dit proces is beschreven in Hoofdstuk 2 van dit proefschrift.

Dit is het meest gebruikte process voor het maken van poreuze membranen. Het polymeer wordt op een gladde glasplaat uitgesmeerd en de fasescheiding wordt gestart. Op deze manier krijgen we een membraan met twee gladde zijden. De nieuwigheid die hier gepresenteerd wordt, is het gebruik van een mal met zeer kleine structuren in plaats van een glasplaat. De structuren in de mal worden gevuld met een polymeer oplossing die uithardt als de fasescheiding voltooid is. Zo krijgen we een membraan met een gestructureerde zijde (degene in contact met de mal) en een gladde zijde (zie pagina 24)

Deze techniek wordt sinds enkele jaren binnen onze groep gebruikt. Optimalisatie vindt momenteel plaats voor verschillende materialen en toepassingen. Echter, nog niet alle fundamentele vragen zijn beantwoord. Deze verschillende aspecten, die ons proces op verschillende manieren beïnvloeden, zijn bestudeerd en beschreven in dit proefschift. Zie hiervoor Hoofdstuk 3 tot en met 6. Het doel van dit onderzoek is om de verschillende factoren te identificeren die de realisatie van verschillende structuren op de membranen beïnvloeden. Door deze factoren te kennen, kan het hele proces (van mal tot polymeer oplossing, inclusief de atmosfeer onder welke het proces wordt uitgevoerd, etc) beheerst en beïnvloed worden om tot de gewenste doelen te komen. In Hoofdstuk 3 is de relatie tussen krimp en de eigenschappen van de gebruikte polymeer oplossing en eigenschappen van de mal beschreven. In Hoofdstuk 4 komen de te verwachten problemen bij het produceren van membranen met polygone (veelhoekige) pilaren aan bod. In Hoofdstuk 5 worden microzeven beschreven, geperforeerde membranen met gedefinieerde kanalen van een kleine diameter. Dit zijn de beste membranen voor het scheiden van vaste stoffen, aangezien ze een grote porositeit vertonen met een zeer regelmatige structuur.

In Hoofdstuk 6 wordt wellicht mijn grootste bijdrage aan deze technologie beschreven: de introductie van flexibele mallen. Met deze mallen is de implementatie van onze techniek in een continu proces eenvoudiger. Deze flexibele mallen hebben het bijkomende voordeel dat de fasescheiding door hen heen plaats kan vinden. Dit stelt ons in staat om membranen met structuren op beide zijden te verkrijgen (zie pagina 90)

Dit is een korte beschrijving van dit proefschrift met uitzondering van de conclusies en de dankwoorden welke volgen.

Una membrana puede ser definida como una barrera entre dos medios. Se trata de una clase de barrera muy especial: algunas substancias pueden atravesarla y otras no. Es casi como un chequeo de pasaporte en la frontera entre dos países: de un lado hay gente, del otro lado hay otro tipo de gente y sólo se puede cruzar si se tiene la visa adecuada.

A diferencia de un control de pasaportes en la Aduana, una filtración a través de una membrana sigue reglas mucho más estrictas acerca de qué puede pasar y qué no. Si una membrana no es porosa, puede usarse para separar gases. Los gases suelen ser moléculas muy pequeñas que atraviesan poros sin mayor impedimento. De esta manera, dos gases distintos no podrían ser separados el uno del otro. Por eso es que se usa una membrana densa. Los gases deben formar una mezcla íntima con el material del cual está hecha la membrana: primero se disuelven en una superficie de la misma, luego la atraviesan y por último, se desprenden de ella del otro lado. Es por esto que la razón principal por la cual se puede separar dos gases tiene su base en la afinidad entre las moléculas de un gas dado y el material del cual se hace la membrana en cuestión.

Las membranas porosas se usan comúnmente para líquidos. Estos están conformados por moléculas más grandes que hacen que (comparados con los gases) los líquidos sean fluidos mucho más viscosos. Así, una mezcla de líquidos (o líquidos con sólidos disueltos en ellos) atraviesa los poros de una membrana, que los separa de acuerdo a su tamaño. En otras palabras, una molécula es lo suficientemente pequeña para penetrar en un poro y seguir adelante hacia la otra superficie de la membrana o no lo es y se queda donde está.

El material del cual se hace una membrana está dado por las condiciones en que se debe realizar la separación y las substancias que se desea separar. Idealmente, se elegirá un material que no sea atacado, permitiendo el funcionamiento por un período más largo. De esta forma, si una aplicación involucra solventes agresivos habrá de tenerse más cuidado que si sólo se usa agua.

Una membrana porosa puede obtenerse de numerosas maneras. En esta tesis, he usado un proceso conocido como separación de fases. Una 'fase' es una porción de un

sistema con propiedades uniformes, como ser una solución de polímero. Puede sonar extraño pero no es distinto de una taza de café: tenemos agua a la cual agregamos algo que está presente homogéneamente en todo el contenido de la taza. La idea es causar la separación de esta fase homogénea en dos fases distintas (también homogéneas). No importa exactamente cómo es que esto ocurre, lo importante es que nuestra solución original se vuelve dos soluciones: una con alto contenido de polímero (A) y una con bajo contenido de polímero (B). La fase B está dispersa en la fase A, como aceite en agua cuando mezclamos bien. Luego de un tiempo, la alta cantidad de polímero causará que A solidifique, formando la membrana. Todas las gotas de B no pueden solidificar, puesto que no contienen suficiente polímero. De esta manera quedan atrapadas en A, formando los poros de la membrana.

Este es el proceso más utilizado para obtener membranas poliméricas porosas. Normalmente, la solución de polímero es untada sobre algo bien liso, como una placa de vidrio y luego se induce la separación de fases. Así, obtenemos una membrana con ambas superficies lisas. La novedad presentada en esta tesis es la utilización de moldes con micro estructuras, en lugar de la placa de vidrio liso. Al untar la solución de polímero, las estructuras en el molde se llenan de solución que al solidificar, nos da una membrana con un lado texturizado (el que estaba en contacto con el molde) y un lado liso (ver página 24).

Esta técnica ha sido utilizada en nuestro grupo durante varios años. Diversas optimizaciones fueron y están siendo llevadas a cabo para su utilización con diversos materiales en varias aplicaciones. Sin embargo, varias cuestiones fundamentales no están del todo comprendidas aún. Estos aspectos afectan la performance del proceso en diversas maneras, que son estudiadas a lo largo de esta tesis (Capítulos 3 a 6). La motivación detrás de este proyecto es el identificar qué factores afectan el resultado de esta técnica al intentar dotar a las membranas de distintas estructuras. Sabiendo esto, es posible ajustar todo el proceso (desde el diseño del molde a la composición de la solución de polímero, incluyendo la atmósfera en la cual se lleva a cabo, etc.) para alcanzar los objetivos deseados. El capítulo 3 explora el encogimiento que acompaña a la separación de fases y cómo depende de la composición de la solución de polímero, así como de las estructuras en el molde. El capítulo 4 muestra qué problemas pueden esperarse al intentar producir membranas con pilares poligonales en su superficie. El capítulo 5 presenta un estudio de micro tamices, membranas perforadas con canales bien definidos en cuanto a tamaño y ubicación. Estas membranas son muy importantes

para la separación de sólidos suspendidos.

El capítulo 6 contiene, tal vez, mi mayor contribución a esta técnica: la introducción de moldes flexibles. Con estos moldes, la implementación de esta técnica en un proceso continuo se vuelve más factible. Estos moldes tienen el beneficio agregado de ser permeables, permitiendo la inducción de la separación de fases a través de sí mismos. Esto nos permite obtener membranas con ambas superficies texturizadas (ver página 90).

Esto describe el contenido de esta tesis, salvo por el capítulo de conclusiones y los agradecimientos que siguen.

These 4+ years have been often intense and even more often calm. They have, however, never been boring at all. In part this had to do with interesting research, in part with the unlimited internet access and in part with the people who helped in different ways to make the day to days more bearable.

I would like to start by thanking Matthias, Dimitris and Rob for our interviews over four years ago. I was off to a rocky start but eventually you all found it in you to allow me into the group with this interesting project. Matthias, thank you for your good response during those times and for helping me in making this happen.

This project has been made possible through the financial support of the MicroNed Consortium. To all the industrial project partners, thank you for the collaboration. I would also like to acknowledge the MESA+ Institute, in particular the Cleanroom Staff for all the support.

Greet, heel erg bedankt voor alles. Jij bent er altijd voor mij geweest, altijd geduldig (vooral wat betreft het optellen van vakantie dagen), altijd behulpzaam. Jij hebt altijd alle zaken op een rijtje en regelt alles snel. Jij bent lief en heel speciaal voor mij, ik zal je missen. Antoine, bedankt voor alle financiële diensten. Het klinkt misschien raar, maar ik zal jou ook missen, vooral met het ontwikkelen van goede strategieën om ondertekeningen na tien uur te kunnen krijgen. Ik kon altijd op jou rekenen en dat betekent veel voor mij.

Rob, mijn begeleider en superdude. Je creativiteit en inzicht hebben mij altijd de goede kant op gestuurd. Zelfs wanneer wij het niet eens waren (vaak dus) heb je mij mijn gang laten gaan. Ik heb altijd veel van jou verwacht en ik ben nooit teleurgesteld geweest. Wetenschappelijk en persoonlijk heb jij altijd een goede instelling gehad om mij te helpen. Ik heb altijd geboft met mijn bazen (ik weet het, alleen honden hebben bazen) maar je bent wel de overtreffende trap tot nu toe.

Anne, Ria, Ruud, Ton en oma De Beus, bedankt voor alle gezelligheid en ondersteuning. Jullie hebben mij altijd in jullie midden opgenomen. Ik voel mij echt op mijn gemak bij jullie en dat maakt het zo ver weg van huis zijn makkelijker.

Ineke, Lydia, Alisia en Paul, bedankt voor jullie enorme hulp en de leuke samenwerking. Ik sta bij jullie in het krijt voor grote delen van het onderzoek en de innovatieve (en zware) technieken en methoden die hier zijn komen te staan. Ineke en Lydia, tevens bedankt voor jullie hulp met het verbeteren van mijn Nederlands. John, bedankt voor het eindeloze geduld met mijn rare opstellingen. Marcel en Wilbert, bedankt voor de vriendschap en jullie goede instelling om altijd te helpen met computer problemen.

I have shared many things with some people here along these years. I will start with my office mates. Ikenna, we have shared the Chicken Box and later the office on the ground floor in Langezijds. I have learned from you not to talk to myself because you did it for the both of us. I've found in you a good friend and I wish you the best in all the great challenges ahead. Afterwards, Al-Hadidi joined us and that made for a lot of fun. Thank you, guys. When we moved to Meander, I got to share an office with Bernke, Jigar and Maik, who got later replaced by Anne Corine. To all of you, people, thank you so much for the great talks and the loads of fun. You have always comforted me during my great rages and complaints.

Now on to who may very well be my official trip mate, Katja. We have been together to many corners of this world, both for work and on holidays. You and Christoph are very dear friends to me and I cherish your honestly greatly. I hope you know that you can count on me for everything you might need.

Jens, Hakan, Ana, Gèráldïnê, Gor, Nico and João: thanks a lot for all the fun in the coffee breaks and the other extracurricular activities we shared. Miriam, sin vos no sé qué habría hecho durante los primeros años de mi estadía en Enschede. Me acompañaste mucho, me contuviste aún más y me ayudaste con muchas cosas. A vos y a Marcel, ¡muchas gracias!

Can… I don't think I know the words I need to begin to describe how much I care about our relationship. You have grown through the years to become the brother I was missing here and an integral person in forming my home away from home. If I could ever repay you the guidance and support you've given me during all the things I have been through, I would only be more grateful. There are great things coming your way, I know. I wish you all the best life has to offer. Well, you've already gotten some of the best life has to offer. Laura, you've brought us brighter (and cleaner) days. Thanks for

the patience.

To the special members of the Think Tank: Michel, Jeroen, Jordi: thanks for all the fun. Jona, thank you for the extensive help with the good looking parts of this work.

Zeynep, it has been my pleasure to share this project with you. Our cooperation has been very smooth and I think we have both learned a great deal from one another. Thank you for this. Joan, mi primer y único estudiante, muchísimas gracias por realizar la mayor parte del trabajo presentado en el capítulo 5. Tu autonomía y responsabilidad son cualidades valorables en todo investigador. (PhD, Carlos!)

Debo gran parte de la posibilidad de estar acá a la sólida educación que he recibido en la escuela secundaria y durante mi carrera universitaria. Al Departamento de Química de las Escuelas Técnicas ORT agradezco por todo el esfuerzo puesto en formar una mente a menudo rebelde, pero con gran aprecio por la infraestructura que me permitió desarrollar la pasión por la disciplina que ejerzo. Al Departamento de Ingeniería Química de la Universidad de Buenos Aires, lo mismo pero por lograrlo con la creatividad y el esfuerzo que se requiere al contar con un presupuesto magro. Gracias por la disciplina y por una base de conocimientos mucho más sólida que las que suelo encontrar por acá.

A toda la pandilla de Boehringer. Panga, Titi, Ingrid y Ana: gracias! Mariela, tu amistad es mucho más de lo que esperaba encontrar el día que fui por una entrevista de trabajo a Boehringer. Te quiero muchísimo y espero tener la misma suerte con mis jefes en el futuro ☺. Ingrid, mi compañera de viajes, la estima que te tengo es grande. Hace bastante ya que dejaste Europa y debo confesar que extraño mis escapadas a Ingelheim y a todos esos pueblitos locos que fuimos a visitar.

Barbi, Camen, Paulita y Anita, muchísimas gracias por todo el apoyo interoceánico que me dieron en este tiempo. Ana espero que en tus momentos de quietud en tu isla de acero recuerdes que hay quien te quiere mucho por estos pagos. Paulita, gracias por hacer de cada una de mis visitas una fiesta. Camen, quizás la comentadora más activa de mi blog, resulta irónico que nuestra amistad haya crecido mucho más conmigo acá que cuando estaba allá. De todos modos, gracias por tu constancia. Barbi, sos lo más. El cariño que te tengo a vos y a toda tu familia (incluido Gera) es grande.

Pachi, Javi, Gonza y Euge: mis compañeros de proyecto. Nos rompimos la cabeza para hidrodesalquilar tolueno, pero la pasamos bien, ¿no? Muchas gracias por las interminables charlas y días de estudio. Muchas gracias por toda la joda y los buenos momentos. Los quiero.

Nadia, Yael y Barbie, aunque ahora sólo estén juntas en este párrafo, tengo grandes recuerdos de todo el tiempo que pasamos juntos. Las quiero a cada una por distintas cosas y las extraño en distintos días, pero sobre todo las quiero porque fueron de gran influencia en la formación de la persona que soy. Gracias!

Jesi, tu amistad y tu apoyo son invaluables. Gracias por todo. Te quiero con el alma. Soli, muchas gracias por venir a la defensa. Me vale de mucho todo tu esfuerzo para hacerlo y el tener una representante de la familia es fabuloso.

Paco y Flor… de los hermanos que se eligen, los mejores. Siempre atentos, siempre dispuestos. La capacidad que tienen para entenderme con pocas palabras y para aceptarme con todas mis cosas tal y como soy me sorprende cada vez. Gracias por ser... y gracias por venir!

A mi familia, a todos en general, muchas gracias por el apoyo y por la cercanía, sin importar las distancias. A mis mayores, gracias por la educación y por todos los esfuerzos invertidos en mí. A mis cuatro abuelos, gracias por una infancia maravillosa. A Dorita, por haber sido tal vez la primera persona que puso en mi cabeza la idea de hacer un doctorado en otro lugar. A mis padres, por hacerme quien soy. En especial a vos, ma, por haberme hecho con alas. Por haberme enseñado que lo que importa ni se tiene ni se lleva, se es. Por el amor incondicional y por todas las veces que me ayudaste a volver a levantarme luego de caerme. Te amo. A mis pares, por la continuidad. Lele y Lulu, mis hermanos, por todo el esfuerzo puesto en remplazar mutuamente todo lo que nos fue faltando. Por ser hasta el día de hoy las personas que me hacen feliz con sus alegrías y me tiran abajo con sus tristezas. Los quiero y los admiro por su capacidad de hacer frente a la vida y elegir volver a triunfar cada vez que se pueda. A mis menores, mi sobrinada, gracias por todo el cariño y por cada uno de los abrazos. Gracias por hacerme derramar lágrimas cada vez que los dejo.

Gert, my bay. Het is vreemd, hoe alles gebeurt. Hoe elke keuze die je maakt je, op een aparte manier, dichterbij je voorbestemming brengt. Nu weet ik dat alles wat ik

in mijn leven gedaan en meegemaakt heb, alle verdriet en alle geluk, maar een proces was om jou te kunnen waarderen zoals je iedere dag verdient. Je geeft mij alle geluk en rust. De rust van een perfect heden en het geluk van een heldere toekomst. Al ben ik af en toe chagrijnig en wispelturig, ik weet zeker dat ik bij jou wil zijn en het lachje dat altijd op jou gezicht staat als jij mij aankijkt is altijd een grote troost. Bedankt voor je ondersteuning en alle liefde. Ik hou zielsveel van je!

Thanks a lot!
M.-